mgr Anna Sosnowska

Zbadanie roli arginaz i mechanizmów przeciwnowotworowego działania inhibitorów arginazy

Rozprawa na stopień naukowy doktora nauk medycznych

w dyscyplinie nauki medyczne

Promotor: prof. dr hab. med. Jakub Gołąb

Zakład Immunologii

Warszawski Uniwersytet Medyczny

Obrona rozprawy doktorskiej przed Radą Dyscypliny Nauk Medycznych

Warszawskiego Uniwersytetu Medycznego

Warszawa 2020

M.Sc. Anna Sosnowska

Investigating the role of arginases and the mechanisms of antitumor activity of arginase inhibitors

Dissertation for the academic degree of doctor of medical sciences

in the discipline of medical science

Promoter: prof. Jakub Gołąb, M. D., Ph.D.

Department of Immunology

Medical University of Warsaw

Defense of the doctoral dissertation in front of the

Medical Science Discipline Council at the Medical University of Warsaw

Warszawa 2020

List of content

LIST OF FIGURES

Figure 1. Role of cells present in the tumor microenvironment in maintaining the balance between immunostimulation and immunoregulation/immunosuppression.

Figure 2. Enzymes participating in the hepatic urea cycle.

Figure 3. ʟ-arginine catabolizing enzymes and their metabolic products.

Figure 4. The influence of Th1 and Th2 cytokines on ʟ-arginine metabolism.

Figure 5. Mechanisms of MDSC-dependent suppression of T-cell function with a focus on ʟ-arginine metabolism.

Figure 6. Suppression of T-cell mediated antitumor immune response by extracellular vesicles containing ARG1.

Figure 7. ʟ-arginine degrading enzymes in the treatment of ʟ-arginine auxotrophic tumors.

Figure 8. Suppression elicited by immune checkpoint molecules and retrieval of activation by the application of monoclonal antibodies directed against immune checkpoint.

Figure 9. Gating strategy used for flow cytometric analysis of in vivo OT-I T-cells proliferation and CD3ζ expression on cells isolated from a tumor-draining inguinal lymph node.

Figure 10. Dot-plot graphs and histograms showing representative examples of gating for Yellow Fluorescence Protein (YFP) positive cells in control C56BL/6 and B6.129S4-Arg1^{tm1Lky}/J (YARG) mice with LLC tumor at the different size.

Figure 11. Percentage of CD45$^+$ immune cells in B6.129S4-Arg1^{tm1Lky}/J (YARG) mice with LLC tumor at the different size 5 mm, 10 mm and 15 mm and gating strategy used for flow cytometric analysis of tumor immune cells (CD45$^+$), macrophages (F4/80$^+$, CD11b$^+$), M-MDSC (Ly6C$^+$, CD11b$^+$) and G-MDSC (Ly6G$^+$, CD11b$^+$).

Figure 12. The percentages of YFP$^+$ cells representing ARG1$^+$ cells and mean fluorescence intensity of YFP shown within populations of immune cells (CD45$^+$), macrophages (F4/80$^+$, CD11b$^+$), M-MDSC (Ly6C$^+$, CD11b$^+$), G-MDSC (Ly6G$^+$, CD11b$^+$) infiltrating the tumors at different development stages.

Figure 13. The relation between increasing LLC tumor volume and the antigen-specific proliferation of OT-I T-cells and CD3ζ expression in mice.

Figure 14. ι-arginine and ι-ornithine concentrations in plasma samples assessed by mass spectrometry.

Figure 15. Comparison of LLC tumor growth between control C57BL/6 and ARG1 Myeloid KO mice (C57BL/6-Arg1$^{tm1Pmu/J}$ × B6.129P2-Lyz2$^{tm1(cre)Ifo/J}$).

Figure 16. Evaluation of OT-I T-cells proliferation as well as ι-arginine and ι-ornithine concentration in control C57BL/6 and ARG1 Myeloid KO mice (C57BL/6-Arg1$^{tm1Pmu/J}$ × B6.129P2-Lyz2$^{tm1(cre)Ifo/J}$).

Figure 17. Timeline of the in vivo experiment exploiting control C57BL/6 and C57BL/6-Arg1^{tm1Pmu}/J × B6.129-Gt(ROSA)26Sor$^{tm1(cre/ERT2)Tyj}$/J (abbreviated as ARGfloxROSA) mice and measurement of ι-arginine concentration in plasma samples by mass spectrometry.

Figure 18. Measurements of tumor growth, volume and weight in experiment exploiting control C57BL/6 and C57BL/6-Arg1^{tm1Pmu}/J × B6.129-Gt(ROSA)26Sor$^{tm1(cre/ERT2)Tyj}$/J (abbreviated as ARGfloxROSA) mice treated with peanut oil or tamoxifen.

Figure 19. Analysis of percentage, absolute numberof CD3$^+$ tumor-infiltrating lymphocytes and CTV$^+$ adoptively transferred OT-I T-cells in inguinal tumor-draining lymph node using flow cytometry.

Figure 20. Measurement of the basal endogenous expression level of ARG1 in various murine tumor cell lines: A20, LLC, E0771, PANC02, ID8, 4T1, B16F10 evaluated by flow cytometry.

Figure 21. Measurement of the basal endogenous expression level of ARG1 in various murine tumor cell lines: A20, LLC, E0771, PANC02, ID8, 4T1, B16F10 evaluated by Western blotting.

Figure 22. Scheme of the lentiviral transduction performed on LLC WT cells in order to generate cell line overexpressing ARG1 and analysis of ARGs activity in control LLC WT, LLC-pLVX and LLC-pLVX-ARG1 cell lines after transductions measured by enzymatic assay shown as urea production.

Figure 23. Comparison of tumor growth in control immunocompetent C57BL/6 and immunodeficient B6(Cg)-Rag2$^{tm1.1Cgn}$/J (RAG2 KO) mice inoculated with ARG1-overexpressing lung carcinoma cell line (LLC-pLVX-ARG1) and control cell lines (LLC WT, LLC-pLVX).

Figure 24. Comparison of tumor growth and ι-arginine plasma concentration in control C57BL/6 and B6(Cg)-Rag2$^{tm1.1Cgn}$/J (RAG2 KO) mice inoculated with ARG1-overexpressing melanoma cell line (B16F10-pLVX-ARG1) and control cell lines (B16F10 WT, B16F10-pLVX).

Figure 25. Evaluation of proliferation potential of OT-I T-cells in increasing concentrations of recombinant mouse ARG1 and ARG2.

Figure 26. Analysis of the effect of recombinant human ARG1 on proliferation and CD3 expression in murine CD4$^+$ and CD8$^+$ T -cells.

Figure 27. Time-course analysis of CD3ε and CD3ζ expression on CD4$^+$ and CD8$^+$ T-cells in presence of high recombinant human ARG1 concentration.

Figure 28. Representative examples of overlay histograms representing CD3ε and CD3ζ expression on CD4$^+$ T-cells in presence of high recombinant human ARG1 concentration and untreated cells at selected time points.

Figure 29. Comparison of CD4$^+$ T-cells proliferation cultured in medium with no (0 μM), low (15 μM), physiologic (150 μM) and high (1500 μM) ι-arginine concentrations.

Figure 30. Comparison of CD3ε and CD3ζ expression on CD4$^+$ T-cells cultured in medium with no (0 μM), low (15 μM), physiologic (150 μM) and high (1500 μM) ι-arginine concentrations.

Figure 31. Analysis of CD4$^+$ T-cells proliferation in medium lacking ι-arginine supplemented with ι-citrulline.

Figure 32. Evaluation of the effect of ARG1 metabolites in various ι-arginine concentrations on the proliferation of murine CD4$^+$ T-cells.

Figure 33. Evaluation of the effect of various concentrations of ABH on the proliferation as well as on CD3ε and CD3ζ expression of human CD4$^+$ T-cells in presence of ARG1.

Figure 34. Evaluation of the effect of various concentrations of OAT-1617 on the proliferation as well as on CD3ε and CD3ζ expression of human CD4$^+$ T-cells in presence of ARG1.

Figure 35. Evaluation of the effect of various concentrations of OAT-1746 on the proliferation of human CD4$^+$ and CD8$^+$ T-cells in presence of ARG1.

Figure 36. Evaluation of the effect of a wide range of OAT-1746 concentrations on the CD3ε expression of human CD4$^+$ and CD8$^+$ T-cells in presence of ARG1.

Figure 37. Evaluation of the effect of a wide range of OAT-1746 concentrations on the CD3ζ expression of human CD4$^+$ and CD8$^+$ T-cells in presence of ARG1.

Figure 38. Evaluation of the effect of a wide range of OAT-1746 concentrations on the percentage of TNF-α^+ and IFN-γ^+ human CD4$^+$ T-cells in presence of ARG1.

Figure 39. Assessment of ABH, OAT-1617 and OAT-1746 inhibitors effectiveness in blocking the activity of tumor cells associated ARG1 and ARG2.

Figure 40. Assessment of ABH, OAT-1746 and OAT-1617 inhibitors effectiveness in blocking the activity of tumor cells secreted ARG1 and ARG2.

Figure 41. Evaluation of antitumor efficacy of therapy with OAT-1746 ARG inhibitor.

Figure 42. Evaluation of antitumor efficacy of therapy with ABH ARG inhibitor.

Figure 43. Comparison of tumor growth in C57BL/6 mice inoculated with LLC WT or LLC-pLVX-ARG1 cell line treated with OAT-1746 or PBS for the whole experiment.

Figure 44. Study of the antigen-specific proliferation in vivo in C57BL/6 mice with advanced tumors treated with OAT-1746.

Figure 45. Analysis of OAT-1746 immunomodulatory mechanisms on the immune cells in the tumor microenvironment of the lung cancer model.

Figure 46. Timeline of the in vivo experiment evaluating antitumor efficacy of the combination of OAT-1746 with anti-PD-1 therapy in the mouse lung cancer model LLC in C57BL/6 mice.

Figure 47. Evaluation of antitumor efficacy of OAT-1746 combined with anti-PD-1 therapy.

Figure 48. Evaluation of antitumor efficacy of OAT-1746 combined with anti-PD-1 and DMXAA therapies.

LIST OF TABLES 1

Table 1. The summary of the immune checkpoint inhibitors approved by Food and Drug Administration for tumor treatment.

Table 2. Antibodies used for flow cytometry staining.

Table 3. Primers used for genotyping of transgenic mice strains.

INDEX OF ABBREVIATIONS

ABH – (S)-2-amino-6-boronohexanoic acid

ADC – arginine decarboxylase

ADI – arginine deiminase

AGAT – arginine:glycine amidinotransferase

ANOVA – analysis of variance

APCs – antigen-presenting cells

ARG – arginase

ASL – argininosuccinate lyase

ASS-1 – argininosuccinate synthase 1

ATCC – American Type Culture Collection

BEC – (S)-(2-boronoethyl)-L-cysteine

BSA – bovine serum albumin

CAR – chimeric antigen receptor

CATs – cationic amino acid transporters

CD – cluster of differentiation

CFSE – CellTrace Carboxyfluorescein Succinimidyl Ester

CTLA-4 – cytotoxic T lymphocyte-associated antigen 4

CTV – CellTrace Violet

DMEM – Dulbecco's Modified Eagle Medium

DMFO – α-difluoromethylornithine

DMSO – dimethyl sulfoxide

DMXAA - 5,6-dimethylxanthenone-4-acetic acid

EIF2α – eukaryotic translation initiation factor 2α

FACS – fluorescence-activated cell sorting

FBS – fetal bovine serum

FDA – Food and Drug Administration

GCN2 – general control non-depressible 2 kinase

IC$_{50}$ – half-maximal inhibitory concentration

IDO – indoleamine 2,3-dioxygenase

IFN – interferon

IL – interleukin

KO – *knock-out*

LLC – Lewis lung carcinoma

M-CSF – macrophage colony-stimulating factor

MDSCs – myeloid-derived suppressor cells

MF13 – L-proline-m-bis (2-chloroethyl) amino-L-phenylalanyl-L-norvaline ethyl ester hydrochloride

MFI – mean fluorescence intensity

MHC – major histocompatibility complex

NK – natural killer

NO – nitric oxide

NOHA – N-hydroxy-L-arginine

nor-NOHA – N-hydroxy-nor-L-arginine

NOS – nitric oxide synthase

NSCLC – non-small cell lung carcinoma

OTC – ornithine transcarbamylase

OVA – ovalbumin

PBS – phosphate-buffered saline

PEG – polyethylene glycol

RNOS – reactive nitrogen-oxide species

ROS – reactive oxygen species

RT – room temperature

SD – standard deviation

SDS – sodium dodecyl sulfate

SDS-PAGE – sodium dodecyl sulfate polyacrylamide gel electrophoresis

STING – stimulator of interferon genes

TAAs – tumor-associated antigens

TAMs – tumor-associated macrophages

TCR – T-cell receptor

TGF – transforming growth factor

TIF – tumor interstitial fluid

TILs – tumor-infiltrating lymphocytes

TNF – tumor necrosis factor

TRIS – tris(hydroxymethyl)aminomethane

VEGF – vascular endothelial growth factor

WT – wild-type

YFP – yellow fluorescent protein

STRESZCZENIE

Coraz więcej danych wskazuje, że mechanizmy immunoregulacyjne w złożonym mikrośrodowisku nowotworu należą do głównych przeszkód w uzyskaniu skutecznej odpowiedzi klinicznej na immunoterapię. Między innymi, jedną z ważniejszych cech mikrośrodowiska nowotworu, która zaburza lokalną odpowiedź immunologiczną przeciwko komórkom nowotworowym, jest metabolizm aminokwasów, w tym ʟ-argininy. Arginaza (ARG) jest enzymem degradującym ʟ-argininę, która ma znaczenie dla prawidłowego funkcjonowania limfocytów T, biorących udział w skutecznej przeciwnowotworowej odpowiedzi immunologicznej. W mikrośrodowisku różnych typów nowotworów odnotowano wysoką aktywność ARG, a coraz więcej obserwacji wskazuje, że koreluje ona z niekorzystnymi wynikami klinicznymi chorych na nowotwory. Dlatego też, w ramach tego projektu skupiono się na zbadaniu roli ARG w mikrośrodowisku nowotworu oraz na badaniach mechanizmu hamowania ARG w celu zmniejszenia immunoregulacyjnych właściwości mikrośrodowiska nowotworu.

Ekspresję ARG zbadano szczegółowo w mikrośrodowisku mysiego guza płuc na różnych etapach progresji nowotworu. W rezultacie ekspresję ARG stwierdzono w komórkach szpikowych związanych z nowotworem, głównie w makrofagach. Podwyższona ekspresja ARG została powiązana z zaawansowanym stadium nowotworu i korelowała z upośledzoną proliferacją *in vivo* antygenowo specyficznych limfocytów T. Dodatkowo, stężenie ʟ-argininy w osoczu zmniejszało się wraz z progresją nowotworu, co sugeruje podwyższoną aktywność ARG. W warunkach *in vitro* zbadano wpływ braku ʟ-argininy w pożywce oraz wpływ rekombinowanej ARG1 na proces namnażania limfocytów T. Deficyt ʟ-argininy spowodował upośledzoną proliferację limfocytów T, obniżenie ekspresji cząsteczek CD3ε i CD3ζ oraz zmniejszenie produkcji cytokin. Wszystkie zaobserwowane zmiany zostały zniesione pod wpływem działania inhibitorów ARG. Do wyjaśnienia immunomodulującego wpływu ARG1 na rozwój antygenowo swoistej odpowiedzi immunologicznej wykorzystano myszy transgeniczne z niedoborem ARG1. Uzyskane wyniki wskazują, że myszy z niedoborem ARG1 rozwijają lepszą odpowiedź immunologiczną i mają wyższy odsetek, a także liczbę limfocytów T naciekających guz. Wyniki przeprowadzonych badań ukazują

również negatywny wpływ zwiększonej ekspresji ARG1 na wzrost guzów *in vivo*, powodując przyspieszoną progresję mysiego raka płuc i czerniaka. Ponadto *in vivo* zbadano działanie przeciwnowotworowe nowego drobnocząsteczkowego inhibitora ARG OAT-1746 w modelu mysiego nowotworu płuc. Aktywność przeciwnowotworową OAT-1746 zbadano w monoterapii, jak również w połączeniu z innymi immunoterapiami, w tym z inhibitorem punktu kontrolnego anty-PD-1 i agonistą stymulatora genów interferonu (STING). Monoterapia z użyciem OAT-1746 znacząco zahamowała wzrost nowotworu, jak również wydłużyła przeżycie myszy. Ponadto, działanie to zostało spotęgowane w terapii skojarzonej. Ostatecznie zbadano mechanizm działania OAT-1746. Uzyskane wyniki sugerują, że OAT-1746 działa poprzez modyfikację proporcji określonych subpopulacji limfocytów T w mikrośrodowisku nowotworu, zwłaszcza poprzez przekierowanie równowagi w kierunku mniej immunosupresyjnego fenotypu limfocytów T.

Podsumowując, wyniki zawarte w niniejszej pracy doktorskiej wskazują, że aktywność ARG1 upośledza odpowiedź limfocytów T, oraz że modulacja właściwości mikrośrodowiska nowotworu poprzez hamowanie enzymatycznej aktywności ARG jest obiecującym podejściem immunoterapeutycznym, które wzmacnia przeciwnowotworową odpowiedź immunologiczną.

ABSTRACT

Accumulating evidence indicates that the immunoregulatory mechanisms in the complex tumor microenvironment are among the main obstacles to successful cancer immunotherapy. One of the most prominent features of the tumor microenvironment that dysregulates the local adaptive immune response against cancer is amino-acid metabolism, also that involving ʟ-arginine. Arginase (ARG) is an enzyme degrading ʟ-arginine, which plays a role in the expansion and proper functioning of T-cells to exert a successful antitumor immune response. High ARG activity in the tumor microenvironment of various types of malignancies has been reported and an increasing number of observations indicate that it correlates with poor clinical outcomes of cancer patients. Therefore, this project focused on investigating the role of ARG in the tumor microenvironment and on studies of ARG inhibition mechanism to reduce the immunosuppressive properties of cancer.

ARG1 expression was studied in detail in the tumor microenvironment of a murine lung carcinoma at the different tumor progression stages. As a result, ARG expression was found in tumor-associated myeloid cells, mostly macrophages. Elevated ARG expression was linked with advanced tumor stage and correlated with impaired *in vivo* proliferation of the antigen-specific T-cells. Additionally, ʟ-arginine plasma concentration decreased with tumor progression, suggesting elevated ARG activity. In *in vitro* settings, the influence of lack of ʟ-arginine in medium or addition of recombinant ARG1 on the process of T-cells expansion was investigated. Depletion of ʟ-arginine caused impaired T-cells proliferation, down-regulation of CD3ε and CD3ζ chains expression and reduced cytokines production. The observed negative changes were abrogated in the presence of ARG inhibitors. Transgenic mice with ARG1 deficiency were used to elucidate the immunomodulatory impact of ARG1 on the development of antigen-specific immune response. The obtained results indicate that mice with *knock-out* of ARG1 develop an improved immune response and have a higher percentage as well as the number of tumor-infiltrating lymphocytes. This study also demonstrates the negative effects of ARG1 overexpression on the *in vivo* tumor growth, causing accelerated progression of lung carcinoma and melanoma. Furthermore,

the *in vivo* antitumor efficacy of the novel small-molecule ARG inhibitor OAT-1746 was investigated in the murine lung tumor model. Antitumor activity of OAT-1746 was studied in monotherapy as well as in combination with other immunotherapies, including checkpoint inhibitor anti-PD-1 and stimulator of interferon genes (STING) agonist. OAT-1746 treatment as monotherapy significantly inhibited tumor growth as well as prolonged the survival of mice and these effects were enhanced in combination therapy. Finally, the mechanism of action of OAT-1746 was investigated. The obtained results suggest that OAT-1746 acts by changing the proportions of specific T-cell populations in the tumor microenvironment, especially by switching the balance towards a less immunosuppressive T-cell phenotype.

Altogether, this study provides the evidence that ARG1 activity impairs T-cell response and that modulation of tumor microenvironment properties by targeting ARG enzymatic activity is a promising immunotherapeutic approach to enhance the antitumor immune response.

1. INTRODUCTION

1.1 Tumor microenvironment

Tumors are formed in the oncogenesis process that may last even several decades. Most often, it is initiated by hereditary or spontaneous mutations induced by chemical, biological and/or physical factors. Accumulation of the genetic changes within the genes responsible for cell cycle control, such as proto-oncogenes and tumor suppression genes, leads to disruption of the balance between apoptosis, differentiation, proliferation and cell aging. This usually results in the alteration of cellular repair systems and the development of inflammation in the affected tissue. Inflammation associated with tumorigenesis leads to the accumulation of immune cells within the tumor and surrounding tissues or organ, contributing to their remodeling and, consequently, impairing their function [1-3].

The tumor microenvironment not only contains tumor cells, but represents a very complex structure that consists of many other types of cells, including fibroblasts, immune cells, endothelial cells of blood and lymphatic vessels, adipocytes, pericytes as well as the extracellular matrix. Together these components constitute the closest surrounding of tumor cells and are in dynamic interactions [4]. Cells and vasculature are supported by a three-dimensional macromolecular network of an extracellular matrix that represents non-cellular components such as collagen, fibronectin, laminin, elastin, hyaluronan, among others. The extracellular matrix helps to maintain homeostasis that is tightly controlled. On the other hand, it undergoes continuous remodeling mediated by several enzymes that degrade the matrix [5]. Cellular components of tumor microenvironment distinct from transformed cells are termed stromal cells. This group consists of cancer-associated fibroblasts, endothelial cells, mesenchymal stem cells and various immune cells [6]. The continuous cross-talk of malignant cells with stromal cells and/or with extracellular matrix can lead to the acquisition of a changed, unfavorable phenotype by cells in the tumor microenvironment that further promotes tumor progression. Cumulatively, the properties of the tumor microenvironment contribute to promoting chronic

inflammation, angiogenesis, invasion, progression and metastasis as well as determine resistance to treatment [7].

1.2 Immune cells in the tumor microenvironment

Apart from the malignant cells, the tumor mass contains a variety of other cells belonging to the immune system. There are cells playing a positive role in the host protection process, called immune surveillance, in which immune cells may detect and eliminate precancerous and malignant cells. These cells include resting and effector T-cells as well as natural killer (NK) cells with the ability to direct killing of tumor cells and dendritic cells relevant for antigen presentation. On the other hand, a characteristic feature of the tumor microenvironment is the formation of the immunoregulatory properties mediated by a group of immune cells playing an unfavorable role. Among immunoregulatory cells contributing to tumor development, the following can be distinguished: tumor-associated macrophages (TAMs), myeloid-derived suppressor cells (MDSCs), T-cells with the regulatory properties [4, 8]. The division of immunostimulatory and immunoregulatory cells in the tumor microenvironment is presented in Figure 1.
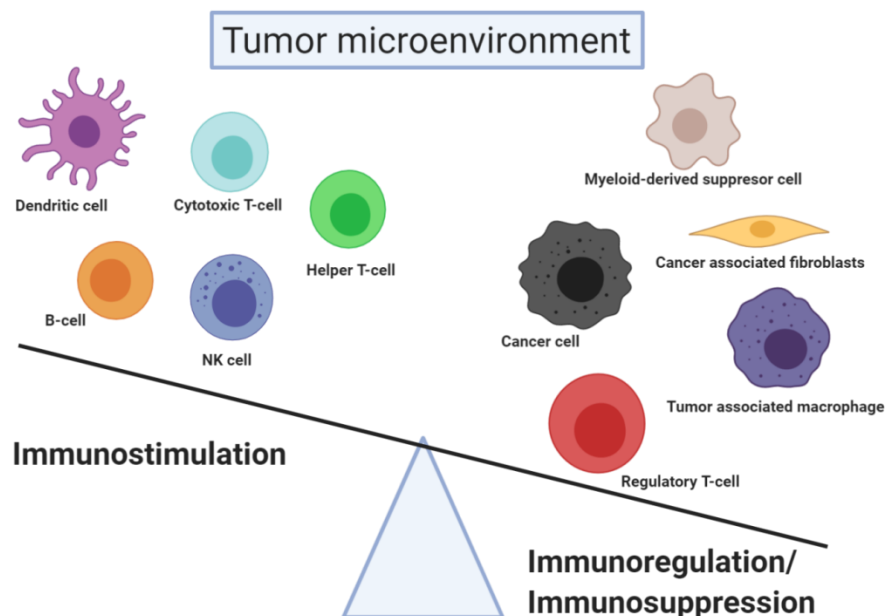
Figure 1. Role of cells present in the tumor microenvironment in maintaining the balance between immunostimulation and immunoregulation/immunosuppression.

1.2.1 Immunoregulatory cells

1.2.1.1 Tumor-associated macrophages (TAMs)

Macrophages originate in the majority from monocytes that are attracted to the tumor niche by tumor-derived chemokines: CCL2, CCL3, CCL4, CCL5, CCL8, CXCL12 and growth factors: macrophage colony-stimulating factor (M-CSF) and vascular endothelial growth factor (VEGF) [9]. In the tumor microenvironment, especially upon the production of cytokines by other cells, macrophages can be further polarized into two distinct subsets: M1 and M2. Currently, this classification is not recommended however, the majority of articles describe the function of macrophages in the tumor in the context of M1 or M2 subsets based on *in vitro* polarization [10]. According to the literature, M1 type is induced upon interferon γ (IFN-γ) exposure, whereas M2 type is favorably generated in the presence of T helper 2 (Th2) cytokines such as interleukin 4 (IL-4) and IL-10. Generally, macrophages are characterized by high functional and phenotypic plasticity. Depending on the signals in the microenvironment, macrophages can undergo a smooth transition between M1 and M2 type or differentiate into similar forms. Differentiated M1 macrophages represent a pro-inflammatory phenotype, whereas M2 macrophages are characterized as immunoregulatory and contribute to the promotion of tumor growth. TAMs commonly represent M2 type and play a protumoral role. Macrophages in the tumor can be identified by immunophenotyping based on CD11b and F4/80 markers expression. Furthermore, major histocompatibility complex (MHC) class II expression might serve as the additional marker for both types, whereas expression of CD206 and immunosuppressive enzyme arginase (ARG) is characteristic for M2 phenotype [11, 12]. It was shown that the increased number of TAMs is associated with advanced tumor stage and shorter survival in a variety of human cancers, including glioblastoma, pancreatic cancer, lymphoma and breast cancer, among others [13-17]. M2 polarized macrophages were shown to express high levels of VEGF and, once injected in tumor-bearing mice, promoted the development of higher vascular density in the tumor [18]. In addition, TAMs can secrete matrix metallopeptidases 1 and 7, which are proteolytic enzymes induced in hypoxia responsible for releasing VEGF from the extracellular

matrix, accelerating angiogenesis [19]. It was shown that the influx of macrophages into healthy tissue is an important step in the formation of a pre-metastatic niche. In the lung, macrophages displaying specific phenotype (CD11b^{+} F4/80[+/-] CD68^{+} CX3CR1^{+}) are recruited before metastasis is formed [20]. Importantly, TAMs by secretion of inhibitory cytokines such as IL-10, transforming growth factor-β (TGF-β) and inflammatory mediator prostaglandin-E2 can inhibit antitumor immune response mediated by T-cells [21, 22]. Liu and colleagues showed that in a model of murine colorectal cancer TAMs recruit regulatory T-cells positive for chemokine receptor 6 (CCR6) by the production of its sole chemokine ligand 20 (CCL20) [23]. A number of unfavorable effects attributed to TAMs arise from the production of immunosuppressive enzyme ARG that causes evasion of immune response.

1.2.1.2 Myeloid-derived suppressor cells (MDSCs)

Accumulation of not fully differentiated myeloid cells displaying abnormal functions is a common feature of cancer. MDSCs are derived from myeloid lineage and represent pathologically activated immature stages of monocytes and granulocytes, which reside in the tumor microenvironment and promote tumor progression. Furthermore, MDSCs can also be found in bone marrow, spleen and peripheral circulation. Similar to TAMs, MDSCs are characterized by considerable heterogeneity and high plasticity depending on the surrounding differentiating conditions. In a healthy state, MDSCs are present only at low numbers because they continuously undergo differentiation to mature forms of monocytes and granulocytes. However, in pathological conditions, the number of MDSCs increases due to a block of differentiation and cytokine-driven proliferation [24, 25]. This accumulation is not only limited to cancer, but also occurs in autoimmunity, infectious diseases, aging, obesity, pregnancy and transplantation. Although MDSCs are linked with so many circumstances, their role has been the most widely studied in the context of cancer [26]. MDSCs rapidly accumulate in the tumors, which has been shown in numerous murine cancer models including lymphoma, sarcoma, melanoma as well as lung, colon and mammary carcinomas [27]. In cancer patients circulating MDSCs were found to be significantly increased in early and late-

stage cancer correlating with clinical stage and metastatic disease. For example, among patients with various advanced-stage cancers, the highest number and percentage of MDSCs were linked with extensive metastatic tumor burden [28]. MDSCs exhibit a very potent suppressive activity towards cells of the immune system and also play a role in angiogenesis, promotion of tumor cells survival and metastases [29, 30]. In mice, MDSCs are defined by the expression of CD11b and GR1 markers on their surface. GR1 marker, initially recognized by monoclonal antibodies as a single antigen, is now known to be one of the two molecules: Ly6G and Ly6C. Based on Ly6G and Ly6C relative expression, MDSCs can be further differentiated into granulocytic identified as Ly6G^{high}, Ly6C^{low} and monocytic expressing Ly6C^{high} and Ly6G^{low}) subpopulations [27]. Human cells do not express GR1 molecule, thus MDSCs identification is different. Youn *et al.* evaluated the MDSCs ratio in mouse tumor models revealing that granulocytic MDSCs are a dominant subpopulation in the spleen of mice with advanced LLC tumors [27]. Several T-cell inhibitory mechanisms employed by MDSCs were established. The first is the production of immunosuppressive enzyme ARG that actively depletes from microenvironment simple amino acid ʟ-arginine needed for T-cells proliferation [31, 32]. Second is the production of peroxynitrite that causes nitration of the T-cell receptor (TCR), altering the binding process of specific antigen and thus impairing proper T-cells activation [33]. The third unraveled mechanism of MDSCs playing a role in immune evasion is the down-regulation of ʟ-selectin (CD62L) on T-cells. ʟ-selectin is an adhesion molecule important in an endothelial attachment that directs the trafficking of naïve lymphocytes to lymph nodes where activation takes place and also allows access of the T-cells to the tissue inflamed by tumor development [34]. Another identified immunomodulatory process of MDSCs is ʟ-cysteine sequestration that limits the availability of this amino acid for T-cells expansion process [35]. Moreover, MDSCs impair cytotoxic activity of NK cells through decrease in perforin production, which was demonstrated *in vivo* in tumor-bearing mice [36]. Special subpopulation of MDSCs expressing M-CSF receptor CD115 apart from GR1 was shown to induce suppressive FoxP3^{+} T regulatory cells [37]. Due to so many negative faces of MDSCs they emerge as promising target in cancer therapy

including their depletion, blockage of expansion or directing efforts towards suppressing their inhibitory mechanisms [38]. Accumulating evidence indicates that elevated number of MDSCs is linked with poor clinical outcomes of cancer patients and hinders the therapeutic efficiency of other immunotherapies such as immune checkpoint inhibitors [39, 40].

1.2.1.3 Regulatory T-cells

Regulatory T-cells belong to $CD4^+$ subpopulation of T lymphocytes and are further characterized by the specific phenotype of nuclear transcription factor FoxP3 and surface CD25 expression. Notably, CD25 molecule constitutes the α chain of a functional receptor for IL-2 with high affinity. Regulatory T-cells have been associated with cancer-related immunosuppression created by a plethora of mechanisms targeting both cellular and humoral activity. One of the key inhibitory activity is competition with conventional T-cells for IL-2 consumption via its surface receptor. This cytokine is crucial for the appropriate expansion of all T-cells therefore, with its limited amount effector T-cells responsiveness is impaired. The well-known action of regulatory T-cells is the production of cytokines such as IL-10, IL-35 and TGF-β that have immunosuppressive activity towards other cells of the immune system including B cells, NK cells and T-cells (naïve, effector, memory) [41, 42]. Besides, regulatory T-cells express the cytotoxic T lymphocyte-associated antigen 4 (CTLA-4) that transmits inhibitory signaling. Through binding of CTLA-4 with CD80 and CD86, co-stimulatory molecules found on antigen-presenting cells (APCs) such as dendritic cells, it impairs their potential in stimulating the T-cells following antigen encounter [43]. Another immunosuppressive mechanism of regulatory T-cells results from the conversion of adenosine triphosphate via ectonucleotidases CD39 and CD73 into adenosine, which is an immunosuppressive metabolite towards T-cells, especially in hypoxic conditions of tumor-affected tissue [44]. Higher frequency of regulatory T-cells in the tumor microenvironment is linked with worse prognosis in several types of cancer including hepatocellular carcinoma and non-small cell lung carcinoma (NSCLC) [45]. However, there is one exception – it is colorectal cancer, where regulatory T-cells play a

beneficial role [46]. Considering a variety of adverse mechanisms promoting tumor development, regulatory T-cells represent an appealing target in cancer immunotherapy that is under intensive investigation [47, 48].

1.2.2 Immune cells playing a positive role in the tumor microenvironment

1.2.2.1 Tumor-infiltrating lymphocytes (TILs)

T lymphocytes can be the most simply divided into CD4$^+$ Th cells and CD8$^+$ cytotoxic T-cells. Further CD4$^+$ T-cells can be divided into functional subsets: Th1 and Th2, characterized by contrasting differentiation cytokines and production of a specific repertoire of cytokines playing a distinct role in immunity. T-cells presence in the tumor microenvironment is considered a positive prognostic factor for cancer patients, especially considering CD8$^+$ T-cells subpopulation. However, CD4$^+$ FoxP3$^+$ CD25$^+$ regulatory T-cells are also included to the T-cells that infiltrate the tumor, and as mentioned above their role is rather unfavorable as contrary to other T-cells subpopulations [49]. Recent studies based on meta-analysis revealed that not only the presence but also TILs histological location such as tumor center or invasive margin is relevant for prognosis [50]. CD8$^+$ T-cells play an essential role in the elimination of cancer cells through their direct cytotoxic activity [51]. Tumor-induced dysfunction of tumor-infiltrating CD8$^+$ T-cells was described in lung cancer patients. It was shown that the lung tumor microenvironment sensitizes these cells to activation-induced cell death, which may be further linked with the poor clinical effects observed in immunotherapeutic trials [52]. The role of CD4$^+$ T-cells is more complex. Th1 type lymphocytes are able to limit tumor progression by secreting cytokines with anti-cancer properties such as tumor necrosis factor α (TNF-α) and IFN-γ. Furthermore, IFN-γ secreted by Th1 T-cells activates the M1 type of macrophages, playing a beneficial pro-inflammatory role in the tumor microenvironment. In contrast, Th2 T-cells by secreting cytokines such as IL-4 and IL-10 activate M2 type of macrophages, the presence of which promotes tumor progression [53]. The evaluation of TILs is utilized to calculate the so-called immunoscore – cancer classification system based on the immunohistochemistry method assessing densities of CD3$^+$ and CD8$^+$ T-cells at the

tumor site and in the invasive margin. It was proposed for the estimation of recurrence risk in colon cancer patients [54, 55].

1.2.2.2 Natural killer (NK) cells

NK cells are cells of the innate immune system that are able to eliminate cells infected with viruses and those that express surface markers related to oncogenic transformation. The signal for the elimination of aberrant cells is also triggered by a lack of MHC class I expression on the target cells. NK cells share some common features with cytotoxic T-cells, however here, detection of a target cell does not solely depend on specific antigen recognition. NK cells can kill target cells (cancerous or virus-infected cells) directly, in a mechanism also known as natural cytotoxicity. The process is mediated by stimulation of activating and/or inhibitory receptors present on the surface of NK cells. The predominance of activating signals or a deficit of inhibitory signals within the immune synapse leads to the activation of NK cells and the release of the content of lytic granules containing perforin, granzymes, granulizine and TIA-1 protein. With the predominance of inhibitory signals, no activation of the cytotoxic reaction in NK cells occurs [56, 57]. NK cells participate in the control of tumor progression by directly interacting with cancer cells or indirectly by affecting other cells of the immune system. The lysis of a transformed cell generates cell debris that can be further engulfed by APCs such as dendritic cells and macrophages. Loss of MHC class I molecules from the surface is a very common feature of mouse and human tumor cells. It consequently leads to decreased antigen presentation and avoiding the detection by the T-cells, which require this interaction to become activated [58]. In mice with impaired NK cell activity, tumor growth was accelerated and more metastases were observed [59]. Similar observations apply to mice treated with an antibody that targets NK cells causing their depletion [60]. Moreover, NK cells isolated from cancer patients exhibit decreased activity [61]. Also, the incidence of familiar cancer was found to be associated with reduced cytotoxicity of NK cells [62]. Numerous studies revealed that impaired activity of NK cells in cancer patients is related to alterations of expression of activating receptors such as NKp30, NKp46,

NKG2D that are relevant for natural cytotoxicity [63, 64]. Several strategies based on the antitumor properties of NK cells are currently in preclinical and clinical development aiming to fight a variety of cancer types, but predominantly hematological malignancies. The therapies encompass adoptive NK cell transfer expanded on the large scale such as autologous and allogeneic NK cells as well as human NK cell lines and recently widely studied NK cells with genetically engineered and modified in laboratory chimeric antigen receptor (CAR) targeting specific receptor. Other therapies include agonists of NK cell activating receptors and modulation of microenvironment towards properties favoring the NK cells activity such as increasing the concentration of IL-15 that enhances NK cells proliferation [65, 66].

1.2.2.3 Dendritic cells

Dendritic cells have unique properties to professionally present antigens and therefore play a key role in the induction of adaptive immune response against developing tumor. Dendritic cells can uptake, intracellularly process antigens associated with cancer cells and then present peptides in the context of MHC class II molecules to the CD4^{+} T-cells. As a result, a cellular antitumor response is activated, as well as the production of antibodies by B-cells, leading to the destruction of cancer cells [67]. Furthermore, in a process termed cross-presentation dendritic cells can present exogenous antigens derived from solid tumors via MHC class I molecules to naïve cytotoxic T-cells. Subsequently, CD8^{+} cytotoxic T-cells recognize and attack cancer cells that have on their surface antigens already presented by dendritic cells [68]. Based on the enormous potential of dendritic cells in the elicitation of antitumor T-cell mediated immune responses, these APCs have been used as active cellular immunotherapy after *ex vivo* expansion on a large scale. The procedures of dendritic cell-based vaccines involve the isolation of CD34^{+} precursors or CD14^{+} monocytes from the peripheral blood of cancer patient, laboratory differentiation into dendritic cells by treatment with IL-4 and granulocyte-macrophage colony-stimulating factor (GM-CSF), loading the dendritic cells with tumor-specific antigens and infusion of expanded cells to the patient circulation. It is expected that administrated dendritic cells will migrate to the

secondary lymphoid organs such as tumor-draining lymph nodes to induce the specific response against cancer [69, 70]. So far, vaccines utilizing dendritic cells have been investigated in many cancer-related clinical trials evaluating patients with prostate cancer, breast cancer, melanoma, renal cancer, ovarian cancer, myeloma and gastrointestinal cancer [71, 72]. Results of prolonged overall survival in 2010 have led to Food and Drug Administration (FDA) approval for clinical use of autologous dendritic cells based vaccine named sipuleucel-T for treatment of metastatic prostate cancer that is castration-resistant [73]. Generally, dendritic cells based immunotherapy has shown favorable safety profiles and such treatment induced antitumor immune responses in some treated patients. However, in some patients, the clinical response is limited and not satisfying. Among the factors influencing this inefficiency is reduced expression of tumor-associated antigens (TAAs) by malignant cells [74]. Furthermore, a study using murine tumor indicated that proinflammatory cytokine IL-6 induces ARG expression in dendritic cells that causes subsequent downregulation of MHC class II molecules leading to CD4^{+} T-cells dysfunction [75]. The presence of dendritic cells in the tumor niche plays a positive role by generating antitumor immunity. However, a subpopulation of tumor-associated regulatory dendritic cells that exhibits defective function and possess immunosuppressive properties has also been described [76, 77].

1.3 ʟ-arginine

In healthy adults, ʟ-arginine is considered as non-essential amino acids. However, it is regarded as conditionally-essential or semi-essential amino acids for adults with pathological conditions such as inflammation, trauma and cancer, since its synthesis might be insufficient. On the other hand, for preterm infants and young children it is classified as an essential amino acid [78]. ʟ-arginine is involved in a number of crucial nutritional and physiological processes in the human body. First, it participates in nitrogen metabolism as a part of the hepatic urea cycle that aims to convert toxic ammonia to urea that can be excreted with the urine. Enzymes participating in the hepatic urea cycle are shown in Figure 2. Second, it is required for the synthesis of creatinine, which supports tissues with high energy demands, such as muscles and the

brain. Third, it constitutes the precursor for the synthesis of a variety of relevant signaling molecules such as glutamate, agmatine and notably nitric oxide that play a particular role in host-defense and vasodilatory mechanisms. Forth, it serves as a simple amino acid for protein synthesis, necessary for all dividing cells. Importantly, it is required for the proliferative ability of both transformed cells as well as cells of the immune system. Thus, ι-arginine is necessary for the proper expansion of T-cells that trigger antitumor immune response [79, 80]. Depending on the health and nutritional status of the individual, normal plasma concentration varies between 50 to 250 μM [81]. More detailed studies counting age and sex of the individual revealed that the usual range is 72.4 ± 6.7 μM, 81.6 ± 7.3 μM, 88.0 ± 7.8 μM and 113.7 ± 19.8 μM for young women, young men, elderly women and elderly men, respectively [82]. In contrast to plasma ι-arginine concentrations, its intracellular concentration is many times higher and range from 1 to 2 mM [83]. Transport of extracellular ι-arginine to the intracellular compartments is enabled via several membrane transporters. The main group of transporters that uptake the majority of ι-arginine consists of cationic amino acid transporters (CATs) including CAT-1, CAT-2A, CAT-2B, CAT-3, also termed as SLC7A1-3 [84]. In myeloid cells, transport of ι-arginine occurs predominantly by CAT-2, whereas in T-cells is mediated by CAT-1. [85, 86] MDSCs in the tumor that are characterized by upregulated ARG activity uptake the extracellular ι-arginine through CAT-2B [87, 88].
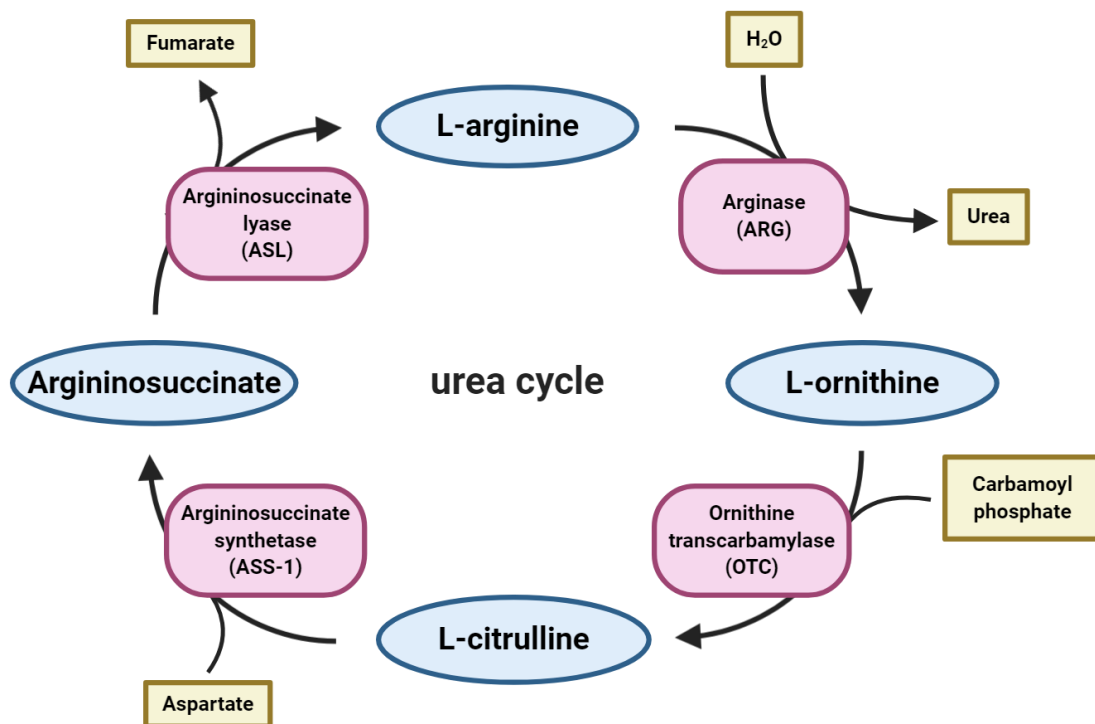
Figure 2. *Enzymes participating in the hepatic urea cycle.*

1.4 ʟ-arginine metabolism

In the human body, the majority of ʟ-arginine can be synthesized by two distinct pathways named intestinal-renal axis and ʟ-citrulline-nitric oxide (NO) cycle. The first pathway allows maintaining the systemic homeostasis of extracellular ʟ-arginine. The intestinal-renal axis pathway begins within intestinal enterocytes, where the amino acids coming from dietary intake (such as glutamine, proline and glutamate) are converted into ʟ-citrulline, that is next transferred to the hepatic portal circulation. From there, it circulates to the systemic circulation to finally reach the kidneys, where it is converted to the ʟ-arginine and released back to circulation. This conversion is possible due to the expression of two pivotal enzymes of the cytosolic urea cycle: argininosuccinate synthase 1 (ASS-1) and argininosuccinate lyase (ASL) [89]. The second pathway termed as ʟ-citrulline-NO cycle occurs in the immune cells and manages the intracellular pool of ʟ-arginine. It evolved to maintain the constant production of NO that is involved in host defense against different pathogens such as

bacteria, parasites and fungi [90]. In this cycle ι-arginine is again synthesized from citrulline in a two-step reaction by ASS and ASL enzymes via the intermediate ι-argininosuccinate, to be next converted into NO by the inducible nitric oxide synthase (iNOS). Apart from the NO, the by-product of the iNOS enzymatic reaction is again citrulline that closes the cycle [91]. It is worth mentioning that iNOS belongs to a family of enzymes existing in three different isoforms that differ in tissue and cellular distribution. iNOS, also known as NOS2, has the highest enzymatic activity and is the most prevalent type in immune cells, including various types of myeloid cells such as macrophages and MDSCs. Besides, NOS1 is found in neuronal tissue, whereas NOS3 is located in endothelial cells [92]. Aside from immune cells, intracellular ι-arginine can be synthesized in most types of cells via the urea cycle enzymes. An additional ι-arginine pool might come from the degradation of intracellular proteins. In mammalian cells, ι-arginine can be further metabolized by four distinct enzymes: ARG, NOS, ι-arginine:glycine amidinotransferase (AGAT), and ι-arginine decarboxylase (ADC) [93]. ι-arginine catabolizing enzymes and their metabolic products are presented in Figure 3. The reaction catalyzed by ARG produces ι-ornithine and urea, mediated by NOS generates ι-citrulline and NO. L-Ornithine constitutes the precursor for proline, which is mandatory for collagen production. Enzymatic conversion by AGAT incorporates glycine and creates ι-ornithine and guanidinoacetate that further leads to the synthesis of creatinine. ADC catalyzed reaction generates agmatine - a precursor for the biosynthesis of polyamines that are necessary to sustain the rapid turnover of the proliferating cells [89, 94]. Additionally, some bacteria including mycoplasma express another enzyme able to convert the ι-arginine: arginine deiminase (ADI), that generates L-citrulline and ammonia [95].
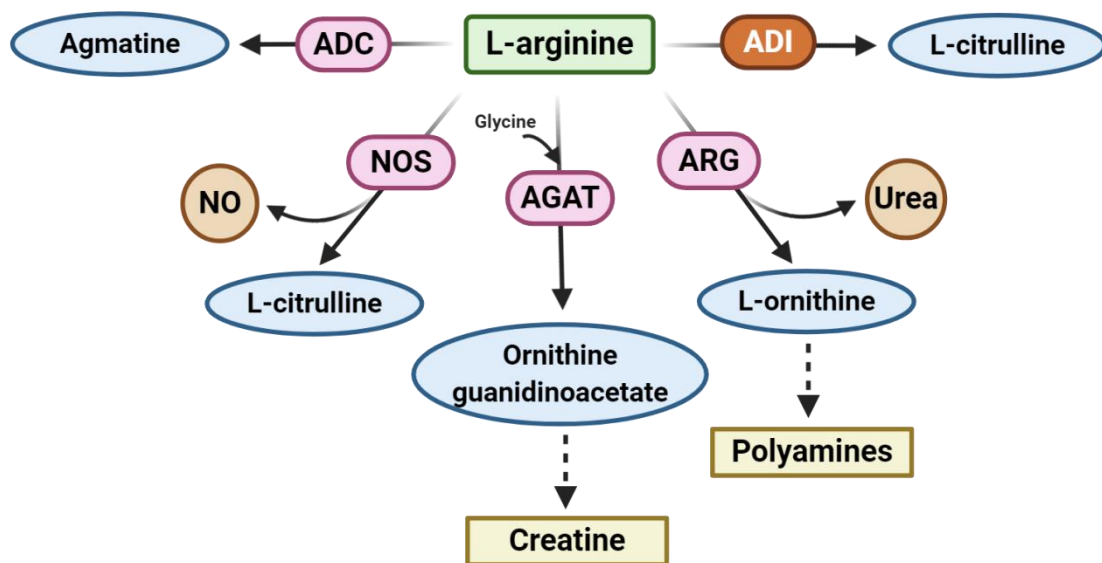
Figure 3. ɩ-arginine catabolizing enzymes and their metabolic products. ADC - arginine decarboxylase; NOS - nitric oxide synthase; AGAT - arginine:glycine amidinotransferase; ARG – arginase; ADI - arginine deiminase, NO – nitric oxide

Degradation of ɩ-arginine by ARG and iNOS enzymes play an essential role in immune cells. Since both enzymes share the same substrate, their activity needs to be balanced. Higher activity of ARG negatively regulates iNOS enzymatic activity by limiting the availability of ɩ-arginine. The kinetic profile of each enzyme needs to be considered once the expression is triggered at the same rate. iNOS has a much higher affinity for the substrate but catalyzes the reaction much slower. Consequently, ɩ-arginine can be depleted approximately at the same rate by both enzymes. ARG functions as a regulator of NO production via regulation of ɩ-arginine supply, and therefore it affects the production of reactive oxygen and nitrogen species [96]. The expression of both enzymes is also controlled by immune mediators – cytokines produced by Th lymphocytes. Th1 cytokines, such as IFN-γ and TNF-α, induce iNOS but inhibit ARG1, whereas Th2 cytokines, such as IL-4, IL-10 and IL-13, have the opposite effect [97, 98]. The influence of Th1 and Th2 cytokines on ɩ-arginine metabolism is presented in Figure 4. Coordinated expression of all ɩ-arginine degrading enzymes plays a crucial role in maintaining the homeostasis and physiological functions of the cells within the body.
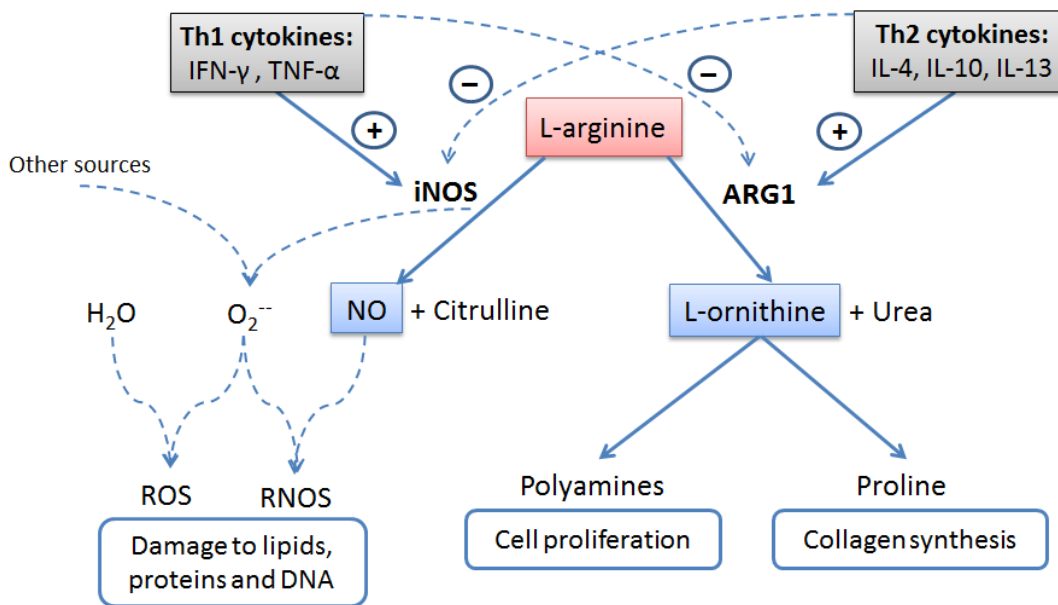
Figure 4. *The influence of Th1 and Th2 cytokines on ɪ-arginine metabolism. ARG1 - arginase-1; IFN-γ - interferon gamma; IL - interleukin; iNOS - inducible nitric oxide synthase; NO - nitric oxide, RNOS - reactive nitrogen-oxide species; ROS - reactive oxygen species; TNF-α - tumor necrosis factor alpha*

1.5 Role of the ɪ-arginine in the tumor microenvironment

In recent years it has been increasingly recognized that obstacles to successful immunotherapy result from the fact of existing immunosuppression mechanisms in the complex microenvironment of the tumor. Among others, one of the most prominent features of the tumor microenvironment that dysregulates the local adaptive immune response against cancer is amino-acid metabolism, most notably that involving ɪ-arginine and ʟ-tryptophan [99]. In the ɪ-arginine depleted conditions, T-cells residing at the neoplastic site commence metabolic competition with the tumor cells and other cells in the surrounding microenvironment for the nutrient needed to sustain the rapid cells proliferation. ɪ-arginine deficiency inhibits T-cells proliferation but is not associated with an elevated incidence of apoptosis. Moreover, the lack of ɪ-arginine also downregulates the expression of TCR-associated CD3ζ chain, a pivotal intracellular signal-transduction element of the TCR complex that is required to transmit the activation signals upon T-cell stimulation [100-102]. It is a clinically relevant mechanism observed in cancer patients – down-regulation of CD3ζ chain was

36

noticed in both CD4$^+$ and CD8$^+$ T-cells isolated from the tumor area as well as from the peripheral blood. Correlation analysis suggested that low or absent expression of the CD3ζ chain might be a reliable predictive factor for an unfavorable prognosis in cancer patients [103, 104]. T-cells cultured without ι-arginine are able to become activated, which was noticed by upregulation of the activation markers expression such as CD25 and CD69 [105]. Therefore, it was concluded that ι-arginine starvation must act on later stages than T-cells activation. Lack of ι-arginine halts the T-cell cycle progression by arresting the cells in the G_0-G_1 phase. The underlying mechanism indicates the inability to upregulate cyclin D3 and mRNA of cyclin-dependent kinase 4 that are necessary to pass through G_1 phase and progression into the subsequent S phase of the cell cycle [106]. Another proposed mechanism for the lymphocyte cell-cycle arrest includes signaling through general control non-depressible 2 (GCN2) kinase. Amino acid starvation causes activation of GCN2 kinase and subsequent phosphorylation of eukaryotic translation initiation factor (EIF2α) that inhibits protein synthesis [107]. Halting the proliferation of cytotoxic lymphocytes might result in much less efficient elimination of cancerous cells, thereby promoting tumor growth. Furthermore, it was shown that T-cells deprived of ι-arginine in culture medium produce lower amounts of IFN-γ that is a key mediator of an inflammatory and antitumor immune response [105]. IFN-γ-mediated mechanisms are responsible for the inhibition of cancer cells proliferation therefore, its reduced amounts result in weakened reactions against tumor [108]. In addition, T-cells with high ι-arginine concentration display better antitumor activity and enhanced survival [109].

1.6 Arginase (ARG)

ARGs constitute a highly conserved family of enzymes that hydrolyze the biochemical conversion of ι-arginine into ι-ornithine and urea. Two ARG isoenzymes can be distinguished: ARG1 and ARG2 that differ in structure, regulation and subcellular localization. ARG1 is localized in the cytoplasm of the cells, whereas ARG2 is a mitochondrial protein. Each of the isoforms is encoded by a separate gene located on distinct chromosomes. Still, they share more than 50% of amino acid residues,

including 100% homology in areas crucial for enzymatic activity. Therefore both enzymes catalyze the same biochemical reaction [110, 111]. Human ARG1 was cloned as the first isoenzyme in 1986, whereas human ARG2 was cloned 10 years later. Human ARG1 is 36 kDa protein built from 322 amino acids, while human ARG2 is approximately 38 kDa protein constructed from 354 amino acids [112, 113]. The chromosomal location of genes was mapped to chromosome 6 (q23) and 14 (q24.1-24.3) for ARG1 and ARG2, respectively [114, 115]. ARG1 is mainly expressed in the liver, where it participates in the detoxification of ammonia as one of the key enzymes of the urea cycle. The enzymes of the urea cycle are distributed between mitochondria and cytoplasm, however ARG1 acts as a cytosolic protein. Besides, ARG1 isoform is also present in red blood cells and some populations of immune cells such as macrophages, granulocytes and MDSCs. Expression of ARG2 is found in a variety of peripheral tissues across the human body. However, the most remarkable expression is found in kidneys. In addition, also brain, prostate, retina, small intestine and lactating mammary gland were established as ARG2 expressing tissues [79, 116]. Based on ARGs crystal structures evaluated in high-resolution, it was established that enzymes have a trimeric structure with identical subunits. The enzyme active site is located at the bottom of a cleft containing two manganese ions bridged by oxygens [117].

1.7 Role of the ARG in the tumor microenvironment

In the tumor microenvironment, ι-arginine deprivation by high ARG activity belongs to fundamental mechanisms of tumor escape from T-cells governed antitumor responses [118]. A high level of either ARG1 or ARG2 has been found in the blood of patients with hematologic malignancies such as acute myeloid leukemia [119] as well as in the tumor microenvironment of solid tumors including lung cancer [120], ovarian carcinoma [121], neuroblastoma [122], pancreatic cancer [123], breast cancer [124], renal carcinoma [125], hepatocellular carcinoma [126, 127], skin cancer [128], cervical cancer [129], colorectal cancer [130, 131], esophageal cancer [132], thyroid carcinoma [133] and head and neck cancer [134] among others. What becomes clinically relevant, upregulated ARG expression has been associated with poor clinical outcomes of patients with some type of cancers mentioned above [119, 121, 122, 125, 129, 130,

134]. In the tumor microenvironment and secondary lymphoid organs, the production of ARGs is mainly attributed to MDSCs and TAMs. Transport of the extracellular ʟ-arginine to the intracellular compartments is enabled by CATs. Thus, these integral membrane pumps found also on MDSCs and TAMs in tumor microenvironment deliver the substrate for degradation by ARG, contributing to reduced levels of environmental ʟ-arginine needed for T-cell functioning [135]. Mechanisms of MDSC-dependent suppression of T-cell function via ʟ-arginine metabolism is presented in Figure 5.
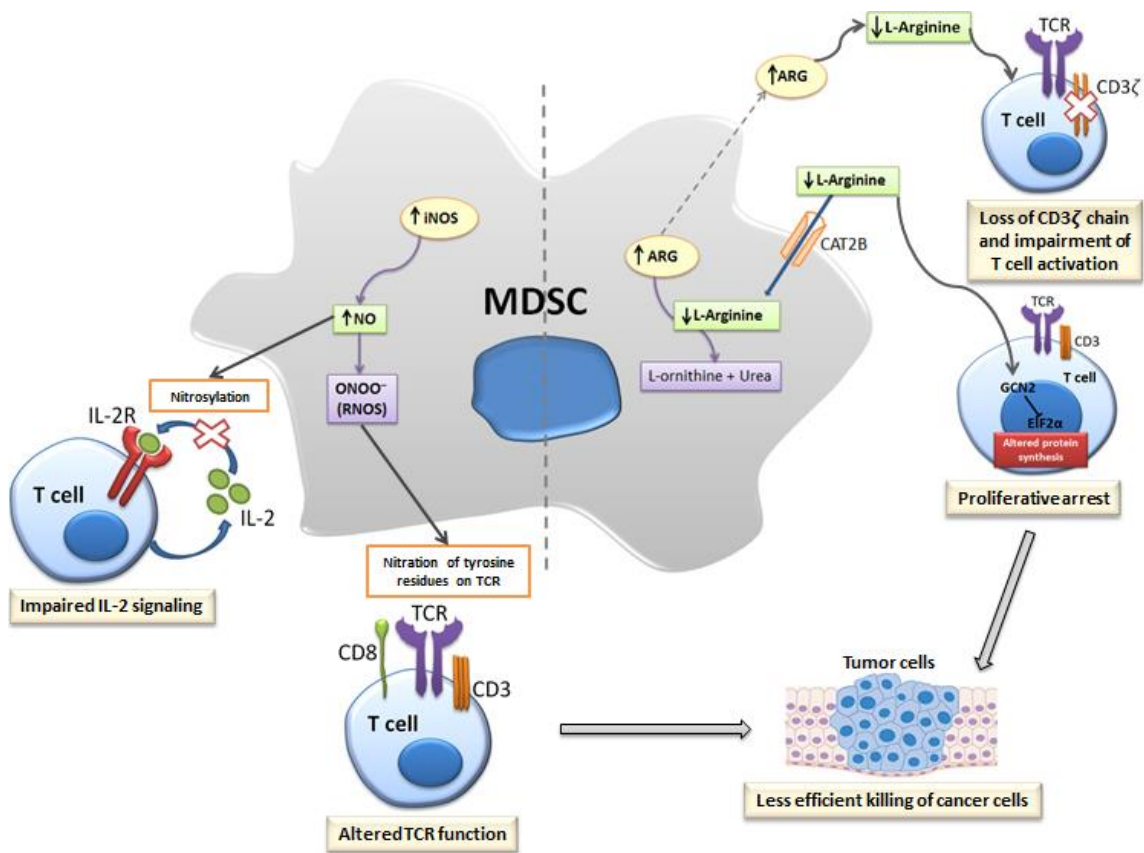
Figure 5. Mechanisms of MDSC-dependent suppression of T-cell function with a focus on ʟ-arginine metabolism. High ARG activity and subsequent ʟ-arginine downregulation in the tumor microenvironment result in proliferation arrest through GCN2 signaling and loss of CD3ζ chain of TCR. Tumor-associated MDSCs release oxidizing molecules, such as peroxynitrite (ONOO−) that cause nitration of components of the TCR signaling complex. iNOS produces NO that nitrosylates cysteine residues, which further interfere with IL-2R signaling pathway. All of these mechanisms influence the intracellular signaling pathways that control T-cell proliferation after antigen stimulation. ARG -arginase; CAT2 - cationic amino acid transporter 2 (ʟ-arginine

transporter); EIF2α - eukaryotic translation initiation factor 2α; GCN2 - general control non-depressible 2 kinase; IL - interleukin; IL-2R - IL-2 receptor; iNOS - inducible nitric oxide synthase; MDSCs - myeloid-derived suppressor cells; NO - nitric oxide; RNOS - reactive nitrogen-oxide species; TCR - T-cell receptor

In vivo depletion of ʟ-arginine via administration of ARG1 leads to the enhanced tumor growth that correlates with higher MDSCs numbers and block of T-cells response [136]. In another report, supplementation with ARG1 substrate (ʟ-arginine) partially inhibited the growth of breast cancer and prolonged survival of mice, which was associated with enhanced adaptive immunity and reduction of MDSCs [137]. The effects of ARG expression on polyclonal activation or cytokines secretion by T-cells have been documented, indicating that ARG negatively influences proliferation and production of T-cells secreted mediators [138, 139]. Furthermore, one report aimed at testing the influence of low ʟ-arginine concentration in the culture medium on antigen-specific cytotoxic T lymphocytes response. Interestingly, researchers found that the percentage of target cells lysis was slightly but insignificantly inhibited, however granzyme B levels and IFN-γ secretion were severely reduced [140]. It is known that the high enzymatic activity of ARG results in functional T-cells hyporesponsiveness due to ʟ-arginine depletion [141]. Therefore, all the mechanisms described above in the chapter 'Role of the ʟ-arginine in tumor microenvironment' that are switched on in the low ʟ-arginine concentration will also apply to elevated ARG expression. Apart from inside tumor and immune cells, an enzymatically active form of ARG1 can also be released in extracellular vesicles by some tumor cells such as ovarian carcinoma [121]. Also, MDSCs were shown to be able to secrete ARG1-containing exosomes that are nanometer-sized extracellular vesicles [142]. Importantly, ARG1 encapsulated by the lipid membrane of extracellular vesicles remains stable and can be transported on far distances from the local tumor site, for instance to the draining lymph nodes where it might further inhibit T-cell mediated responses [121]. This mechanism of distant immunosuppression utilizing extracellular vesicles is presented graphically in figure 6. As contrary to a vesicle-bound enzyme, locally secreted free form of ARG is much more unstable due to the short half time in circulation, which is approximately 30 min [143].
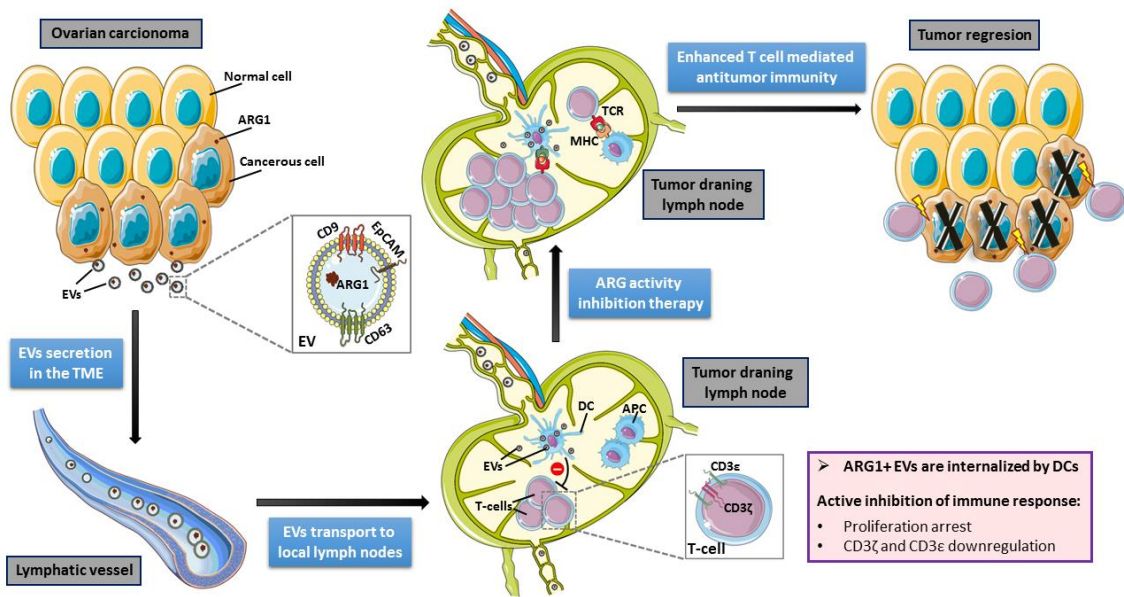
Figure 6. Suppression of T-cell mediated antitumor immune response by extracellular vesicles containing ARG1. Adapted from [144].

1.8 ι-arginine depletion therapy in ι-arginine auxotrophic tumors

ι-arginine is a critical amino acid within the tumor niche since its availability determines the proliferation ability of both immune and tumor cells. Therefore, it can be regarded as an immuno-nutrient and onco-nutrient as well. In terms of therapeutic approaches, both strategies undergo intensive experimental research [89]. Next to the inhibition strategy of ARGs in order to increase the availability of ι-arginine for T-cells, opposite therapy regards inhibition of tumor growth by ι-arginine deprivation. This therapeutic approach can be achieved by employing the engineered human recombinant enzymes that catabolize the ι-arginine. To the most popular enzymes belong human ARG and ADI that are currently being tested in multiple clinical trials [145, 146]. Based on basic research, it is known that bare ι-arginine degrading enzymes are very unstable and degrade within hours due to short half-time [143]. Therefore, a lot of effort was put into the enhancement of the enzyme stability and the most durable conditions were achieved by pegylation technology. The pegylated form of the enzyme is mainly obtained by attachment of polyethylene glycol (pegylation process) that enhances the bioavailability and reduces immunogenicity of the enzyme [147, 148]. It is important that this strategy does not apply to all the tumor types but is

relevant only in ʟ-arginine auxotrophic tumors that are reliant on extracellular ʟ-arginine supply, as a result of downregulation of ASS-1 or ornithine transcarbamylase (OTC) - key enzymes necessary for the intracellular ʟ-arginine recycling and synthesis. This translates into lack to ability of auxotrophic tumor cells for generation of own ʟ-arginine needed to sustain the intensive process of dysregulated cells proliferation. Consequently tumor cells are left as dependent on uptake of the extracellular amino acid found in the nearest microenvironment [149, 150]. The examples of ʟ-arginine auxotrophic tumors associated with loss of ASS-1 include: hepatocellular carcinoma, malignant melanoma mesothelioma, renal and prostate cancers [151]. The pegylated form of ARG, denominated as ADI-PEG20, has shown positive outcomes concerning the treatment of malignant melanomas and hepatocellular carcinoma. Therefore, it was approved many years ago, in 1999 by the FDA for a group of these oncologic patients [152]. Furthermore, intensive clinical trials evaluating the antineoplastic activity of a pegylated form of human recombinant ARG named BCT-100 are underway. So far, it has shown promising anticancer results in various malignancies including melanoma [153], hepatocellular carcinoma [154], leukemia [155, 156], small cell lung cancer [157] and malignant pleural mesothelioma [158]. ʟ-arginine degrading enzymes in the treatment of ʟ-arginine auxotrophic tumors are presented in Figure 7. The main mechanism by which pegylated ARG exerts the antitumor effect is the induction of apoptosis of cancer cells [159, 160]. Once non-malignant cells are deprived of ʟ-arginine, it leads to quiescence due to the arrest in the cell cycle at $G_0 - G_1$ phase. On the other hand, when malignant cells are exposed to lack of ʟ-arginine it does not necessarily stop the cell cycle but triggers dysregulated growth finally resulting in activation of apoptotic pathways [161]. Moreover, ʟ-arginine is not the only amino acid considered for tumor depletion strategy. High nutrients demands to satisfy the elevated energy requirements together with altered metabolism in tumor cells leads to development of auxotrophy for different nutrients [162]. Interests were also put into starvation of tumor cells deprived of ʟ-methionine, ʟ-glutamine among others [163, 164]. Promising results of clinical trials with pegylated form of ʟ-asparaginase lead to the first approval of such modified enzyme for cancer treatment. Escherichia

coli-derived L-asparaginase is indicated for treatment of paediatric and adult patients with acute lymphoblastic leukaemia [165].
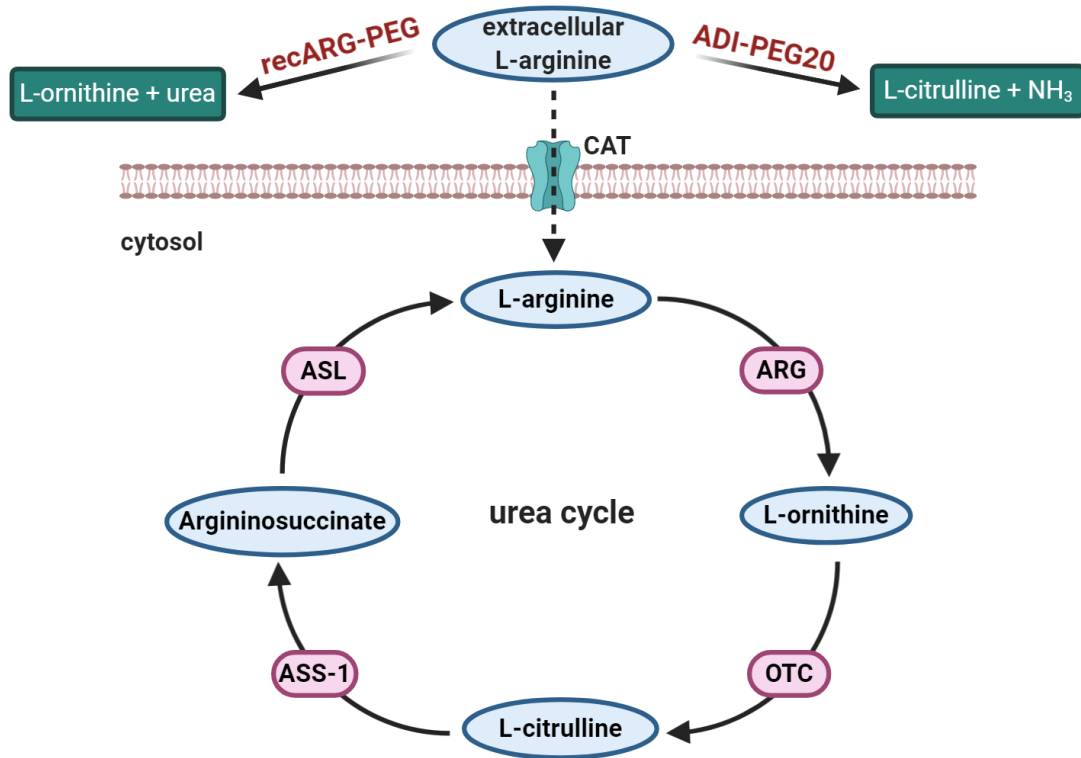
***Figure 7.** ι-arginine degrading enzymes in the treatment of ι-arginine auxotrophic tumors. ADI - arginine deiminase; ASL - argininosuccinate lyase; ASS - argininosuccinate synthase; ARG – arginase; CAT - cationic amino acid transporter; OTC - ornithine transcarbamylase; PEG - polyethylene glycol;*

To sum up, targeting ι-arginine in tumors lacking ASS-1 in most cases results in an anti-proliferative effect on auxotrophic tumors [143]. However, the drawback of this approach is that due to ι-arginine depletion it can render the immune system tumor-unresponsive. Therefore, a thin line can be drawn between the demand for ι-arginine by malignant and immune cells. As it is tumor-type dependent, thorough studies are needed to decide which of the above strategies would be the most effective in a specific tumor type. Indeed, one should be very careful in designing the therapies aiming at modulating the ι-arginine level and always remember about its dual role in the tumor microenvironment.

1.9 Immune checkpoints

Cancer cells utilize many mechanisms to escape from immune system surveillance. One of them is the alteration in expression and signaling of checkpoint molecules present on the major players of the immune system: T-cells. T-cells govern robust activity against cancer cells being able to eradicate transformed cells. On the other hand, the functionality of T-cells might be impaired by the engagement of immune checkpoint molecules such as PD-1 and CTLA-4 with their inhibiting ligands [166]. It is worth mentioning that in 2018 Tasuku Honjo and James P. Allison were awarded jointly with the Nobel Prize in Physiology or Medicine "for their discovery of cancer therapy by inhibition of negative immune regulation." On the way of his research career, Japanese immunologist Tasuku Honjo discovered a PD-1 protein on immune cells. In parallel, American immunologist James P. Allison studied the interaction of an already known protein CTLA-4. They both realized that these molecules function as the brakes of the immune system. Subsequently, they implemented the idea of blocking these T-cells brake molecules with antibodies that ultimately allowed to unleash the T-cells activity, giving spectacular results in animal studies. Later, pharmaceutical companies further developed this breakthrough into life-saving anticancer immunotherapy being applied in several types of cancer [167].

1.9.1 Programmed death protein 1 (PD-1)

PD-1 is an immunoglobulin superfamily protein found at a large quantity on the surface of the activated T-cell membrane that negatively regulates the T-cell function. The cytoplasmic part of PD-1 chain contains an immunoreceptor tyrosine-based inhibitory motif and an immunoreceptor tyrosine-based switch motif that transmit the inhibitory signal. The latter seems to be more decisive for mediating the suppression of lymphocyte activation [168]. First, PD-1 was identified as a protein that is up-regulated on the apoptotic T-cells, whereas later, it was assigned as the marker of exhausted T-cells [169]. PD-1 ligands belong to the B7-family and are represented by PD-L1 (B7-H1) and PD-L2 (B7-DC) molecules, which can be found on the tumor cell as well as on other cells present in the tumor microenvironment. PD-L1 is expressed constitutively, but at

low levels, however upon IFN-γ stimulation, its expression is induced in nearly all tissues. The expression of PD-L1 is characteristic for macrophages, among others. Particularly classically activated macrophages (representing M1 type) can significantly upregulate PD-L1 upon induction by Th1 cells [170]. Aside from tumor cells, PD-L2 is expressed on APCs such as dendritic cells and macrophages. It was shown that alternatively activated macrophages (representing M2 type) induced by IL-4 markedly upregulate PD-L2. PD-L2 has a 4-fold higher affinity for PD-1 than PD-L1 but is generally expressed at lower levels [171]. Interaction between PD-1 and their ligands negatively modulates the T-cell proliferation, production of cytokines as well as their cytotoxic activity [172]. Regarding autoimmune diseases, where the immune system is abnormally activated, this inhibitory process is of great importance in controlling the excessive reactions. In fact, mice deficient in PD-1 are prone to develop autoimmune disorders, indicating a peripheral tolerance defect [173, 174]. However in the context of cancer this mechanism leads to unfavorable effects especially by inhibiting T-cells present in the tumor microenvironment. In such circumstances the more activated T-cells the better response against developing tumor. It was shown that TILs have upregulated expression of PD-1 and PD-L1 in contrast to peripheral T-cells [175, 176]. In general, elevated expression of PD-1 or its ligands is linked with poor prognosis for cancer patients [177, 178]. Moreover, the prognostic value of a soluble PD-L1 was evaluated in unresectable pancreatic cancer, indicating that patients with low levels show better overall survival [179]. Furthermore, in a cohort of patients with esophageal cancers, cases with PD-L2 expression showed unfavorable survival prognosis compared to cases that were negative for PD-L2 [180]. It was also found that tumor-infiltrating T regulatory cells can upregulate PD-1 and play a role in suppressing the proliferation of CD8$^+$ T-cell through PD-1 and PD-L1 interactions [181]. Apart from PD-1, PD-L1 is also able to bind to costimulatory molecule CD80 expressed on T-cells, thus delivering another blocking signal [182].

1.9.2 Cytotoxic T lymphocyte-associated antigen 4 (CTLA-4)

CTLA-4 represents another key inhibitory molecule present on the T-cells. It transmits the negative signal to the interior of cells. It is constitutively expressed by T regulatory cells, but upon activation, it is upregulated by other subsets of T-cells, especially by CD4^{+} T-cells [183]. Especially, exhausted T-cells, both CD8^{+} and CD4^{+} highly express CTLA-4 [166]. Interestingly, CTLA-4 expression was also attributed to cancer cell lines derived from a diversity of human malignant solid tumors [184]. CTLA-4 binds to two known ligands: CD80 (B7.1) and CD86 (B7.2) molecules that are present on the surface of APCs [166]. Aside from binding to CTLA-4, these ligands play a crucial role in the standard activation pathway of a T-cell. During that process, TCR binds to the antigen that is presented by the MHC found on APCs. Simultaneously, the second obligatory event to fulfill the activation process is the interaction of CD28 protein found on T-cells with the mentioned before co-stimulatory molecules CD80 and CD86. CTLA-4 shares 30% homology with CD28 [185]. Therefore, the competitive binding of CTLA-4 to CD80 and CD86 impedes the interaction with CD28. These results in obstruction of the successful activation process of a T-cell. In addition, CTLA-4 has 40-100 times greater avidity for these ligands than CD28 as well as much higher affinity [186]. Moreover, it was shown that CTLA-4 is able to capture its ligand from the APCs via the process called trans-endocytosis. Subsequently, ligands are degraded inside the cell expressing CTLA-4, limiting the availability of costimulatory molecules for CD28 interaction [187]. The main role of CTLA-4 signaling is to extinguish the activation process, which occurs for instance at the end of every infection. However, in the context of cancer progression, up-regulated expression of a CTLA-4 on T-cells is not desired. Tumor antigens belong to so-called weak antigens, therefore elevated T-cell activation threshold by limitation of CD28 signaling via CTLA-4 generates reduced immune responses [166]. By using computational methods, it was estimated that increased CTLA-4 expression correlates with worse overall survival of patients with breast cancer [188]. The role of CTLA-4 expression was studied in mice with its specific deficiency in Foxp3^{+} CD4^{+} T-cells, revealing fatal systemic lymphoproliferative disorder [43].

Likewise, studies in humans indicated susceptibility for autoimmune diseases that were associated with CTLA-4 gene polymorphism [189].

1.10 Cancer immunotherapy

Cancer immunotherapy is the application of fundamental immunology knowledge in oncology clinics. Cancer immunotherapy exploits the idea of boosting the immune system so that it undertakes the naturally occurring efforts to eradicate the cancer cells. The immune system often lacks enough power to act fully and utilize its own potential in the fight against cancer. It might result from mechanisms developing in cancer, such as avoiding the host immune response. This strategy is termed as immune evasion and applies not only to tumors but also to pathogenic organisms that attack the body. Therefore, immunotherapy acts on the immune system directing the treatment to improve its potential maximally. Some cancer immunotherapy approaches use the very basic immunology expertise such as the fact of the presence of specific molecules on cancer cells like TAAs that can be targeted by the antigen-specific T-cells or antibodies. Others focus on removing the blockade, which is immunosuppression generated mostly in the tumor microenvironment. Generally, immunotherapy can be categorized into several main branches: cellular therapies, antibody therapies, cancer vaccines, immunomodulators and, previously famous but now not so popular, cytokine therapies [190, 191].

In the second half of the XX century, MacFarlane Burnet and Lewis Thomas proposed the cancer immunosurveillance hypothesis. They claimed that emerging cancer cells could induce the development of an effective immune response due to the presence of antigens specific for tumor [192, 193]. At that moment, the limited research tools and the lack of enough knowledge about the complexity of interactions of the immune system made it difficult to confirm this assumption fully. With the development of more specific methods including improved mouse models with immunodeficiency, it becomes possible to perform more profound studies. Finally, in 2001 Lloyd Old and Robert Schreiber experimentally proved the cancer immunosurveillance hypothesis to be correct. They studied the development of sarcoma tumors induced by chemical

carcinogen methylcholanthrene in immunocompetent mice in comparison with immunodeficient mice lacking recombination-activating gene-2 (RAG2) gene crucial for the proper development of lymphocytes [194]. They also confirmed the finding that the intact functionality of the immune system protects from cancer in another strain of mice lacking the signaling for IFN [195]. Studies of others provided evidence that untouched components of immune system defense such as perforin or NK and natural killer T (NKT) cells play a role in preventing cancer development [196, 197]. Perforin is a cytolytic protein stored in the granules of NK cells and cytotoxic T lymphocytes that is released upon activation of these cells and is involved in the process of killing of target cells [196].

1.10.1 Monoclonal antibodies against immune checkpoints

The discovery of immune checkpoint PD-1 and CTLA-4 and the subsequent development of their inhibitors, that is blocking monoclonal antibodies, has totally revolutionized cancer therapy. A considerable benefit of the immune checkpoint blockade strategy was that this treatment has the potential to be applied to a variety of cancer types not being limited to only one specific origin of cancer. Therefore, some hopes returned to patients that have failed standard treatment such as resection surgery, radiotherapy or chemotherapy. The scheme showing suppression elicited by immune checkpoint molecules and retrieval of activation by the application of monoclonal antibodies is presented in Figure 8.
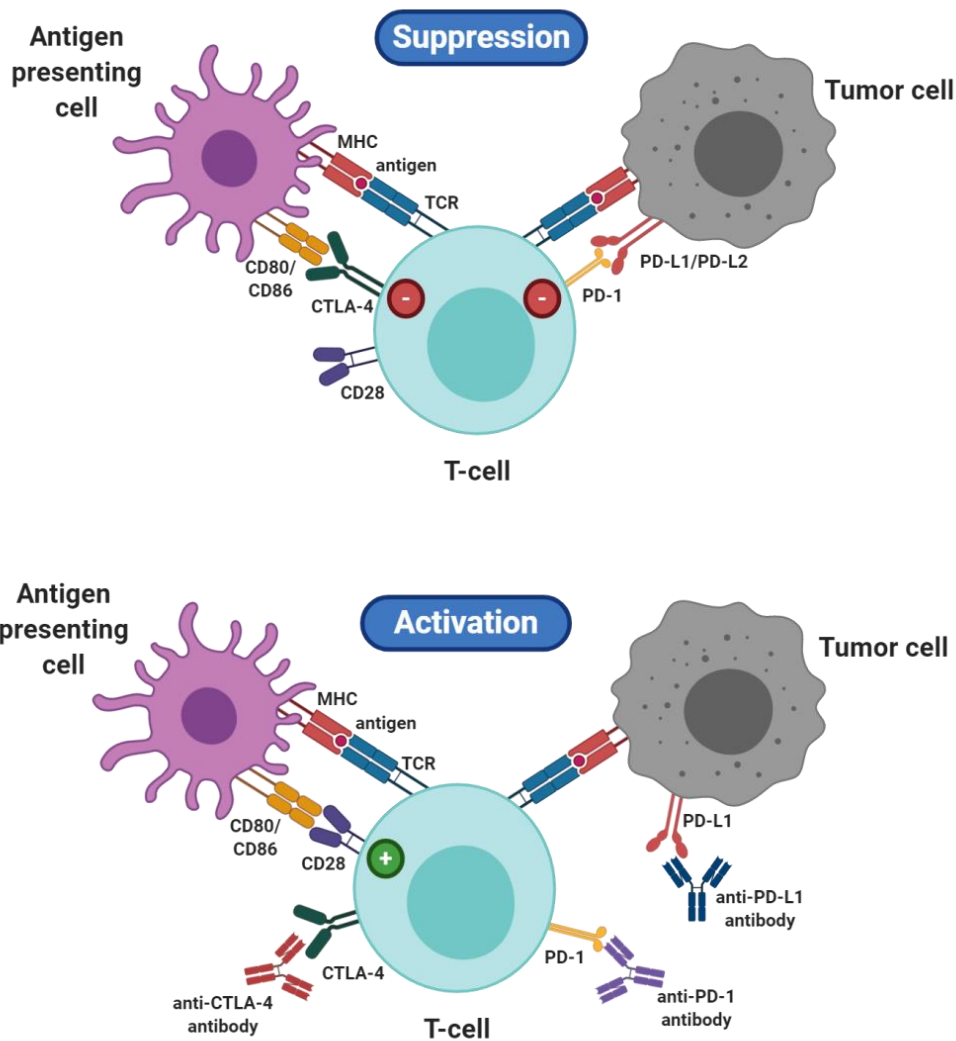
Figure 8. *Suppression elicited by immune checkpoint molecules and retrieval of activation by the application of monoclonal antibodies directed against immune checkpoint. MHC - major histocompatibility complex; TCR – T-cell receptor; CTLA-4 - cytotoxic T lymphocyte-associated protein 4; PD-1 - programmed death protein 1; PD-L1 - Programmed death-ligand 1*

The antibody against CTLA-4 called ipilimumab was the first in the class of immune checkpoint blockade immunotherapeutics that was approved by FDA. It was registered in 2011 to treat patients with advanced metastatic melanoma as clinical trials showed improved overall survival [198, 199]. This approval triggered great optimism for this group of patients that, together with the diagnosis, were informed about a miserable estimated prognosis based on previously available therapies. Later on, in 2014, fully

human IgG4 monoclonal antibodies against PD-1 named nivolumab were approved for by the FDA and registered to treat patients with inoperable or metastatic melanoma. Clinical studies revealed that nivolumab given as monotherapy prolongs survival in comparison with dacarbazine chemotherapy group in previously untreated melanoma patients with BRAF mutation, which is a typical aberration in this type of cancer [200]. Concurrent clinical trials summarized that the combination therapy of these two immunomodulatory agents (nivolumab plus ipilimumab) displays beneficial effects in melanoma than only ipilimumab monotherapy [201]. What is important, combinatorial therapy was concluded to have an acceptable and manageable safety profile [202]. Therefore, dual therapy was approved in 2015 by FDA for the therapy of melanoma without BRAF mutation [203]. Another humanized monoclonal antibody against PD-1 was registered in 2014 for melanoma clinical management. As developed by another company, it was named pembrolizumab and also represents IgG4 antibody class [204]. In the meantime, clinical studies evaluating nivolumab or pembrolizumab showed antitumor activity in patients suffering from advanced non–small-cell lung cancer, which resulted in the next registrations of these agents [205]. Consecutive years brought several subsequent approvals of the mentioned immune checkpoints in new medical conditions including renal cell carcinoma, Hodgkin lymphoma, urothelial carcinoma, head and neck squamous cell carcinoma, hepatocellular carcinoma, gastric and gastroesophageal carcinoma among others [203]. Furthermore, PD-L1 has become a target for blocking by newly designed monoclonal antibodies named atezolizumab, avelumab and durvalumab [206]. The summary of the immune checkpoint inhibitors approved by FDA for tumor treatment is shown in Table 1.

Table 1. *The summary of the immune checkpoint inhibitors approved by Food and Drug Administration (FDA) for tumor treatment (data are current as at 30/06/2020). Based on [203, 207].*

Year of FDA approval	Immune checkpoint target	Therapeutic agents	Medical indication
2011	CTLA-4	Ipilimumab	Melanoma
2014	PD-1	Nivolumab	Melanoma
2014	PD-1	Pembrolizumab	Melanoma
2015	PD-1	Nivolumab	Non–small cell lung cancer

2015	PD-1	Pembrolizumab	Non–small cell lung cancer
2015	CTLA-4 + PD-1	Ipilimumab + Nivolumab	Melanoma with BRAF wild-type
2015	CTLA-4	Ipilimumab	Melanoma (as adjuvant)
2015	PD-1	Nivolumab	Renal cell carcinoma
2016	PD-1	Nivolumab	Hodgkin lymphoma
2016	PD-L1	Atezolizumab	Urothelial carcinoma
2016	PD-1	Nivolumab	Head and neck squamous cell carcinoma
2016	PD-1	Pembrolizumab	Head and neck squamous cell carcinoma
2016	CTLA-4 + PD-1	Ipilimumab + Nivolumab	Melanoma (any BRAF status)
2016	PD-L1	Atezolizumab	Non–small cell lung cancer
2017	PD-1	Pembrolizumab	Hodgkin lymphoma
2017	PD-L1	Avelumab	Merkel cell carcinoma
2017	PD-L1	Avelumab	Urothelial carcinoma
2017	PD-L1	Durvalumab	Urothelial carcinoma
2017	PD-1	Nivolumab	Urothelial carcinoma
2017	PD-1	Pembrolizumab	Urothelial carcinoma
2017	PD-1	Pembrolizumab	Solid tumors of any histology: MSI-high or MMR-deficient
2017	PD-1	Nivolumab	Metastatic colorectal cancer: MSI-high, MMR-deficient
2017	CTLA-4	Ipilimumab	Pediatric melanoma
2017	PD-1	Nivolumab	Hepatocellular carcinoma
2017	PD-1	Pembrolizumab	Gastric and gastroesophageal carcinoma
2018	PD-L1	Durvalumab	Non–small cell lung cancer
2018	CTLA-4 + PD-1	Ipilimumab + Nivolumab	Renal cell carcinoma
2018	PD-1	Pembrolizumab	Cervical cancer
2018	PD-1	Pembrolizumab	Primary mediastinal large B-cell lymphoma
2018	CTLA-4 + PD-1	Ipilimumab + Nivolumab	Metastatic colorectal cancer: MSI-high, MMR-deficient
2018	PD-1	Nivolumab	Metastatic small cell lung cancer
2018	PD-1	Cemiplimab	Metastatic cutaneous squamous cell carcinoma
2018	PD-1	Pembrolizumab	Advanced, treatment-resistant hepatocellular carcinoma
2018	PD-1	Pembrolizumab	Merkel cell carcinoma
2019	PD-1	Pembrolizumab	Advanced melanoma (pre-surgical treatment)
2019	PD-L1	Atezolizumab	Triple-negative breast cancer
2019	PD-L1	Atezolizumab	Small cell lung cancer (extensive stage)
2019	PD-1	Pembrolizumab	Non-small cell lung cancer (stage III)
2019	PD-1	Pembrolizumab	Colorectal and uterine cancer
2019	PD-L1	Avelumab	Renal cell carcionoma
2019	PD-1	Pembrolizumab	Metastatic or unresectable recurrent head and neck squamous cell carcinoma
2019	PD-1	Pembrolizumab	Metastatic small cell lung cancer

2019	PD-1	Pembrolizumab	Esophageal cancer
2019	PD-1	Pembrolizumab	Endometrial cancer
2019	PD-L1	Atezolizumab	Metastatic nonsquamous non-small cell lung cancer
2020	PD-1	Pembrolizumab	Non-muscle invasive bladder cancer
2020	CTLA-4 + PD-1	Ipilimumab + Nivolumab	Hepatocellular carcinoma
2020	PD-L1	Durvalumab	Extensive-stage small cell lung cancer
2020	CTLA-4 + PD-1	Ipilimumab + Nivolumab	Metastatic non-small cell lung cancer PD-L1+ and no mutations in EGFR or ALK)
2020	PD-L1	Atezolizumab	Hepatocellular carcinoma
2020	PD-1	Nivolumab	Esophageal squamous cell carcinoma
2020	PD-1	Pembrolizumab	Unresectable or metastatic solid tumor with mutational burden
2020	PD-1	Pembrolizumab	Cutaneous squamous cell carcinoma
2020	PD-1	Pembrolizumab	Unresectable or metastatic colorectal cancer: MSI-high, MMR-deficient
2020	PD-L1	Avelumab	Advanced or metastatic urothelial carcinoma

Despite many promising outcomes across various types of cancers, the number of patients that fully benefit from this immunotherapeutic treatment is limited. Thus, the important issue is to find the criteria that will be helpful for the selection of a group of patients that would respond to implemented immune checkpoint inhibitor therapy. Researchers started to analyze the treated patients' samples as well as the tumor microenvironment in order to find the clues and identify the potential biomarkers that would be useful as selection criteria [208]. Generally, tumor microenvironment can be divided into three types based on the presence of immune cells: immunological desert, immunologically excluded and immune inflamed. The first type lacks the T-cells and there is no priming nor activation. In the second, a variety of mediators such as chemokines or vascular factors are present but there is no substantial T-cells accumulation. The third type represents the infiltration of all kinds of immune cells particularly including T-cells [209]. It is known that patients with immune inflamed tumors respond to immunotherapies at a higher rate than those that have not infiltrated tumors. Antibodies against immune checkpoint inhibitors act by removing the suppressive signaling and allow the T-cells to recover its functionality. Therefore, to unleash their antitumor potential, it is essential that treated tumors are reachable for T-cells to develop its activity [208]. Analysis of the tumor tissue infiltrations

requires invasive methods such as biopsy. On the other hand, studies revealed that simple, non-invasive methods like a collection of peripheral blood and analysis of absolute lymphocyte count might be suggestive for the response to therapy. It was confirmed as a predictive biomarker in a group of melanoma patients treated with ipilimumab. The subgroup of patients with an initially higher absolute lymphocyte count displayed better overall survival upon treatment [210]. Furthermore, levels of lactate dehydrogenase, absolute monocyte counts and absolute eosinophil counts emerged as other easily accessible prognostic biomarkers for ipilimumab treatment [211]. It was concluded that anti-PD-1 and anti-CTLA-4 treatment differs in the candidates for predictive biomarkers. For anti-PD-1 therapy - NK cells, whereas for anti-CTLA-4 - memory CD4^{+} and CD8^{+} T-cells were classified as relevant for obtaining better clinical response [212]. In addition to immune cells infiltrations and biomarkers found in the peripheral blood, genetic background and signatures comprise essential indicators of therapy responsiveness [213]. Importantly, pembrolizumab was approved in 2017 for the treatment of any solid tumor that is characterized as microsatellite instability-high or that is deficient in DNA mismatch repair [214]. Active mismatch repair mechanisms utilize enzymes that are crucial for identifying and repairing mismatched bases in the process of DNA replication as well as genetic recombination in both cancer and normal cells. Consequently, inactive genes, proteins dysfunction or defects in a process of mismatch repair may generate high microsatellite instability. This, in turn, might lead to the accumulation of a high load of mutations in genes related to cancer resulting in the expression of tumor-associated neoantigens. Neoantigens act stimulatory for triggering enhanced T-cells mediated immune response against malignant cells. Therefore, tumors with defective mismatch repair and/or high microsatellite instability are generally successfully treated with immune checkpoint inhibitors [214]. The leading type of cancer that is characterized by high genetic instability is colorectal cancer, therefore nivolumab was readily approved for its treatment in 2017 [215].

A relevant issue arises with the emerging adverse effects of the immunotherapy that blocks the inhibitory signaling in the T-cells. It results from the fact that PD-1 and CTLA-

4 molecules are involved in controlling autoimmune diseases and play an essential role in maintaining self-tolerance. As a consequence, negative side effects concern chiefly immune-related incidents. Their occurrence is frequent and diagnosed in even up to 90% of anti-CTLA-4 treated patients and in 70% of anti-PD-1 or PD-L1 treated patients [216]. Combinatorial therapy with antibodies blocking two types of molecules increases the incidence of immune-related adverse effects. It may include: colitis, rash, hepatitis, pneumonitis and endocrinopathies [217]. However, with the enlarged number of studied cases and broadening knowledge of the exact underlying mechanisms, side effects become predictable and their management is affordable [218].

1.10.2 ARG inhibitors

Over the years, several compounds exhibiting ARG inhibition activity have been developed. Immunosuppressive properties of MDSCs and TAMs present in the tumor microenvironment can be modulated by the use of ARGs inhibitors aiming at reducing the immunotherapy brakes and potentiating T-cell mediated antitumor immune response. This chapter focuses on outlining the existing ARG inhibitors, whereas their antitumor efficacy concerning *in vitro* and *in vivo* applications in a variety of cancer types is summarized in the discussion section.

The discoveries of ARG inhibitors reach the 1990s when the first inhibitor has been identified [219]. N-hydroxy-nor-L-arginine (nor-NOHA) [220], (S)-2-amino-6-boronohexanoic acid (ABH) [221] and (S)-(2-boronoethyl)-L-cysteine (BEC) [222] belongs the group of the first generation of synthesized ARG inhibitors. These three compounds represent reversible ARG inhibitors widely cited in the literature, but all of them possess very modest inhibition activity. Nonetheless, these compounds served over the years as the best inhibitors to study the pathways regulating ʟ-arginine metabolism across many science fields – not only oncoimmunology. ARG inhibition seems to be a reasonable approach in various pathogenic disorders such as hypertension, diabetes, asthma, erectile dysfunction, atherosclerosis and heart failure. Moreover, ARG inhibitors might be applied in the treatment of infectious diseases

since many pathogenic bacteria express ARG that aid them to survive in the host organism [81]. Nor-NOHA represents alpha-amino acid of ʟ-arginine and has a half-maximal inhibitory concentration (IC_{50}) value equal to 12±5 µM [223]. Despite nor-NOHA is one of the first synthesized compounds widely cited in the literature as the well-established ARG inhibitor until now, there is no clinical trial involving cancer patients [224]. It might be due to the fact that nor-NOHA has a very poor half-life (minutes after administration *in vivo*) and does not penetrate the plasma membrane, thus mostly inhibits extracellular ARG found in the tumor microenvironment [225]. ABH and BEC inhibitors represent boronic acid analogs of ʟ-arginine and their pharmacokinetic profiles and bioavailability are characterized as relatively poor [226]. Nevertheless, ABH at 200-400 µM was used to provide evidence that human embryonic stem cells express an active form of ARG enzyme [227]. Later on, ABH served for the chemists as the template to start with for the development of novel inhibitors with increased activity against target enzymes. Second generation inhibitors were improved by the addition of α,α-disubstituted amino acid substituents that provided the additional interactions for binding with the target protein [228]. Among synthesized compounds, the best properties were displayed by (R)‑2-amino-6-borono-2-(2-(piperidin-1-yl)ethyl)hexanoic acid abbreviated as compound 9 [229] and 2-amino-6-borono-2-(difluoromethyl)hexanoic acid known as FABH [230]. Compound 9 inhibits human ARG1 and ARG2 with IC_{50} of 223 nM and 509 nM, respectively [229]. Recently, the new set of modified ARG inhibitors were discovered comprising third generation represented by N‑substituted 3‑amino-4-(3-boronopropyl)pyrrolidine-3-carboxylic acids. Extraordinary binding and activity was attributed to N-2-amino-3-phenylpropyl substituent called NED-3238, that inhibits ARGs at a very low nanomolar IC_{50} values of 1.3 nM and 8.1 nM for ARG1 and ARG2, respectively [231]. In the meantime, there were trails to generate the irreversible inhibitors of ARGs that showed the potential in docking with active site of ARGs [232].

The most recently developed small-molecule inhibitor of both ARG1 and ARG2, a potential clinical drug candidate, was synthesized by OncoArendi Therapeutics, a Polish drug discovery company, and its denoted in literature as OAT-1746 [121] or on

posters presented during conferences as OATD-02 [233]. OAT-1746 has IC_{50} values equal 32 nM and 75 nM towards recombinant human ARG1 and recombinant human ARG2, respectively [234]. Another small-molecule ARG inhibitor is a compound named CB-1158 developed by Calithera Biosciences. CB-1158 inhibited both recombinant human ARG1 and recombinant human ARG2 with IC_{50} values of 86 ± 25 nM and 296 ± 5 nM, respectively. Yet, CB-1158 is the only ARG inhibitor that has been introduced into clinical studies in the immunooncology field [235]. Clinical trial inclusion criteria required patients with metastatic or locally advanced solid tumors of various origins. It is investigated as a single agent or in combination with immune checkpoint therapy such as anti-PD-1 or chemotherapy based on drugs including oxaliplatin, leucovorin, 5-fluorouracil, gemcitabine, cisplatin or paclitaxel. One clinical trial recruits patients suffering from refractory or relapsed multiple myeloma, where CB-1158 is going to be tested in combination with anti-CD38 antibody daratumumab (NCT03837509) [72]. A report from the first completed clinical trial (NCT03361228) in which CB-1158 was tested as a monotherapy in patients with microsatellite stable colorectal carcinoma concluded the increase in plasma ʟ-arginine in a dose-dependent manner. It summarized the disease control rate was equal to 27%. Combination therapy with PD-1 inhibitor pembrolizumab resulted in increased total intratumoral CD8^{+} T-cells whereas the six month progression free survival rate was 20% [236].

Apart from the compounds described above, there are other often naturally occurring molecules/compounds/substances displaying ARG inhibition activity, including a hydroxy derivative of ʟ-arginine: Nω-hydroxy-ʟ-arginine (NOHA), α-difluoromethylornithine (DMFO), ʟ-norvaline, ʟ-ornithine, ʟ-citrulline, ʟ-lysine. Their chemical structure and activity against ARG as the target has been well summarized in the exhaustive reviews of ARG inhibitors published in 2017-2018 [237-239]. N-hydroxy-L-arginine (NOHA) is a stable intermediate product formed during the biosynthesis of nitric oxide from ʟ-arginine and it has been shown to possess the ability to inhibit ARG [240]. DFMO targets ornithine decarboxylase - a key enzyme for polyamine synthesis and has been characterized as a putative but nonspecific ARG inhibitor [241]. ʟ-norvaline is an unbranched-chain amino acid isomer of valine and has been described

as an ARG inhibitor [242]. However, based on studies on human endothelial cells, it is known that ʟ-norvaline exhibits anti-inflammatory properties that are independent of inhibition of ARG [243]. Besides, ʟ-norvaline is a part of synthetized tripeptide, L-proline-m-bis (2-chloroethyl) amino-L-phenylalanyl-L-norvaline ethyl ester hydrochloride (abbreviated as MF13), that possess anticancer properties [244]. One old study points at the antitumor potential of irreversible extrahepatic ARG inhibitors (+)-S-2amino-5-iodoacetamidopentanoic acid (2-AIPA) and (+)-S-2-amino-6-iodoacetamidohexanoic acid (2-AIHA) that were tested in Balb/c mice inoculated with L5178Y lymphosarcoma cells [245]. A recent study shows that 6-gingerol may act as ARG inhibitor and play a role in exerting anticancer effects [246].

2. AIMS

- to investigate the effects of ARG1 expression or deficiency in the tumor microenvironment on *in vivo* tumor growth and the development of antitumor immune response

- to investigate the effects of recombinant ARGs and the treatment with ARG inhibitors on the *in vitro* T-cells proliferation, CD3 expression and cytokines production

- to compare the *in vitro* activity of ARG inhibitors in blocking the ARG1 and ARG2 associated with tumor cells

- to evaluate the antitumor efficacy and the mechanism of action of ARG inhibitors in *in vivo* lung cancer model

3. MATERIALS AND METHODS

3.1 Cell culture

Murine tumor cell lines Lewis Lung Carcinoma (LLC, CRL-1642™), melanoma B16F10 (CRL-6475™), lymphoma A20 (TIB-208™), breast cancer 4T1 (CRL-2539™) and human embryonic kidney cell line HEK293T (CRL-3216™) were obtained from American Type Culture Collection. Murine pancreatic cancer cell line PANC02 was purchased from Division of Cancer Treatment and Diagnosis, NCI, NIH Tumor Repository, whereas breast cancer cell line E0771 was purchased from CH3 Biosystems. Murine ovarian cancer cell line ID8 was kindly provided by Kathy Roby from the University of Kansas, whereas modified murine melanoma B16F10-ARG2 and human monocytic leukemia THP-1-ARG2 cell lines were kindly provided by Vincenzo Cerundolo from the University of Oxford. LLC, B16F10, B16F10-ARG2, PANC02, ID8, HEK293T and THP-1-ARG2 cell lines were cultured in Dulbecco's Modified Eagle's Medium (DMEM, Sigma-Aldrich). A20, 4T1 and E0771 cell lines were cultured in Roswell Park Memorial Institute (RPMI) medium (Gibco). Media were supplemented with heat-inactivated 10% (v/v) fetal bovine serum (FBS, Thermo Fisher Scientific) 2 mM ʟ-glutamine (Lonza), 100 U/ml penicillin and 100 µg/ml streptomycin (Lonza), and cells were cultured in cell culture incubator (NuAire) at 37°C in an atmosphere of 5% CO_2 in the air and 95% humidity. Cell lines have been cultured no longer than 3 weeks after thawing and were kept at the lowest possible passage. Cells were passaged according to the growth rate of the given line, usually every two or three days. Before passage adherent cells were washed with phosphate-buffered saline (PBS, Corning) without calcium and magnesium ions followed by the addition of a 0.25% trypsin-EDTA solution (Sigma-Aldrich). After incubation for a few minutes at 37°C, trypsin was inactivated with complete medium and the cells' suspension was transferred into conical tubes (Corning) and then centrifuged at 300 × g for 5 minutes at room temperature (RT). The supernatant from the centrifuged cells was aspirated with the vacuum system and the cells' pellet was re-suspended in an appropriate volume of medium, pipetted, and part of the suspension was transferred to culture bottles (Corning) containing a fresh portion of the medium. The remaining cells were used to conduct experiments. The viability of

tumor cells, assessed by trypan blue (Sigma-Aldrich) staining, was not less than 95%. Non-adherent cell line A20 was passaged by centrifugation with the same conditions as above followed by changing the medium for a fresh one. All tumor cell lines were regularly tested for *Mycoplasma* contamination using polymerase chain reaction (PCR) technique and were confirmed to be negative.

3.1.1 Counting and assessing cell viability

Cells were counted by automatic cell counter EVE™ (NanoEnTek) or by a microscopic technique using a Bürker camera (Heinz Herenz) and inverted microscope Axiovert 25 (Zeiss). At the same time, the cell viability was assessed after staining with 0.4% trypan blue solution. To this end, the cell suspension was mixed in a 1:1 or 1:10 ratio with trypan blue. Cells lacking cell membrane integrity absorb the dye and are visible under the microscope as blue while living cells remain unstained. Using the microscope, live cells were counted within 25 small squares (excluding cells lying on the left and bottom sides of the square). The obtained number was multiplied by the chamber factor ($\times 10^4$) and dilution ($\times 2$ or x10), thereby the number of cells in 1 ml of suspension was obtained.

3.1.2 Freezing, storage and thawing of cells

Cells were frozen in a 90% FBS solution with 10% dimethyl sulfoxide (DMSO, Sigma-Aldrich). The suspension of cells at a density of 1-5 $\times 10^6$/ml in FBS and DMSO was transferred to sterile cryotubes (Sarstedt), which were placed in a container with isopropanol allowing the cells to cool slowly at 1°C/minute. The container was then placed at -80°C. The next day, the cryotubes were transferred to liquid nitrogen containers. Cells were thawed by placing cryotubes removed from liquid nitrogen to a 37°C water bath (BioSan) with gentle mixing. Upon dissolution of the last ice crystals, the cell suspension was immediately transferred to a 15 ml tube, the culture medium was added and centrifuged at 300 $\times$ g for 5 minutes at RT. The supernatant was aspirated to remove DMSO and the cells were re-suspended in an appropriate medium and transferred to a culture flask.

3.2 Western blotting

Western blotting is a semi-quantitative molecular biology technique that allows assessing the amount of a specific protein in protein extracts. This method consists of several stages: electrophoretic separation of proteins in a polyacrylamide gel, transfer of separated proteins into a membrane, usually nitrocellulose, on which specific proteins are detected with specific primary antibodies. Then the primary antibodies are detected by secondary antibodies conjugated with reagents for their subsequent detection.

3.2.1 Preparation of protein lysates

To prepare protein extracts, cells were harvested from cell line culture and washed 3 times in refrigerated PBS by centrifugation at $500 \times$ g for 7 minutes, at 4°C. After the last centrifugation, the supernatant from the cell pellet was thoroughly removed, and the cells were suspended in 100-200 µl of Lysis buffer for Western Blotting (10% glycerol, 1% Triton X-100, 150 mM NaCl, 5 mM EDTA, 50 mM HEPES, pH 7.4), depending on the type and number of cells lysed, with added protease inhibitors cocktail (Thermo Fisher Scientific). Samples were frozen at -80°C for at least 24 hours for better cells' disruption. Next, samples were thawed and incubated on ice for 30 minutes with occasional vortexing and centrifuged at $12,000 \times$ g for 10 minutes at 4°C to remove non-lysed cell fragments. After centrifugation, the protein lysates were transferred to new eppendorf tubes (Corning).

3.2.2 Measurement of protein concentration

Protein concentration in the obtained lysates was measured using the Pierce BCA Protein Assay Kit (Thermo Fisher Scientific). The measurement was carried out in a 96-well flat-bottomed plate (Corning). 10 µl of a 10-fold diluted protein lysate was added to each well. The protein concentration was measured for each sample tested in three technical replicates. in parallel, a standard curve was prepared using a known concentration of albumin solution by serial dilution. 10 µl standard curve solutions were added to the appropriate wells. Then 200 µl of a solution resulting from mixing

Reagent A (containing sodium carbonate, sodium bicarbonate, dinquinic acid, sodium tartrate in 0.1 M sodium hydroxide) and Reagent B (containing 4% copper sulfate) in a ratio of 50:1 was added. The contents of the wells were mixed, then incubated for 30 minutes at 37°C and absorbance was measured using an Asys UVM 340 (Biochrom) spectrophotometer at $\lambda = 562$ nm.

3.2.3 Protein electrophoresis in polyacrylamide gel (SDS-PAGE)

For the electrophoresis of proteins in polyacrylamide gel, 20-30 µg of lysate was used and 5-fold concentrated sample buffer (62 mM Tris-HCl pH 6.8; 5% β-mercaptoethanol; 10% glycerol; 2.5% sodium dodecyl sulfate, SDS; 0.004% bromophenol blue) and water were mixed to give a final volume of 25 µl. Then the sample lysates were incubated for 5 minutes at 95°C. At this temperature, protein denaturation occurs and the presence of β-mercaptoethanol provides reducing conditions leading to the reduction of disulfide bridges. Moreover, SDS contained in the sample buffer gives the proteins the negative charge necessary for their electrophoretic separation. The prepared protein lysates were next applied to a polyacrylamide gel (Bio-Rad or self-made). For electrophoresis, 1.5 mm thick polyacrylamide gels containing 12% of polyacrylamide were prepared. Electrophoresis was carried out in electrophoretic apparatus (Bio-Rad) contacting running buffer (14.4 g Glycine, 3.0 g Tris, 1 g SDS, diH20 up to 1 L). The electrophoresis in the stacking gel was carried out at a voltage of 80-90 V (intensity <40 mA), while in the resolving gel the voltage was increased to 120-130 V (intensity <40 mA). Electrophoresis lasted until the proteins and prestained marker (Thermo Fisher Scientific) were fully resolved on the gel.

3.2.4 Transfer of proteins to the membrane

After electrophoretic separation, the proteins were transferred from the gel to the nitrocellulose membrane (Amersham) during the so-called semi-dry transfer, in which proteins with a negative charge migrate towards the anode. Before semi-dry transfer, the nitrocellulose membrane was soaked in the transfer buffer (192 mM glycine, 25 mM Tris, 10% methanol) and then was located between the polyacrylamide gel and

the anode. The semi-dry transfer was carried out in Trans Blot apparatus (Bio-Rad) for 30 minutes at 25 V constant conditions.

3.2.5. Protein detection on nitrocellulose membrane

After the transfer, the nitrocellulose membrane was stained with Ponceau S Staining Solution (Fluka) - a dye that binds non-specifically to proteins, allowing to verify whether the transfer was carried out completely and without interference. The membrane was then washed in Tris Buffered Saline with Tween (TBST) buffer (50 mM Tris-HCl pH 7.4; 150 mM NaCl and 0.1% Tween 20) to remove Ponceau S Staining Solution. In the next step, the membrane was incubated for 1 hour with mixing in 5% non-fat dry milk solution dissolved in TBS. Incubation was carried out to block nonspecific antibody binding to the membrane. Then the excess milk solution was rinsed in TBST and the membrane was incubated overnight at 4°C with a solution of the primary antibody in an appropriate dilution (anti-ARG1 1:2000, GeneTex) in a TBST. After incubation, the membrane was washed 3 times in TBST, then incubated for 1 hour at RT with a solution of the appropriate secondary antibody (anti-rabbit, dilution 1:10,000, Jackson Immuno-Research), conjugated to horseradish peroxidase, recognizing the Fc fragment of the primary antibody. Finally, the membrane was washed 3 times in TBST. Signal detection for horseradish peroxidase was performed using two sets: SuperSignal West Femto Maximum Sensitivity Substrate (Thermo Fisher Scientific) with high sensitivity and SuperSignal West Pico Chemiluminescent Substrate (Thermo Fisher Scientific) with standard sensitivity. To this end, the reagents contained in the kit were mixed in a 1:1 ratio, applied to the membrane, incubated for 2 minutes, followed by chemiluminescence readout using a ChemiDoc Imaging System (Bio-Rad). To verify the equal protein loading housekeeping protein β-actin was detected. Briefly, the membrane was incubated for 15 minutes in stripping buffer (Thermo Fisher Scientific) followed by twice washing in TBST for 15 minutes and blocking for 1 hour with mixing. Next, the membrane was incubated with anti-β-actin–peroxidase antibody (Sigma-Aldrich) for 30 minutes, washed 3 times in TBST and chemiluminescence signal was again detected using a ChemiDoc Imaging System.

3.3 Arginase activity assay

Supernatants from tumor cell culture were collected and urea was depleted using a Amicon Ultra 10 kDa molecular weight cut-off filters (Merck Millipore)and twice centrifugation at 14,000 × g for 30 minutes. $1x10^6$ of tumor cells were lysed in 100 μl of lysis buffer (the same as in Western blotting) containing protease inhibitors. Enzymatic activity was measured using ARG Activity Assay Kit (Sigma-Aldrich) according to the manufacturer's instructions. Briefly, samples were loaded into flat-bottom 96-well plate (4 μl/well), representing the sample well and the sample blank well, and ultra-pure water was added to reach a final volume of 40 μl in each well. Together with samples, the plate was loaded with urea standard to plot the standard curve. 100 ng of recombinant human ARG1 (provided by OncoArendi Therapeutics) and ultra-pure water served as positive and negative controls, respectively. Next, 10 μl of 5X substrate buffer, composed of ι-arginine buffer and manganese solution, was added to the wells except from sample blank wells, and the plate was incubated for 2 hours at 37°C. Following the incubation, 200 μl of urea reagent, composed of mixed reagents A and B, as added to each well to stop the reaction. Finally, 10 μl of 5X substrate buffer was added to the sample blank wells to have the same reagents proportion as in the sample wells. After mixing, the plate was incubated for 60 minutes at RT. Finally, the absorbance, proportional to the amount of the produced urea, was measured at 430 nm using ASYS UVM 340 microplate reader (Biochrom). ARG activity in samples was determined based on urea accumulation calculated using a standard curve.

3.4 Generation of tumor cells stably expressing murine ARG1

LLC, B16F10 and ID8 cells stably expressing an increased amount of murine ARG1 (LLC-pLVX-ARG1 and B16F10-pLVX-ARG1, ID8-pLVX-ARG1) were generated using lentiviral transduction. Transduction is a method of permanently introducing genetic material into a cell using a viral vector. HEK293T cell lines were used to produce lentiviral particles. In the first stage, HEK293T cells were transfected with the calcium chloride

method. This method involves the simultaneous delivery of the following plasmids to the cells:

- a plasmid containing the gene encoding ARG1,

- a plasmid containing elements encoding capsid proteins - pMD2.G (Addgene)

- a plasmid containing genes encoding the structural and packaging elements of the virus and regulatory elements necessary for amplification of the virus genetic material – psPAX.2 (Addgene)

HEK293T cells were seeded on the day preceding transfection into a 10 cm diameter dish in $2.6×10^6$ cells in 10 ml DMEM medium with 10% FBS without the addition of antibiotics. Cells were cultured in an incubator for 24 hours. The next day, a plasmid mixture was prepared in an eppendorf tube:

- 8.6 μg of the psPAX.2 plasmid,

- 5.5 μg envelope plasmid pMD2.G,

- 8.6 μg plasmid coding ARG1 gene or 8.6 μg control plasmid pLVX-IRES-Puro

Then 55 μl $CaCl_2$ and 375 μl ultra-pure water were added. The mixture was added dropwise to 450 μl of HBS solution (280 mM NaCl, 10 mM KCl, 1.5 mM Na2HPO4, 12 mM glucose, 20 mM HEPES) placed in a tube with capacity 15 ml. During the addition of the mixture, the HBS solution was constantly mixed using a vortex. Then the mixture was immediately added dropwise to HEK293T cell plate. Cells were cultured for 16-18 hours in an incubator. The next day, medium was gently removed from the culture and 6 ml fresh DMEM medium was added, then the cells were cultured for another 30-34 hours. After this time, the medium from the cells was collected, transferred to 15 ml centrifuge tubes and centrifuged to remove HEK293T cell debris. The centrifuged supernatant from the HEK293T culture was passed through a 0.45 μm syringe filter (Minisart) and centrifuged overnight at 3000 × g at 4°C to concentrate the virus particles. The same day target tumor cells LLC or B16F10 or ID8 were seed at the number $0.1x10^6$ in 6 well plate in 1,5 ml of medium. After overnight centrifugation, the supernatant was carefully removed from the tube, leaving about 0.5-1 ml of concentrated virus particles at the bottom. Such concentrated virus suspension was added in a dropwise manner to the seeded LLC, B16F10 or ID8 target cells in a 6-well

plate and then cells were incubated for 24 hours. To enhance the transduction efficiency polybrene (Sigma-Aldrich) was added at the concentration of 8 µg/ml. Next, the medium was changed for the fresh one with no virus and transduced cell lines were selected with 4.5 µg/ml, 1.5 µg/ml, 2 µg/ml puromycin antibiotic (Sigma-Aldrich), respectively. Cells transduced with the empty pLVX-IRES-Puro plasmid served as control cell lines.

3.5 *In vitro* T-cells proliferation assay

Murine CD4$^+$ and CD8$^+$ T-cells were isolated from spleens of healthy 8-9-week-old C57BL/6 mice using EasySep™ Mouse CD4$^+$/CD8$^+$ T-Cell Isolation (STEMCELL Technologies) according to the manufacturer's instructions. Human CD4$^+$ and CD8$^+$ T-cells were negatively isolated from peripheral blood of healthy volunteers using EasySep™ Human CD4$^+$/CD8$^+$ T-Cell Isolation Kit (STEMCELL Technologies) according to the manufacturer's instructions. For T-cell proliferation assay, T-cells were labeled with CellTrace Violet (CTV, Thermo Fisher Scientific) or CellTrace Carboxyfluorescein Succinimidyl Ester (CFSE, Thermo Fisher Scientific) dye for 20 minutes at 37°C at a final concentration of 2.5 µM. CTV and CFSE dyes form stable complexes with the free amino residues of proteins, therefore the dye is retained inside the cells and does not leak even in a loss of cell membrane integrity. The labelled T-cells were plated in round-bottomed 96-well plates (0.2×10^6 cell/well) in RPMI medium with 10% (v/v) FBS (Thermo Fisher Scientific), 2 mM glutamine (Lonza), 1% (v/v) penicillin/streptomycin (Lonza), 1% (v/v) MEM non-essential amino acids solution (Sigma-Aldrich), 50 µM 2-Mercaptoethanol (Thermo Fisher Scientific) and 30 U/ml of recombinant human IL-2 2 (PeproTech). In selected experiments, instead of a regular medium and FBS, T-cells were cultured in ʟ-arginine-free RPMI SILAC medium SILAC (without ʟ-arginine, ʟ-glutamine, ʟ-lysine, Thermo Fisher Scientific) supplemented with 10% dialyzed FBS (Thermo Fisher Scientific), 273 µM ʟ-lysine (Sigma-Aldrich) and ʟ-arginine (Sigma-Aldrich) at various concentrations as indicated in the figures. To trigger proliferation, T-cells were stimulated with Dynabeads Mouse/Human T-Activator CD3/CD28 beads (Thermo Fisher Scientific) in a 1:1 ratio. Recombinant mouse ARG1 (provided by Vincenzo Cerundolo laboratory from the University of Oxford), recombinant human

ARG1 (provided by OncoArendi Therapeutics), recombinant mouse ARG2 (provided by Vincenzo Cerundolo laboratory from the University of Oxford), 1 mM ι-citrulline (Sigma-Aldrich), 15 μM or 150 μM ι-ornithine (Sigma-Aldrich), 15 μM or 150 μM urea (Sigma-Aldrich) and ARG inhibitors ABH or OAT-1617 or OAT-1746 (synthesized and provided by OncoArendi Therapeutics) were added as indicated in the figures. Murine T-cells were incubated for 3 days whereas human T-cells were incubated for 5 days at 37°C in 5% CO_2. Then, cells were harvested, stained with live/dead Zombie NIR dye (BioLegend) and corresponding anti-CD3 and anti-CD4/anti-CD8 (and in some experiments also with anti-IFN-γ and anti-TNF-α) antibodies and analyzed by flow cytometry (FACSCanto II or FACS Aria II, BD Biosciences). Antibodies used for the flow cytometric staining are summarized in Table 2. The gate for proliferating cells was set based on the unstimulated control. Percentages of proliferating cells were calculated using the FlowJo Software v10.6.1 (Tree Star).

Table 2. *Antibodies used for flow cytometry staining.*

Directed against	Antibody target	Antibody clone	Manufacturer
Mouse	ARG1	polyclonal	R&D Systems
Mouse	CD3ε	17A2	eBioscience
Mouse	CD3ε	145-2C11	Tonbo Biosciences
Mouse	CD3ζ	H146-968	Abcam
Mouse	CD4	GK1.5	eBioscience
Mouse	CD4	RM4-5	eBioscience
Mouse	CD8	53-6.7	eBioscience
Mouse	CD11b	M1/70	eBioscience
Mouse	CD45.2	104	eBioscience
Mouse	F4/80	BM8	eBioscience
Mouse	Ly6C	HK1.4	eBioscience
Mouse	Ly6G	1A8	BioLegend
Mouse	MHC class II	M5/114.15.2	eBioscience
Human	CD3ε	OKT3	eBioscience
Human	CD3ζ	6B10.2	eBioscience
Human	CD4	RPA-T4	eBioscience
Human	CD8	SK1	eBioscience
Human	IFN-γ	B27	BD Biosciences
Human	TNF-α	MAb11	BD Biosciences

3.6 Flow cytometry analysis

Flow cytometry is a method enabling multi-parametric cell assessment, associated with the determination of morphological features such as size or granularity, analysis of the amount of surface and intracellular proteins after labeling with appropriate monoclonal antibodies conjugated with fluorochromes. During cytometric analysis, cells are analyzed in suspension, passing one after the other due to the negative pressure generated in the hydraulic system, which sucks the cells individually. Passing the laser beam, the cell cause it to disperse and deflect, which provides information on the size and granularity of cell based on FSC and SSC detectors. In turn, the excitation of fluorochromes conjugated with monoclonal antibodies and fluorescent dyes by appropriate lasers enables the analysis by measuring the emission spectrum of the dye.

Tumors were disassociated mechanically by cutting into smaller pieces using scissors (Chirmed). The resulting material was digested enzymatically in a solution of RPMI medium containing type IV collagenase (600 U/per tumor, Sigma-Aldrich) and DNAse (400 U/per tumor, Sigma-Aldrich) for 1 hour at 37°C with simultaneous shaking. The samples were then mechanically homogenized using a tissue dissociation system gentleMACS (Miltenyi Biotec). To obtain a single cell suspension, the homogenate was passed through a 100 μm cell strainer (Corning) and diluted with PBS. The homogenate was centrifuged at $400 \times g$ for 5 minutes. When necessary, erythrocytes were lysed using red blood cell lysis buffer (155 mmol/L NH4Cl, 10 mmol/L NaH2CO3, and 0.1 mmol/L EDTA, pH 7.3) for 5 minutes on ice. For flow cytometric analysis of tumor cells from cell line culture, tumor cells were harvested and washed in PBS. For cell surface staining, cells were stained with Zombie Viability Kit according to manufacturer's instructions, blocked on ice with 5% normal rat serum (Sigma-Aldrich) in fluorescence-activated cell sorting (FACS) buffer (PBS; 1% BSA, 0.01% NaN3) and then incubated for 30 minutes on ice with appropriate fluorochrome-conjugated antibodies that are listed in the material section. When necessary, controls for background staining such as isotype control or FMO control were applied. After washing with FACS buffer, cells were immediately acquired. For intracellular staining (such as ARG1 or CD3ζ or

cytokines), membrane-stained cells were fixed using Fixation Buffer for 30 minutes at RT, followed by washing in Permeabilization Buffer, and staining with antibody diluted in Permeabilization Buffer for 30 minutes at RT (Intracellular Fixation & Permeabilization Buffer Set, eBioscience). When necessary, CountBright™ Absolute Counting Beads (Thermo Fisher Scientific) were used to calculate the absolute number of cells according to manufacturer instructions. Flow cytometry analysis was performed on FACSCanto II or FACS Aria II flow cytometers (BD Biosciences) operated by FACSDiva software. For data analysis Flow Jo v7.6.5 software (Tree Star) was applied.

3.7 Analysis of ʟ-arginine and ʟ-ornithine by mass spectrometry

Blood was collected into Microvette® tubes with lithium heparin (Sarstedt) by retro-orbital terminal bleeding from orbital venous sinus performed under terminal anesthesia (overdosed anesthetic mixture 2:2:1 (v/v) ketamine/xylazine/0.9% NaCl solution, Polypharm). Samples were centrifuged at $1000 \times g$ for 10 minutes, plasma was separated and kept frozen at - 20°C until analysis. Measurements of ʟ-arginine and ʟ-ornithine were performed as paid external service by ultra-performance liquid chromatography tandem mass spectrometry (UPLC-MS/MS) method on Waters Xevo TQ-S mass spectrometer equipped with Waters Acquity UPLC chromatograph (Waters).

3.8 *In vivo* experiments

All experiments were performed on female mice. 8- to 12-week-old *wild-type* (WT) C57BL/6 mice were obtained from the Animal House of the Polish Academy of Sciences, Medical Research Center (Warsaw, Poland). Transgenic mice C57BL/6-Tg(TcraTcrb) 1100Mjb/J (abbreviated as OT-I), B6.129S4-*Arg1*^{tm1Lky}/J (YARG), B6.Cg-Foxp3^{tm2Tch}/J (Foxp3-GFP), B6(Cg)-Rag2$^{tm1.1Cgn}$/J (RAG2 KO), C57BL/6-Arg1^{tm1Pmu}/J (ARG1flox), B6.129P2-Lyz2$^{tm1(cre)Ifo}$/J (Lyz2), B6.129-Gt(ROSA)26Sor$^{tm1(cre/ERT2)Tyj}$/J (ROSA) were purchased from The Jackson Laboratory. Animals were housed in controlled environmental conditions in specific-pathogen free (SPF) (transgenic mice) or non-SPF (WT mice) facility of the Medical University of Warsaw with water and food

provided ad libitum. The experiments were performed in accordance with the guidelines approved by the 2nd Local Ethics Committee of the Medical University of Warsaw (approval No. 68/2013), 1st Local Ethics Committee of the University of Warsaw (approval No. 193/2016, 289/2017 and 317/2017) and in accordance with the requirements of EU (Directive 2010/63/EU) and Polish (Dz. U. poz. 266/15.01.2015) legislation.

3.8.1 Inoculation of tumor cells

Immortalized tumor cell lines were thawed from cryovial, cultured, passaged once, again cultured and after next trypsinization were washed twice with PBS followed by centrifugation at $300 \times g$ for 5 minutes at RT. Then, cells in the appropriate number were suspended in PBS and placed on ice. Cell viability was assessed by blue trypan staining and account for at least 95%. Mice were anesthetized intramuscularly using a mixture of ketamine (87 mg/kg, Polypharm) and xylazine (13 mg/kg, Polypharm) diluted with saline to the appropriate volume (in a 2: 2: 1 ratio). Sedated mice were shaved around the injection site. Tumor cells were inoculated in 30 µl of PBS subcutaneously into the right thigh using a special tuberculin syringe with an inserted a 27-gauge needle (BD Biosciences). The number of injected tumor cells was as indicated in the description below each figure.

3.8.2 Tumor growth monitoring

Tumor growth was monitored in 2 (experiments using ABH) or 3 dimensions (all remaining experiments) using a digital caliper (Yato) starting from 6-8 days after tumor cells inoculation. Tumor volume was calculated according to the formula:

$$V \ (\text{mm}^3) = (\text{longer diameter}) \times (\text{shorter diameter})^2/2$$

$$\text{or}$$

$$V \ (\text{mm}^3) = \text{length} \times \text{width} \times \text{height} \times \pi/6$$

for 2 or 3 dimensions measured, respectively. Length measurement includes partially the healthy leg measurement, that was not subtracted from shown results of tumor volume.

3.8.3 Treatment schemes and drug doses

The day of tumor cell administration was designated as day 0. In experiments aiming at the evaluation of antitumor efficacy, ARG inhibitor OAT-1746 was administered twice daily by an intraperitoneal route at the dose of 20 mg/kg for the first 14 days, whereas control groups received PBS. In experiments using ABH, it was administered twice daily by oral gavage route at the dose of 100 mg/kg for the first 14 days, while the control group received PBS. In combinatorial therapies experiments, anti-PD-1 (RMP1-14, BioXCell) or rat IgG2a isotype control (2A3, BioXCell) antibodies were administered by an intraperitoneal route at the dose of 10 mg/kg on days: 6, 9, 12, 15, 18 and 21. 5,6-dimethylxanthenone-4-acetic acid (DMXAA, Selleckchem) was given by intratumoral injection at 0.5 µg/mouse when tumor volume reached approximately 100 mm^3 (day 8), whereas control groups received NaHCO$_3$ (DMXAA diluent). To induce ARG1 Total KO in ARGfloxROSA mice tamoxifen (Sigma-Aldrich) diluted in peanut oil (Sigma-Aldrich) was administered by oral gavage at the dose of 75 mg/kg per mouse on day 7 until day 11 (5 days total), whereas control groups received only peanut oil. For the survival evaluation experiment, humane endpoints were applied including criteria such as severe cachexia or any tumor diameter > 22mm. At the end of the experiment, mice were sacrificed and selected organs such as inguinal lymph nodes, spleens, blood and tumors were used for further analysis.

3.8.4 Generation of ARG1 Myeloid KO and ARG1 Total KO mice and genotyping

Transgenic mice with constitutive ARG1 Myeloid KO were created by crossing C57BL/6-Arg1^{tm1Pmu}/J (ARG1flox mice) with B6.129P2-Lyz2$^{tm1(cre)Ifo}$/J (Lyz2 mice). Transgenic mice with tamoxifen-inducible ARG1 Total KO were created by crossing C57BL/6-Arg1^{tm1Pmu}/J (ARG1flox mice) with B6.129-Gt(ROSA)26Sor$^{tm1(cre/ERT2)Tyj}$/J (ROSA mice). The remaining transgenic mice strains B6.129S4-*Arg1*^{tm1Lky}/J (YARG mice), C57BL/6-Tg(TcraTcrb) 1100Mjb/J (OT-I mice) and B6(Cg)-Rag2$^{tm1.1Cgn}$/J (RAG2 KO mice) were bred using homozygote × homozygote mating system. The progeny was genotyped using the tip end of tail material. DNA was isolated using DNeasy Blood & Tissue Kit (QIAGEN) according to the manufacturer's instructions. Subsequently, the purity and

concentration of isolated DNA were measured by NanoDrop 2000c spectrophotometer (Thermo Fisher Scientific). PCR reaction was set up using OneTaq® 2X Master Mix with Standard Buffer (New England Biolabs) and appropriate primers summarized in Table 3. PCR and agarose gel developing conditions were set according to genotyping protocols available on The Jackson Laboratory website. Bands were visualized using ChemiDoc Imaging System (Bio-Rad). Only mice confirmed to have the desired genotype (homozygotes) were used in the studies.

Table 3. Primers used for genotyping of transgenic mice strains.

F - Forward; R - Reverse; WT - wild-type; MUT - Mutant

Transgenic mice strain	Primers
C57BL/6-Arg1^{tm1Pmu}/J (ARG1flox mice)	TGC GAG TTC ATG ACT AAG GTT (oIMR9556 F) AAA GCT CAG GTG AAT CGG (oIMR9557 R)
B6.129P2-Lyz2^{tm1(cre)Ifo}/J (Lyz2 mice)	CCC AGA AAT GCC AGA TTA CG (oIMR3066 – MUT) CTT GGG CTG CCA GAA TTT CTC (oIMR3067 – COMMON) TTA CAG TCG GCC AGG CTG AC (oIMR3068 – WT)
B6.129-Gt(ROSA)26Sor^{tm1(cre/ERT2)Tyj}/J (ROSA mice)	CTG GCT TCT GAG GAC CG (21306 – WT F) CGT GAT CTG CAA CTC CAG TC (oIMR3621 – MUT F) CCG AAA ATC TGT GGG AAG TC (oIMR9021 – WT R) AGG CAA ATT TTG GTG TAC GG (oIMR9074 – MUT R)
C57BL/6-Tg(TcraTcrb) 1100Mjb/J (OT-I mice)	AAG GTG GAG AGA GAC AAA GGA TTC (oIMR0675 F) TTG AGA GCT GTC TCC (oIMR0676 R) Internal positive control - Tcra: CAA ATG TTG CTT GTC TGG TG (oIMR8744 F) GTC AGT CGA GTG CAC AGT TT (oIMR8745 R) AAG GTG GAG AGA GAC AAA GGA TTC (oIMR0675 F) TTG AGA GCT GTC TCC (oIMR0676 R) Internal positive control - Tcrb: CAA ATG TTG CTT GTC TGG TG (oIMR8744 F)

	GTC AGT CGA GTG CAC AGT TT (oIMR8745 R)
B6.129S4-*Arg1*^{tm1Lky}/J (YARG mice)	TGA GCA AAG ACC CCA ACG AGA AGC (12129) AGA GCA AGC ACC CCG TTT CTT CTC (12130) GCT GTG ATG CCC CAG ATG GTT TTC (12131)
B6(Cg)-Rag2^{tm1.1Cgn}/J (RAG2 KO mice)	ATC AAT GGT TCA CCC CTT TG 25602 – WT F TCA TGT GAA AGC AGT TCA GGA C 25603 – WT R CCG CCA TAT GCA TCC AAC 25604 – MUT F CAG CGC TCC TCC TGA TAC TC oIMR8330 – MUT R

3.8.5 *In vivo* T-cell proliferation assay

Ovalbumin (OVA)-derived peptide 257-264 SIINFEKL-specific CD8$^+$ T-cells were isolated from the spleen and lymph nodes of C57BL/6-Tg(TcraTcrb) 1100Mjb/J (OT-I mice), labeled with CTV (as described above) and freshly transferred into the lateral tail vein of host C57BL/6 mice at a cell number of 4-6×10^6 in 150 µl of PBS. The next day, after OT-I T-cells inoculation, host mice were challenged with 5 µg of full-length OVA protein (Sigma-Aldrich) injected subcutaneously in a total volume of 30 µl into the tumor area (experimental groups) or right thigh (positive control group). The negative control group did not receive OVA protein nor the tumor cells. In some experimental settings, 20 mg/kg of the ARG inhibitor OAT-1746 was administered intraperitoneally twice daily, starting from the day before OT-I T-cells transfer until the end of the experiment. On day 3 post OVA immunization, draining inguinal lymph nodes from OVA injection site were harvested, mashed through a 70 µm nylon strainer, and cells were stained with OVA peptide-specific MHC class I tetramers (MBL International) to detect OT-I CD8$^+$ T-cells, followed by anti-CD3 and anti-CD8 staining and samples were analyzed for proliferation by flow cytometry. The gate for proliferating cells was set based on the unstimulated negative control. The gating strategy of flow cytometric analysis is presented in Figure 9.
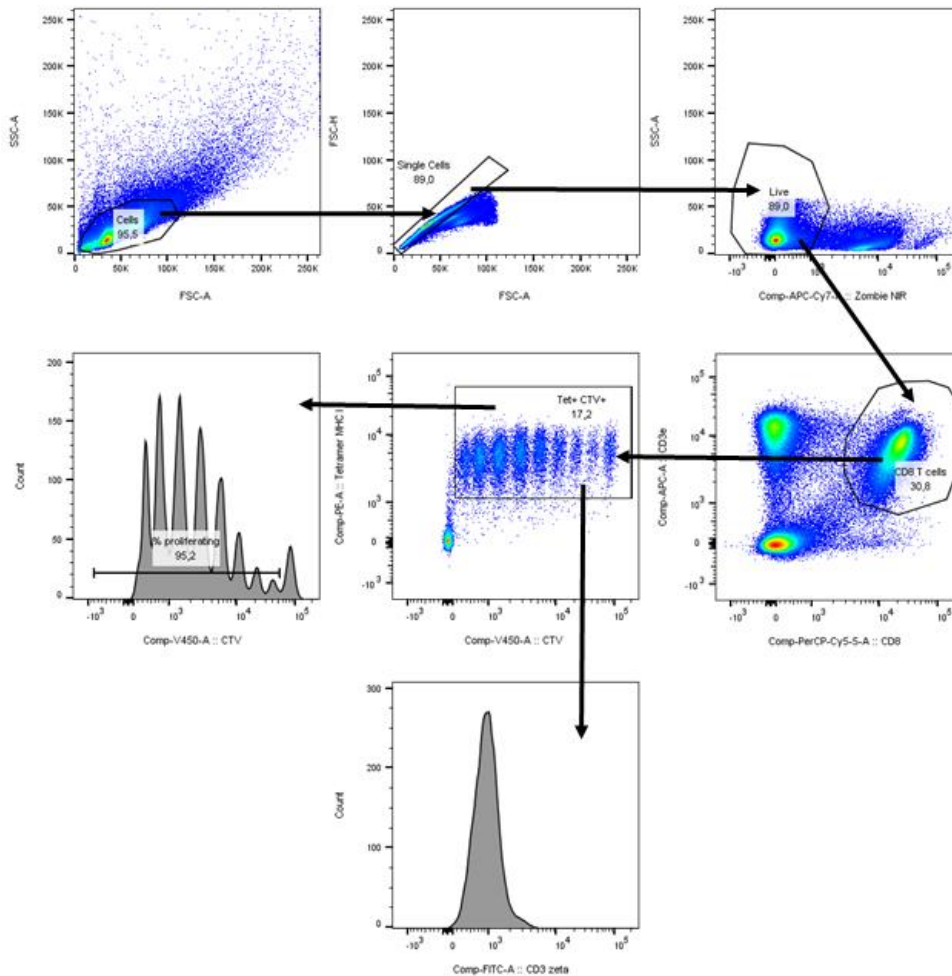
Figure 9. Gating strategy used for flow cytometric analysis of in vivo OT-I T-cells proliferation and CD3ζ expression on cells isolated from a tumor-draining inguinal lymph node.

3.9 Statistical analysis

Data are shown as means ± SD. GraphPad Prism 5 or 8.3.0 software (GraphPad Software) was used to calculate statistical analyses. The normality of data distribution was tested using the Shapiro-Wilk test. Statistical analyses of two groups were compared using unpaired *t*-test. Statistical analyses of three or more groups were compared using a one-way analysis of variance (ANOVA) followed by Tukey's multiple comparisons test. $P<0.05$ at 95% confidence interval was considered statistically significant. Statistically significant results were marked with asterisks depending on the p-value: * p <0.05, ** p <0.01, *** p <0.001. The survival rate of mice in *in vivo* experiments was computed using the Kaplan-Meier plot and comparisons between groups were analyzed using the log-rank test.

4. RESULTS

4.1 Evaluation of ARGs expression in the tumor microenvironment of murine lung cancer model

First, in order to study ARG1 positive cells in the progression of selected LLC lung cancer model, flow cytometry method and genetically engineered B6.129S4-Arg1$^{tm1Lky/J}$ mice called YARG were used. These mice express a yellow fluorescent protein (YFP), downstream of the endogenous stop codon of the *Arg1* gene, facilitating to track the cells with ARG1 expression in the tumor microenvironment. LLC tumor cells were inoculated subcutaneously and established tumors were measured in order to perform isolation at the different advancement stages. Tumors were isolated when they reached approximately 5, 10 or 15 mm in diameter and samples were analyzed by flow cytometry. In tumors of *wild-type* (WT) C57BL/6 mice there was no YFP signal, and cut off was set based on these histograms as the control. Gating used to identify ARG1^{+} cells is shown in Figure 10.
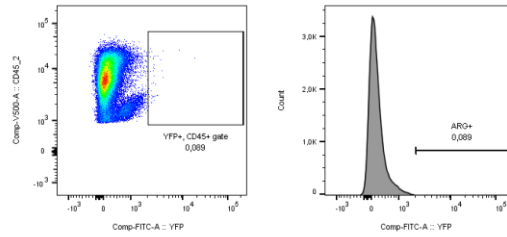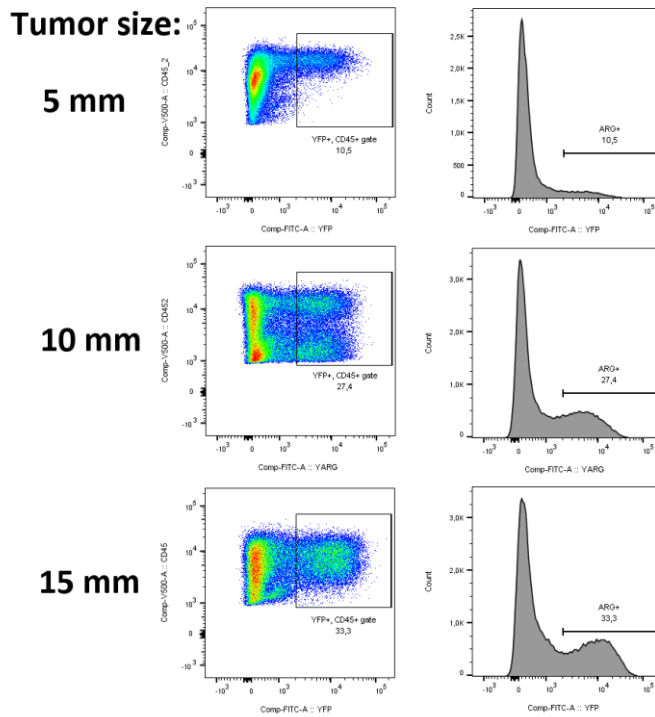
Figure 10. *Dot-plot graphs (left) and histograms (right) showing representative examples of gating for Yellow Fluorescence Protein (YFP) positive cells in control C56BL/6 and B6.129S4-Arg1[tm1Lky]/J (YARG) mice with LLC tumor at the different size. Gate is set on CD45$^+$ immune cells positive for YFP that reflects ARG1 expression in YARG mice.*

LLC is a type of tumor model which is highly infiltrated with immune cells (expressing CD45$^+$ marker) that consists of 74.8 ± 7.1%, 48.1 ± 2.7%, 53.6 ± 5.9% (mean ± standard deviation, SD) of the whole tumor microenvironment at the tumor size 5 mm, 10 mm and 15 mm in diameter, respectively (Figure 11). The gating strategy of tumor samples is presented in Figure 11.
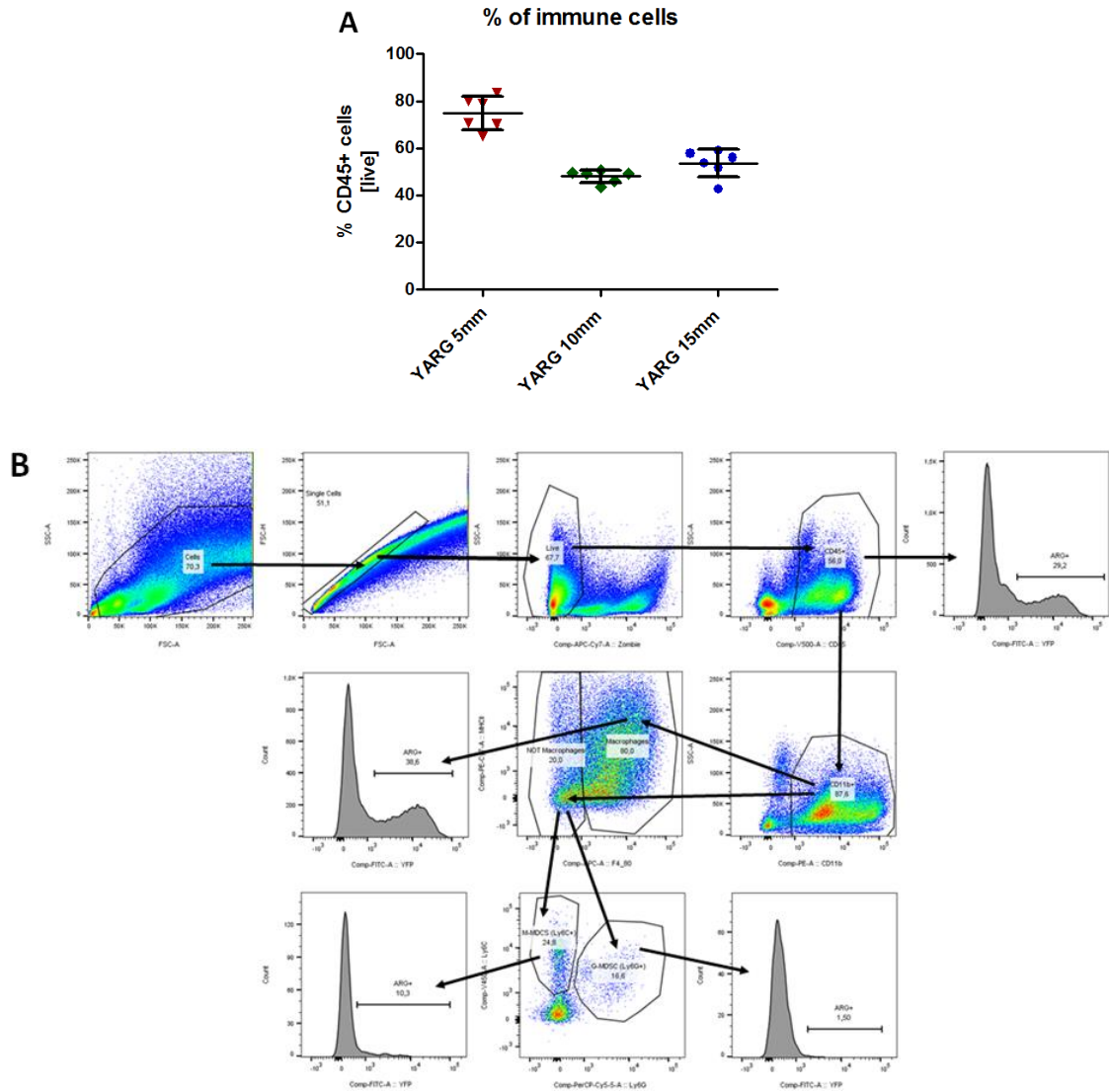
Figure 11. *Percentage of CD45+ immune cells in B6.129S4-Arg1tm1Lky/J (YARG) mice with LLC tumor at the different size 5 mm, 10 mm and 15 mm (A) and gating strategy used for flow cytometric analysis of tumor immune cells (CD45+), macrophages (F4/80+, CD11b+), M-MDSC (Ly6C+, CD11b+) and G-MDSC (Ly6G+, CD11b+) (B).*

Within this mentioned percentages of CD45+ immune cells, 10.9 ± 3.2%, 28.3± 8.1% and 28.4 ± 5.0% represent YFP+ ARG1 expressing cells, respectively (Figure 12). Furthermore, in order to reveal for which specific population of cells ARG1 expression is characteristic, detailed immunophenotyping of tumor microenvironment was performed using a wide panel of antibodies directed against markers that differentiate various subsets of cells. ARG1 expression was found in TAMs, M-MDSCs and G-MDSCs.

In case of TAMs, identified as CD11b$^+$ and F4/80$^+$ cells, ARG1 positivity and expression level were increasing proportionally to tumor growth. It was reflected as an increase in the percentage of ARG1 positive cells (0.7 ± 0.4%, 16.5 ± 5.1%, 27.2 ± 8.9% and 37.9 ± 5.7% for control C57BL/6, 5 mm, 10 mm and 15 mm tumors in YARG mice, respectively) as well as mean fluorescence intensity (MFI) of YFP within this population (1159 ± 278, 2016 ± 336, 3834 ± 1401 and 4843 ± 1059, respectively). In CD11b$^+$ and Ly6C$^+$ cells referred as M-MDSC, ARG1 expression was the most pronounced at 10 mm size-point (MFI = 846 ± 193 vs 510 ± 52 and 624 ± 81 at 5 mm and 15 mm, respectively), whereas percentages of ARG1 positive cells were equally increased at 10 mm (9.4 ± 3.7%) and 15 mm (9.5 ± 2.3%) as compared to 5 mm tumors (3.8 ± 2.0%). Considering G-MDSC identified as CD11b$^+$ and Ly6G$^+$ cells, some ARG1-positive cells were found at all stages, however overall ARG1 expression in this population (MFI = 948 ± 248, 756 ± 219 and 747 ± 127 at 5 mm, 10 mm and 15 mm tumors size-point in YARG mice, respectively) was not higher than in control group of mice (MFI = 941 ± 261). Altogether, in this experiment cells of the myeloid origin that express ARG1 enzyme and that can contribute to overall immunosuppression in the tumor microenvironment have been identified (Figure 12).
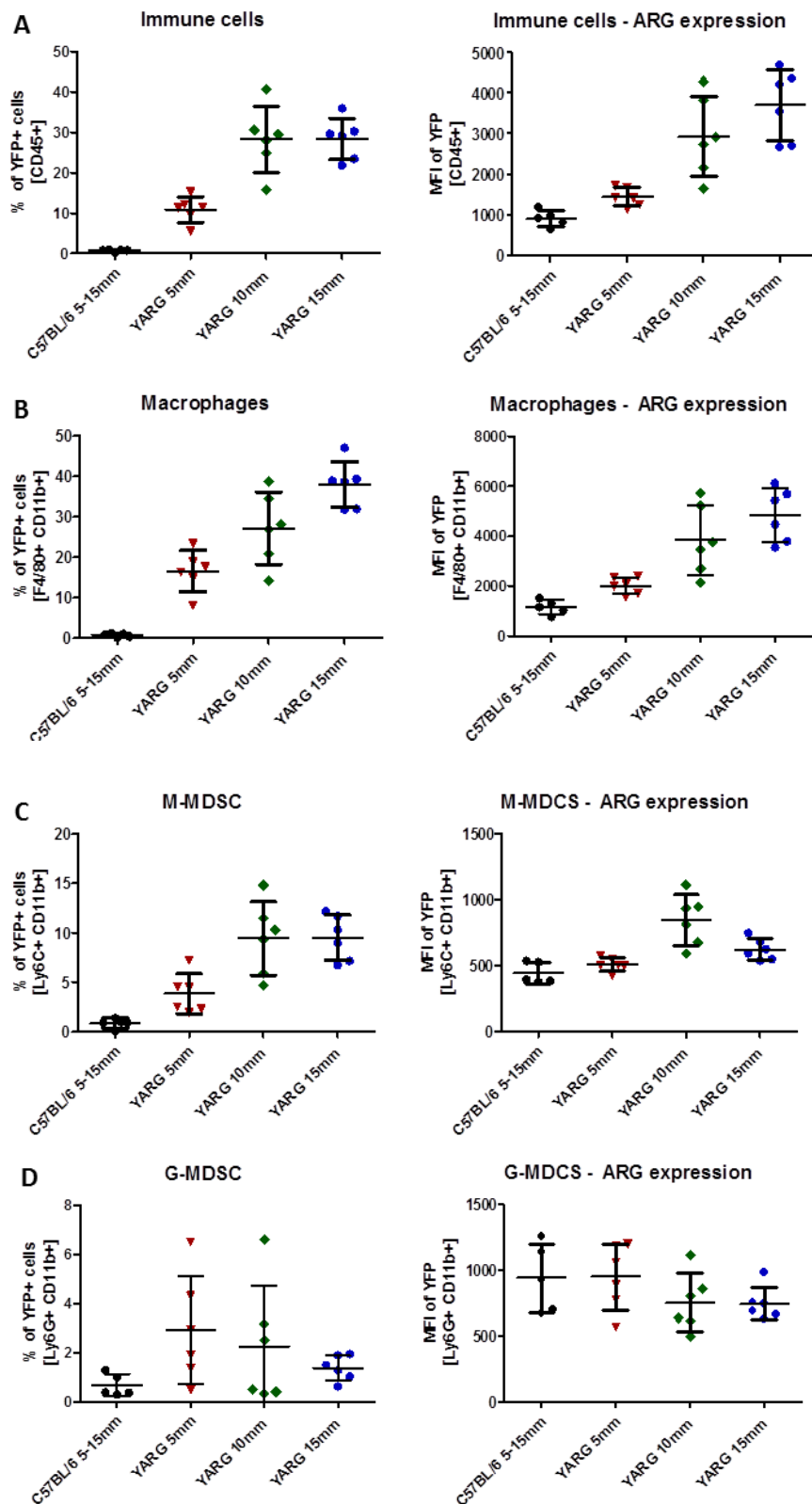
Figure 12. The percentages (right) of YFP⁺ cells representing ARG1⁺ cells and mean fluorescence intensity (MFI, left) of YFP shown within populations of (A) immune cells (CD45⁺), (B)

macrophages (F4/80^{+}, CD11b^{+}), (C) M-MDSC (Ly6C^{+}, CD11b^{+}), (D) G-MDSC (Ly6G^{+}, CD11b^{+}) infiltrating the tumors at different development stages. C57BL/6 or B6.129S4-Arg1[tm1Lky]/J (YARG) mice were inoculated subcutaneously with 1x10^{6} of LLC tumor cells and tumors were harvested when reached approximately 5, 10 or 15 mm in diameter. Tumor samples were digested, stained with antibodies and analyzed by flow cytometry. YARG mice groups consisted of n=6 mice per each size-point, whereas C57BL/6 mice group contained 5 mice. Data show means ± SD.

4.2 Evaluation of *in vivo* antigen-specific immune response in the progression of lung carcinoma model in normal mice

Next, it was questioned whether the increasing number of ARG1 expressing myeloid cells in the tumor microenvironment of LLC murine model might correlate with the proliferative potential of antigen-specific OT-I T-cells in the tumor-draining lymph node. To address this issue the proliferation was studied in C57BL/6 mice with tumors at the different progression stages. Tumors were inoculated subcutaneously at the distant time-points (on days 14, 7 and 0 of the experiment) in order to generate initial, intermediate and advanced tumors, respectively (Figure 13). Tumor measurements performed 20.5 days after inoculation confirmed distinct tumor volumes between groups (155 ± 43 mm^3, 849 ± 190 mm^3 and 2920 ± 269 mm^3 for initial, intermediate and advanced tumors, respectively). Flow cytometric analysis of tumor-draining lymph node revealed that proliferation of adoptively transferred OT-I T-cells was impaired in mice with advanced tumors ($63.58 \pm 21.43\%$ vs $89.53 \pm 5.49\%$, $p < 0.0001$ and $83.57 \pm 5.15\%$, $p = 0.0017$ in initial and intermediate tumors, respectively, one-way ANOVA with Tukey multiple comparison tests). Additionally, in comparison with initial and intermediate tumors groups, these mice had also decreased CD3ζ expression - a critical component that transmits an activation signal in T lymphocytes ($p = 0.0087$ and $p < 0.0001$, respectively, one-way ANOVA with Tukey multiple comparison tests). Importantly, these mice had also the lowest ι-arginine and the highest ι-ornithine plasma concentrations indicating high ARG activity (Figure 14). Collectively, these results suggest that the impaired proliferation of OT-I T-cells is dependent on ARG activity in the tumor microenvironment.
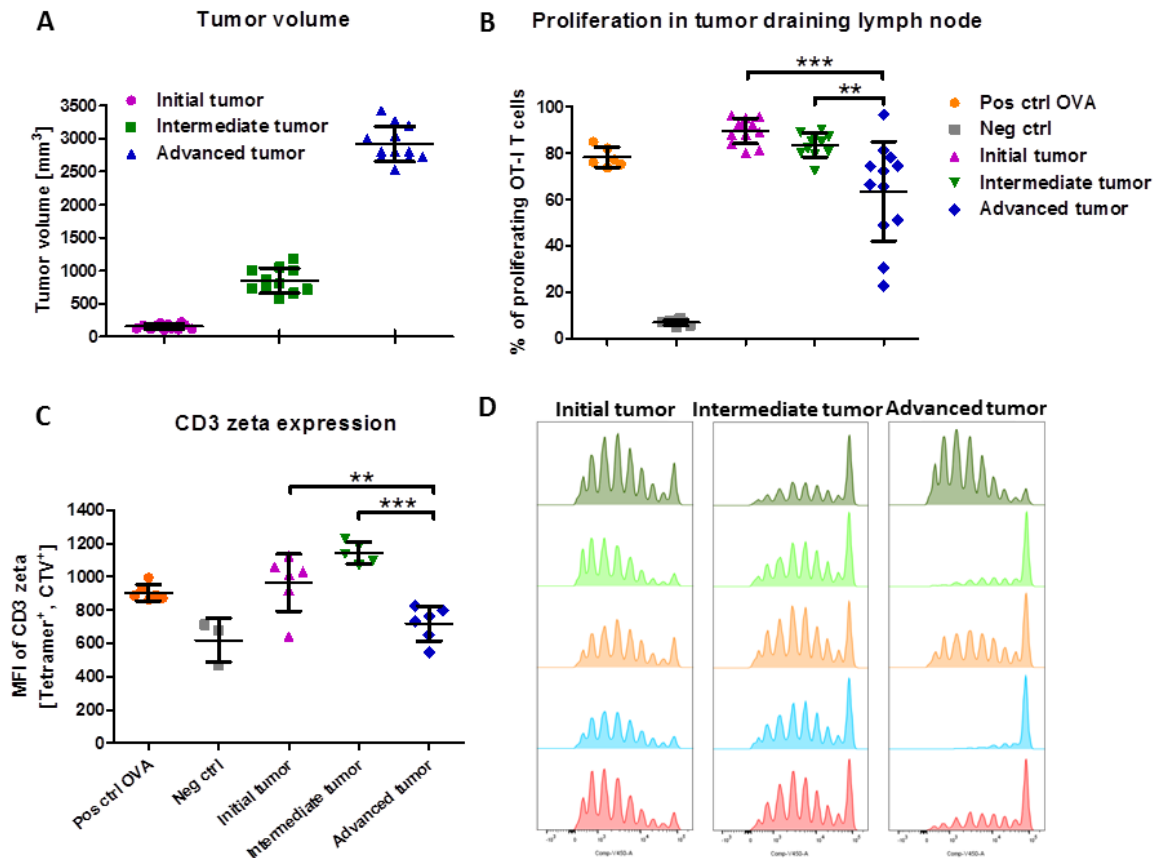
Figure 13. *The relation between increasing LLC tumor volume and the antigen-specific proliferation of OT-I T-cells and CD3ζ expression in mice. 0.5×10^6 of LLC tumor cells were inoculated subcutaneously into C57BL/6 mice on days 0, 7 and 14 of the experiment in order to generate advanced, intermediate and initial tumors, respectively (A). Isolated, CTV stained, OT-I CD8$^+$ lymphocytes were transferred intravenously on day 17. Antigen-specific proliferation was triggered with ovalbumin (OVA) protein injected subcutaneously in the tumor area on day 18. The proliferation of OT-I (B). Mean fluorescence intensity (MFI) of CD3ζ on OT-I T cells from tumor-draining lymph node evaluated by flow cytometry (C). Representative examples of OT-I proliferation histograms (D). Tumor volume and proliferation are shown as a cumulative graph from 2 independent experiments, whereas CD3ζ expression graph represents data from a single experiment. Data are presented as means ± SD. One-way ANOVA with Tukey post-hoc test was used to compare groups. **p≤0.01, ***p≤0.001.*
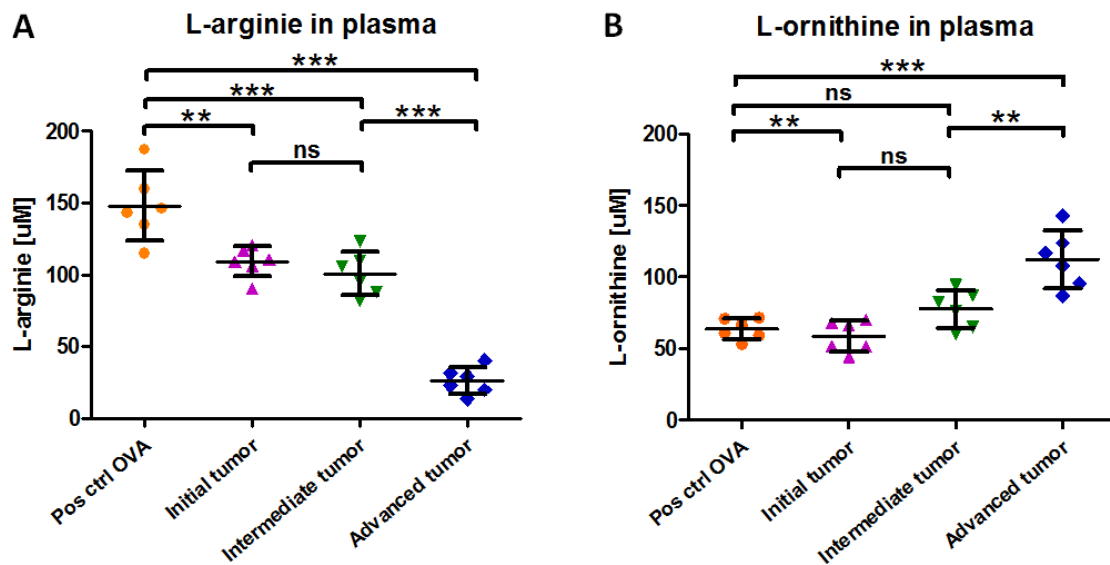
Figure 14. ʟ-arginine (A) and ʟ-ornithine (B) concentrations in plasma samples assessed by mass spectrometry. Each data point represents a mouse from 1 out of 2 experiments described in Figure 13. The positive control (Pos ctrl) group represents mice with no tumor but with ovalbumin (OVA) injected subcutaneously. Data are presented as means ± SD. One-way ANOVA with Tukey post-hoc test was used to compare groups. **$p \leq 0.01$, ***$p \leq 0.001$.

4.3 Evaluation of *in vivo* antigen-specific immune response in the progression of lung carcinoma model in ARG1 *knock-out* (KO) mice

4.3.1 Studies using ARG1 Myeloid KO mice

To further investigate the dependence between ARG1 expression and the local immune response in LLC tumor-bearing mice the transgenic mice models imitating ARG1 deficiency were utilized. To verify the hypothesis that the unfavourable effect is caused by ARG1 produced by myeloid cells in the tumor microenvironment, mice with ARG1 KO in myeloid lineage were exploited. The first observation was that tumor volume in these mice is reduced in comparison with control C57BL/6 mice (p = 0.0052, unpaired two-tailed t-test; Figure 15).
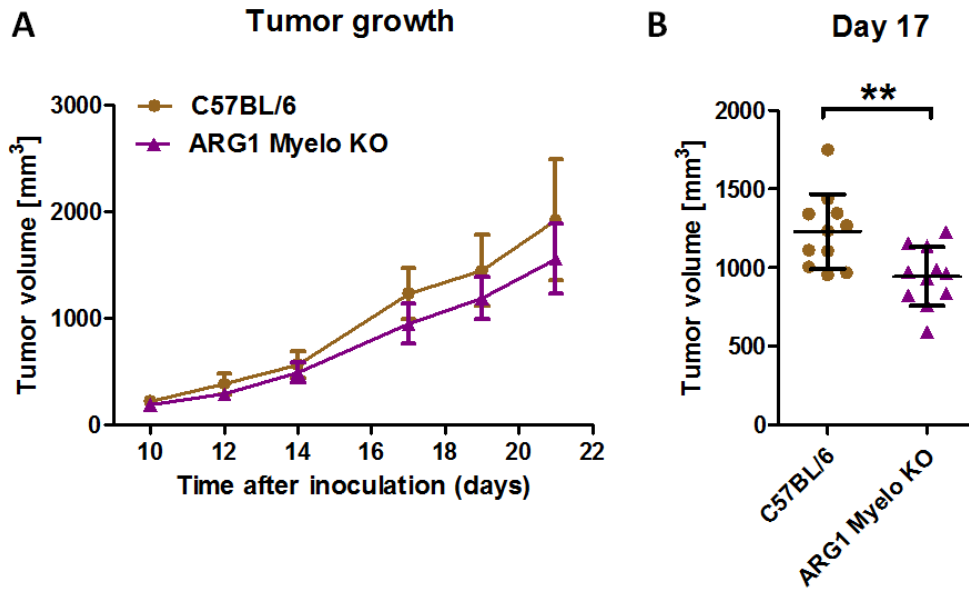
Figure 15. *Comparison of LLC tumor growth between control C57BL/6 and ARG1 Myeloid KO mice (C57BL/6-Arg1$^{tm1Pmu/J}$ × B6.129P2-Lyz2$^{tm1(cre)lfo/J}$). Both groups of mice received 0.5x10^6 of LLC tumor cells injected subcutaneously on day 0 and tumor volume was measured. Summary of linear tumor growth (A) and individual mice display of tumor volume on day 17 (B). Each experimental group consisted of 11 mice. Data show means ± SD. An unpaired two-tailed t-test was used to compare groups. **p≤0.01.*

Then, the antigen-specific proliferation of OT-I T-cells was studied in mice with advanced tumors showing that ARG1 KO in myeloid lineage protects mice against worsening the proliferation at late tumor progression stages. Furthermore, these results were supported by no changes like ʟ-arginine down-regulation and ʟ-ornithine up-regulation in plasma, in contrast to control C57BL/6 mice with advanced tumors, suggesting the lack of activity of ARG1 in myeloid cells in the tumor microenvironment of ARG KO mice (Figure 16). Collectively, these data suggest that high ARG1 activity in mice with advanced tumors might negatively affect the development of antigen-specific immune response in local secondary lymphoid organs.
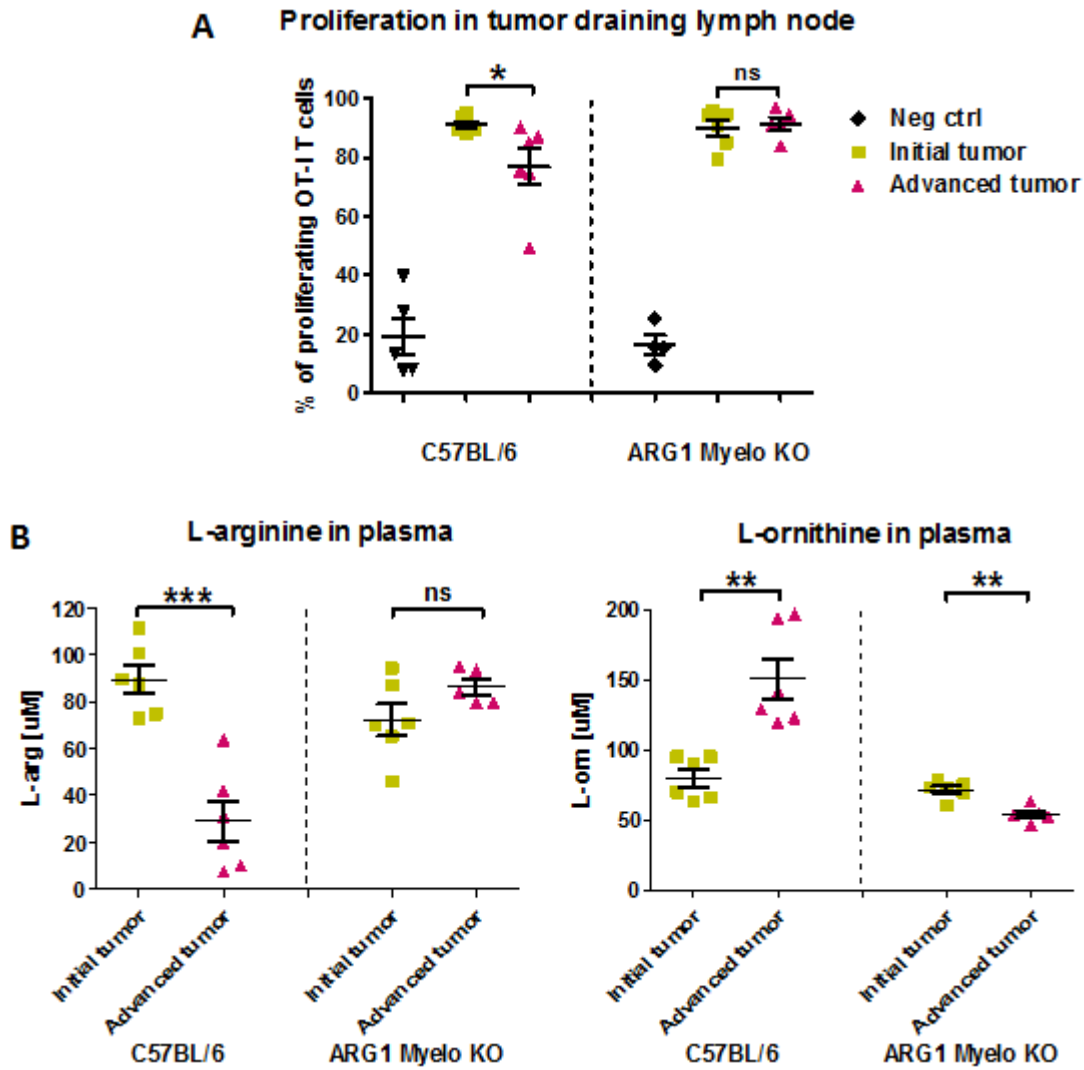
Figure 16. *Evaluation of OT-I T-cells proliferation as well as ι-arginine and ι-ornithine concentration in control C57BL/6 and ARG1 Myeloid KO mice (C57BL/6-Arg1$^{tm1Pmu/J}$ × B6.129P2-Lyz2$^{tm1(cre)Ifo/J}$). Mice received $0.5x10^6$ of LLC tumor cells injected subcutaneously on days 0 and 14 of the experiment in order to generate advanced and initial tumors, respectively. Adoptive cells transfer of isolated, CTV stained, OT-I CD8$^+$ lymphocytes was performed on day 17 by intravenous route. Antigen-specific proliferation was triggered with ovalbumin (OVA) protein injected subcutaneously in the tumor area on day 18. Proliferation of OT-I T-cells in tumor-draining lymph node (inguinal) was evaluated on day 21 by flow cytometry (A). ι-arginine and ι-ornithine concentrations in plasma samples were assessed by mass spectrometry (B). Data are presented as means ± SD. An unpaired two-tailed t-test was used to compare groups. *p<0.05, **p≤0.01, ***p≤0.001.*

4.3.2 Studies using ARG1 Total KO mice

Next, the effects of total ARG1 KO on the LLC tumor growth and probable modifications in the tumor microenvironment were investigated. For that purpose, a mouse model of tamoxifen-inducible ARG1 deficiency in all types of cells was generated. The scheme of the performed experiment is presented in Figure 17. In concordance with genotyping results (data not shown), the expected ARG1 KO phenotype was confirmed since transgenic mice (abbreviated as ARGfloxROSA) treated with tamoxifen showed significant accumulation of plasma ʟ-arginine (458,3 µM ± 141,8 µM) in comparison with ARGfloxROSA control mice treated with tamoxifen diluent which is a peanut oil (45,86 µM ± 11,39 µM, $p < 0.0001$, one-way ANOVA with Tukey multiple comparison test; Figure 17).

Figure 17. *Timeline of the in vivo experiment exploiting control C57BL/6 and C57BL/6-Arg1^{tm1Pmu}/J × B6.129-Gt(ROSA)26Sor^{tm1(cre/ERT2)Tyj}/J (abbreviated as ARGfloxROSA) mice (A) and measurement of ʟ-arginine concentration in plasma samples by mass spectrometry (B). 0.5x10^6 LLC tumor cells were inoculated subcutaneously in induced by tamoxifen (75 mg/kg of a mouse) ARG1 Total KO mice and WT controls C57BL/6. In control groups, peanut oil (tamoxifen diluent) was administered orally from day 7 until day 12 accordingly. Isolated, CTV stained, OT-I CD8^+ lymphocytes were transferred intravenously on day 17. Antigen-specific proliferation was triggered with ovalbumin (OVA) protein injected subcutaneously in the tumor area on day 18. Each experimental group consisted of n = 6-7 mice. Data show means ± SD. One-way ANOVA with Tukey post-hoc test was used to compare groups. *p<0.05, **p≤0.01, ***p≤0.001.*

Mice were inoculated with LLC tumor cells on day 0, whereas tamoxifen oral administration was performed from day 7 until day 12 and in the meantime, tumor growth was monitored. As the result, LLC tumors progression was delayed in ARG1 Total KO mice in comparison with the same transgenic mice injected only with peanut oil ($p = 0.0001$, measurements from day 21, one-way ANOVA with Tukey multiple comparison test; Figure 18). Also, tumor mass weight isolated during harvest was significantly different between these two groups (2.25 ± 0.23 and 1.51 ± 0.27 in ARGfloxROSA mice treated with peanut oil and tamoxifen, respectively; $p = 0.0056$ one-way ANOVA with Tukey multiple comparison tests). Taking into account that tamoxifen itself is an antitumor drug used for breast cancer treatment, it was important verification that this agent given to control C57BL/6 mice did not show antitumor efficacy in the lung cancer model. To further delineate the immunoregulatory mechanisms of ARG1 KO, tumor samples were extracted to perform flow cytometric analysis of TILs. It revealed that inhibited progression of LLC tumors in ARG Total KO mice was associated with both a higher percentage and number of CD3^{+} TILs. Moreover, CTV-labelled adoptively transferred OT-I T-cells were found in tumors of ARG1 total KO mice at the increased percentage in comparison with control mice suggesting that lack of ARG1 expression facilitates the T-cell tumor penetration (Figure 19).

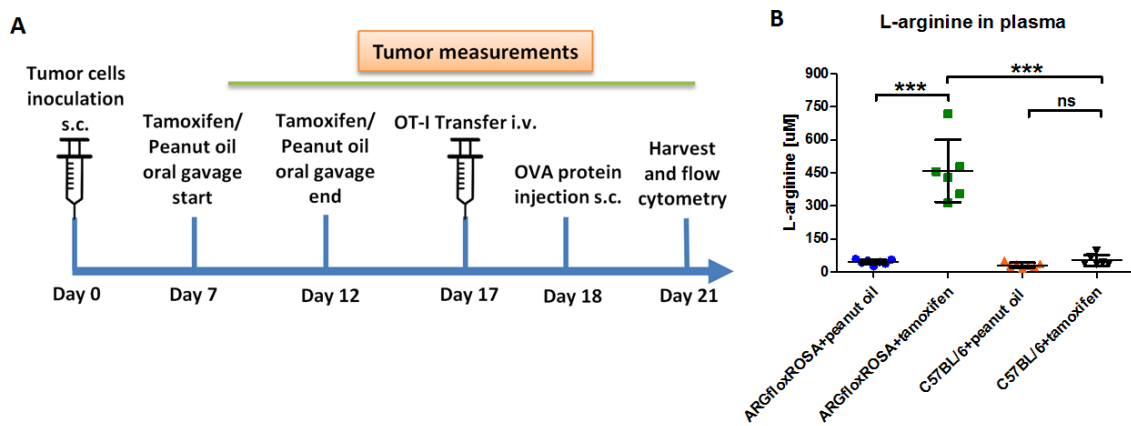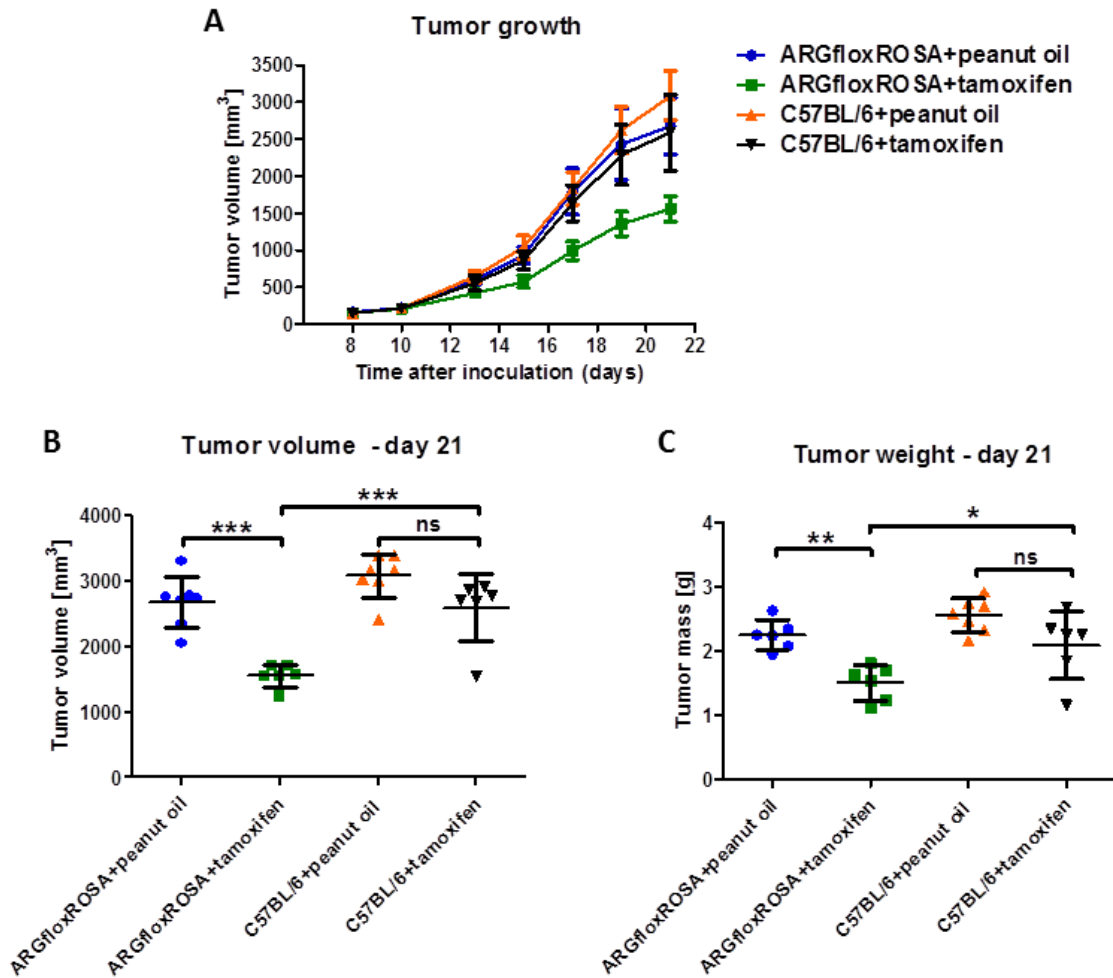***Figure 18.*** *Measurements of tumor growth (A), volume (B) and weight (C) in experiment exploiting control C57BL/6 and C57BL/6-Arg1^{tm1Pmu}/J × B6.129-Gt(ROSA)26Sor$^{tm1(cre/ERT2)Tyj}$/J (abbreviated as ARGfloxROSA) mice treated with peanut oil or tamoxifen. Each experimental group consisted of n = 6-7 mice. Data show means ± SD. One-way ANOVA with Tukey post-hoc test was used to compare groups. *p<0.05, **p≤0.01, ***p≤0.001.*
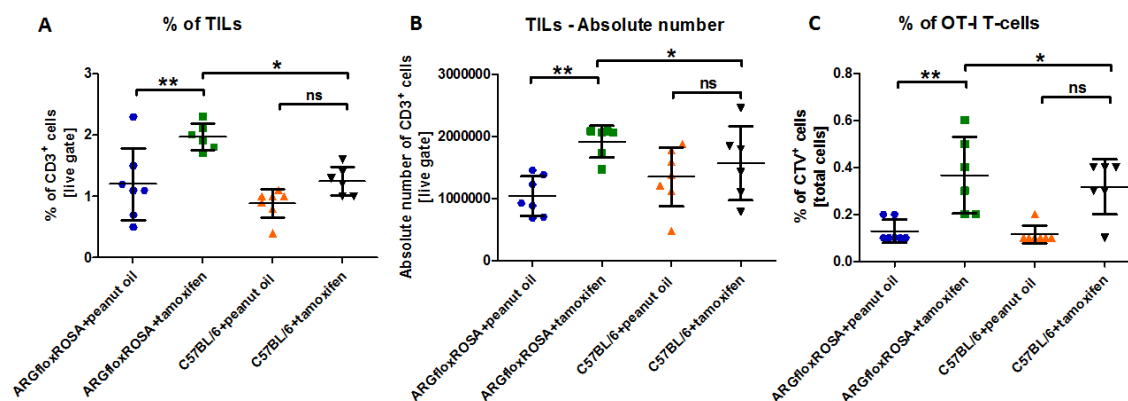
Figure 19. *Analysis of percentage (A), absolute number (B) of CD3$^+$ tumor-infiltrating lymphocytes (TILs) and CTV$^+$ adoptively transferred OT-I T-cells in inguinal tumor-draining lymph node (C) using flow cytometry. Each experimental group consisted of n = 6-7 mice. Data show means ± SD. One-way ANOVA with Tukey post-hoc test was used to compare groups. *p<0.05, **p≤0.01.*

4.4 Assessment of ARG1 expression in murine tumor cell lines

In the course of the project, it was important to find a murine tumor model cell line with sufficiently high endogenous ARG1 expression, therefore several cell lines available within the laboratory including A20, LLC, E0771, PANC02, ID8, 4T1, B16F10 were compared. As initially verified by flow cytometry (Figure 20) and additionally confirmed by immunoblotting (Figure 21) none of them had prominent ARG1 expression level.

Figure 20. *Measurement of the basal endogenous expression level of ARG1 in various murine tumor cell lines: A20, LLC, E0771, PANC02, ID8, 4T1, B16F10 evaluated by flow cytometry.*

Mean fluorescence intensity (MFI) of signal from tumor cell line samples stained with anti-ARG1 antibody in comparison to Fluorescence Minus One (FMO) controls.

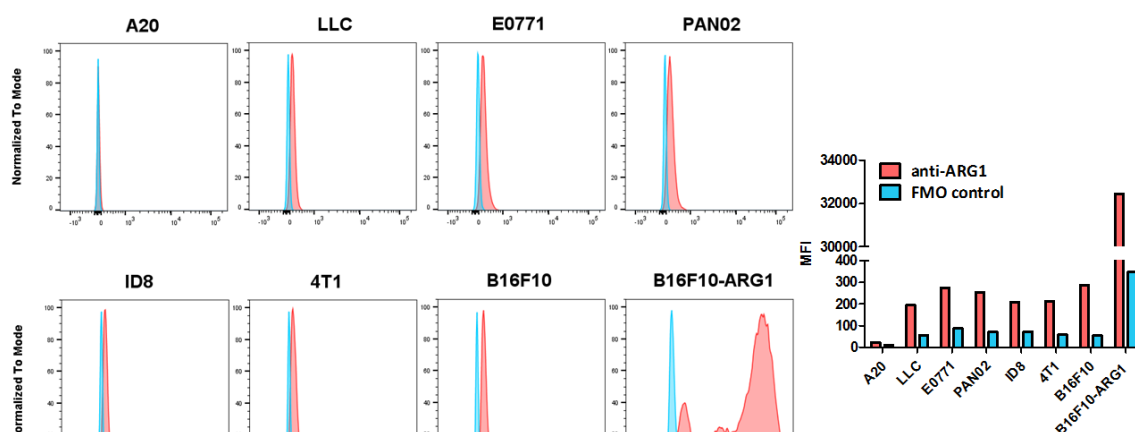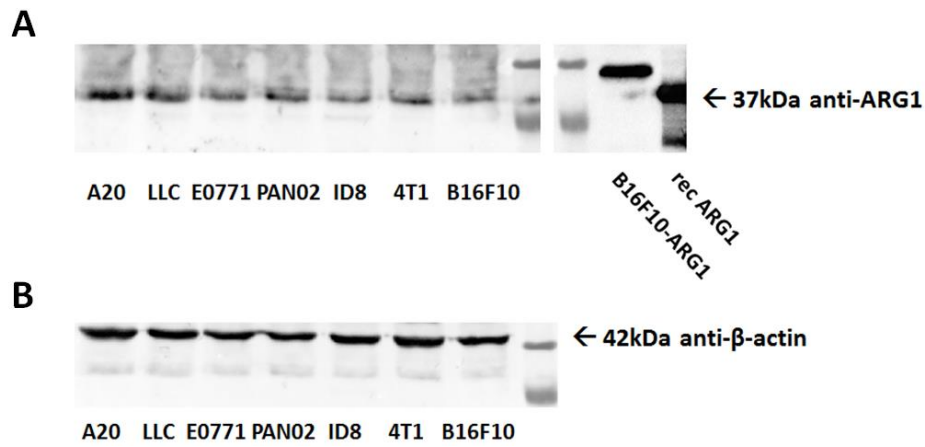**Figure 21.** *Measurement of the basal endogenous expression level of ARG1 in various murine tumor cell lines: A20, LLC, E0771, PANC02, ID8, 4T1, B16F10 evaluated by Western blotting (A). β-actin served as an equal protein loading control (B).*

Hence, it was crucial to generate the tumor model cell lines with ARG1 overexpression using the lentiviral transduction method. The scheme of the experiment is presented in Figure 22. Transductions were successful as the generated LLC cell line overexpressed ARG1 enzyme, which was verified in an enzymatic assay in which it was actively converting ʟ-arginine into urea (Figure 22).
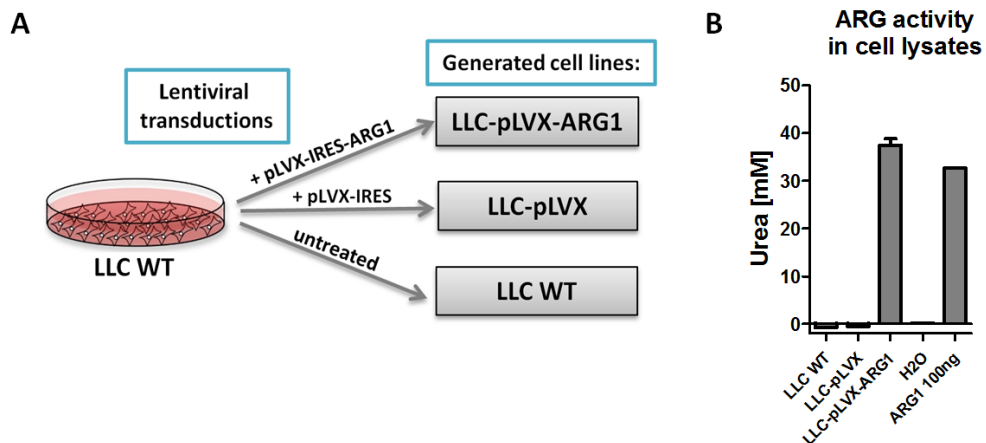
Figure 22. *Scheme of the lentiviral transduction performed on LLC WT cells in order to generate cell line overexpressing ARG1 (A) and analysis of ARGs activity in control LLC WT, LLC-pLVX and LLC-pLVX-ARG1 cell lines after transductions measured by enzymatic assay shown as urea production (B). 100 ng of recombinant ARG1 and double-distilled water were used as positive and negative controls, respectively. Data show means ± SD.*

4.5 Evaluation of ARG1 overexpression on tumor growth *in vivo*

In vivo, ARG1 overexpression by LLC tumor cells resulted in accelerated progression of tumor growth in immunocompetent C57BL/6 mice in comparison with control WT and -pLVX groups (p < 0.0001 and p = 0.0006, respectively comparing measurements performed on day 18; one-way ANOVA with Tukey multiple comparison tests). To address whether this effect was dependent on lymphocytes, the same experiment was performed in immunodeficient B6(Cg)-Rag2$^{tm1.1Cgn}$/J RAG2 KO mice. These mice have impaired T and B-cell development due to arrest at the pro-B and the pro-T-cell stage, respectively. Results of the experiment were not reproduced in RAG2 KO mice that lack mature T and B cells suggesting the mechanism dependent on lymphocytes' presence (Figure 23).
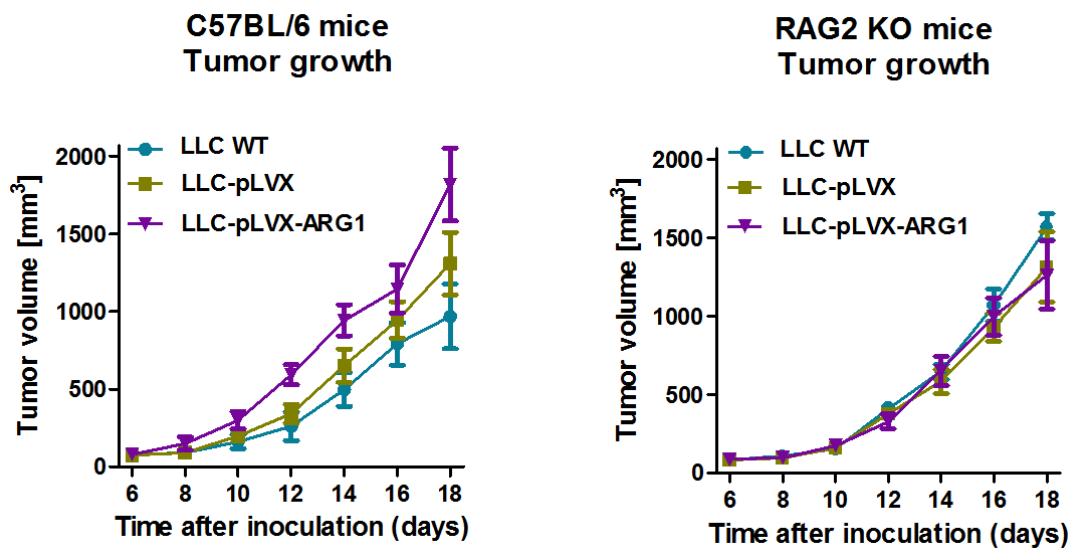
Figure 23. *Comparison of tumor growth in control immunocompetent C57BL/6 and immunodeficient B6(Cg)-Rag2$^{tm1.1Cgn}$/J (RAG2 KO) mice inoculated with ARG1-overexpressing lung carcinoma cell line (LLC-pLVX-ARG1) and control cell lines (LLC WT, LLC-pLVX). Each experimental group consisted of n = 7-8 mice. Data show means ± SD.*

To broaden the studies similar experiment was repeated with the use of B16F10 tumor cell line overexpressing ARG1 as well as matching control cell lines: B16F10 WT and B16F10-pLVX. In accordance with LLC model very consistent results were obtained in B16F10 model in both immunocompetent C57BL/6 and immunodeficient RAG2 KO

(B6(Cg)-Rag2$^{tm1.1Cgn}$/J) mice. Additionally, blood samples were collected and ι-arginine concentration was measured in separated plasma. Results indicate the tremendous down-regulation of ARG substrate in mice inoculated with B16F10-pLVX-ARG1 cell line in comparison to both control ones (Figure 24).
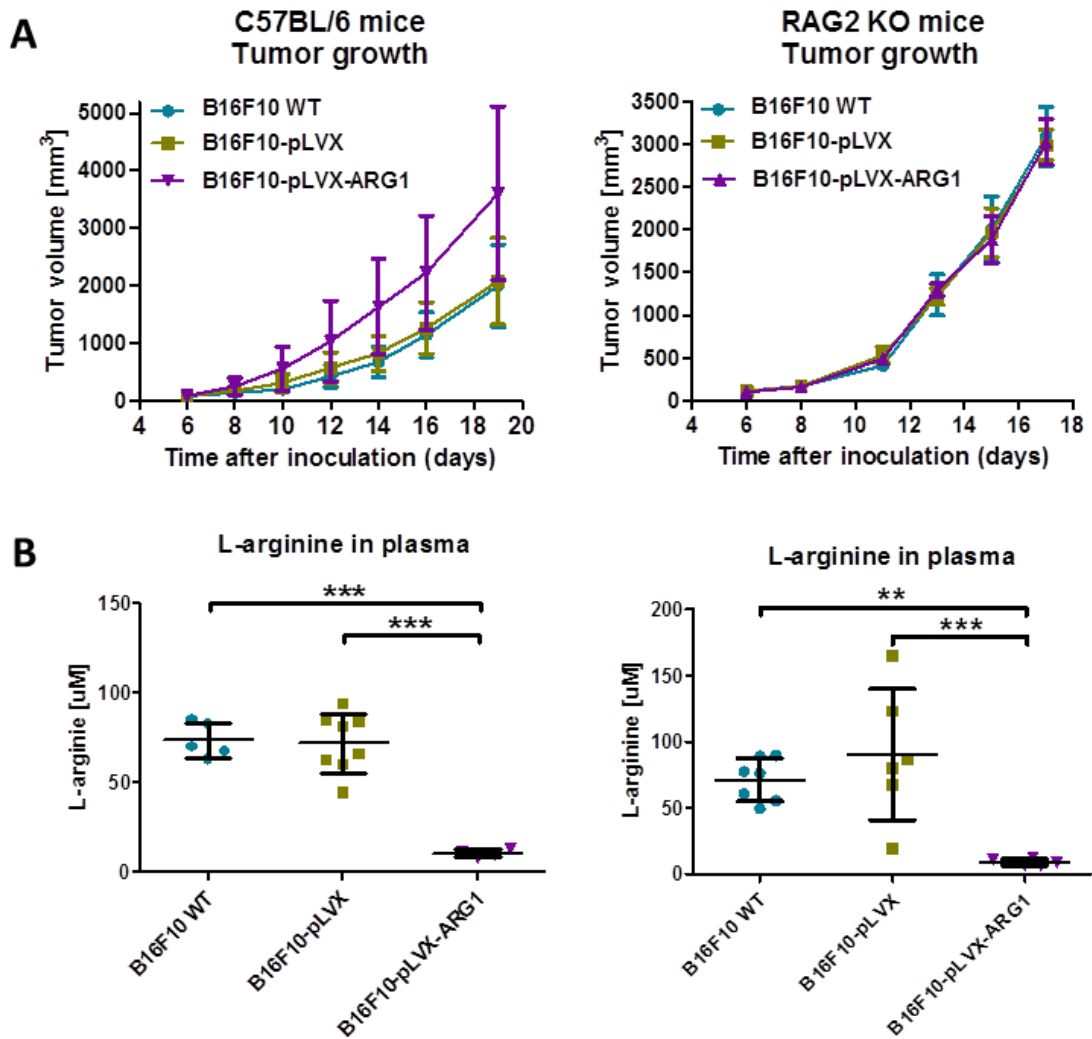
Figure 24. Comparison of tumor growth (A) and ι-arginine plasma concentration (B) in control C57BL/6 and B6(Cg)-Rag2$^{tm1.1Cgn}$/J (RAG2 KO) mice inoculated with ARG1-overexpressing melanoma cell line (B16F10-pLVX-ARG1) and control cell lines (B16F10 WT, B16F10-pLVX). The experimental group consisted of n = 4-8 mice. Data show means ± SD. One-way ANOVA with Tukey post-hoc test was used to compare groups. **p≤0.01, ***p≤0.001.

4.6 Evaluation of ARGs effect on the *in vitro* T-cells proliferation and CD3 expression

To gain deeper insights into the mechanisms beyond the immunomodulatory effects of ARGs on T-cells in the tumor microenvironment *in vivo*, a series of experiments *ex vivo* utilizing splenic antigen-specific OT-I T-cells activated with OVA peptide were performed. Isolated OT-I CD8$^+$ T-cells were stained with CFSE dye allowing to track each cell division and increasing concentrations of recombinant mouse ARG1 or ARG2 were added. In both cases, T-cells divisions were totally abrogated at 4 μg/ml concentration of ARG1 and ARG2, with visible changes in proliferation pattern also at the lower ARGs concentrations. In comparison with the positive control, ARG1 concentration of 1 μg/ml and ARG2 concentration of 2 μg/ml diminished the proliferative potential of antigen-specific OT-I CD8$^+$ T-cells (Figure 25).

Figure 25. *Evaluation of proliferation potential of OT-I T-cells in increasing concentrations of recombinant mouse ARG1 and ARG2. Splenocytes were isolated from OT-I mouse, next were*

stained with CFSE dye and cultured in vitro. To trigger antigen-specific proliferation cells were stimulated with 10 nM of OVA$_{257-264}$ peptide. Samples were assessed by flow cytometry 3 days later using antibodies detecting T-cells.

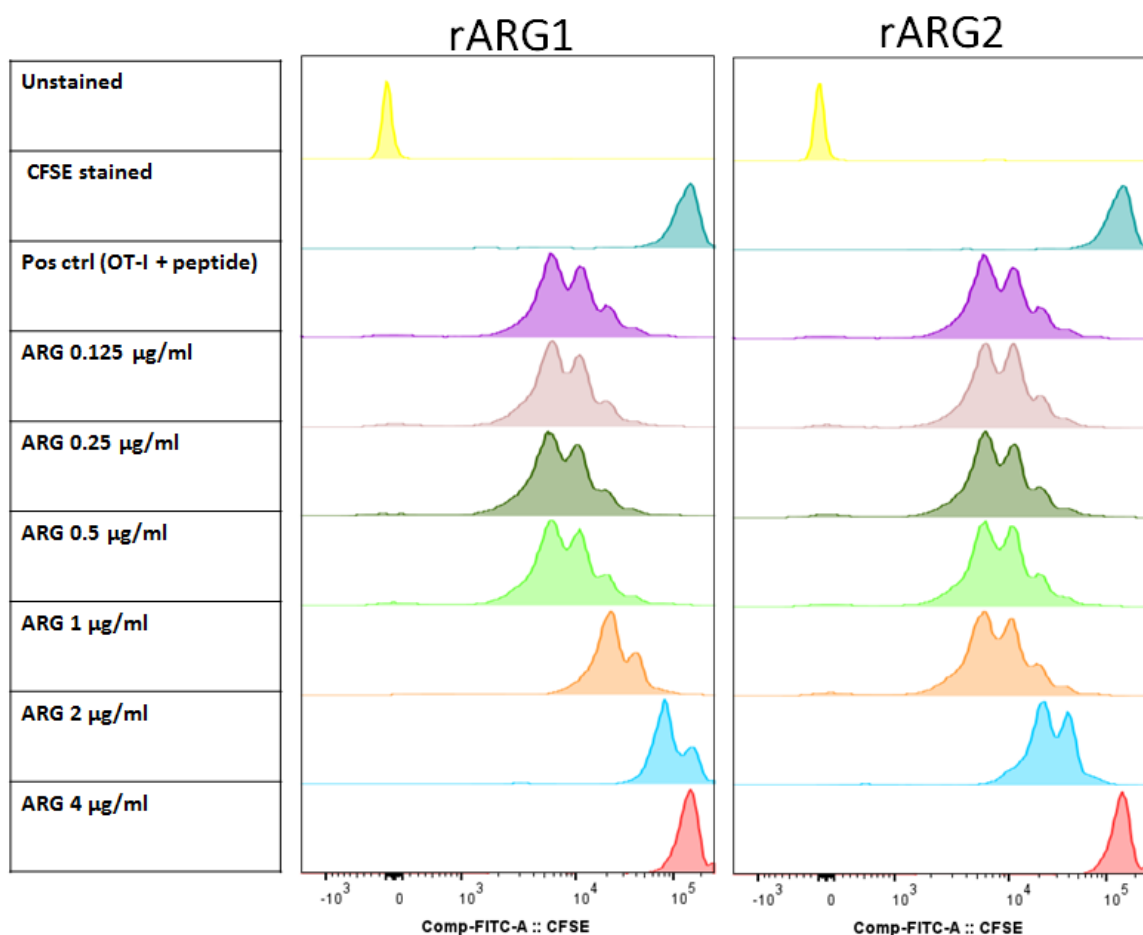Also, a series of experiments utilizing normal splenic CD4$^+$ and CD8$^+$ T-cells activated with anti-CD3/CD28-coupled beads were carried out. Isolated T-cells were stained with CTV dye and increasing concentrations of recombinant human ARG1 were added. In both cases, CD4$^+$ and CD8$^+$ T-cells divisions were completely abolished at 250 μg/ml concentration of ARG1. This indicates that the activity of used human ARG1 was much higher than the activity of applied mouse ARG1 enzyme. Partial impairment of full proliferation profile was observed at the lower ARG1 concentrations – 150 μg/ml and 200 μg/ml in the case of CD4$^+$ and CD8$^+$ T-cells, respectively. The observed reduction of proliferation corresponded to diminished CD3ε and CD3ζ chains expression that was also dose-dependent (Figure 26).
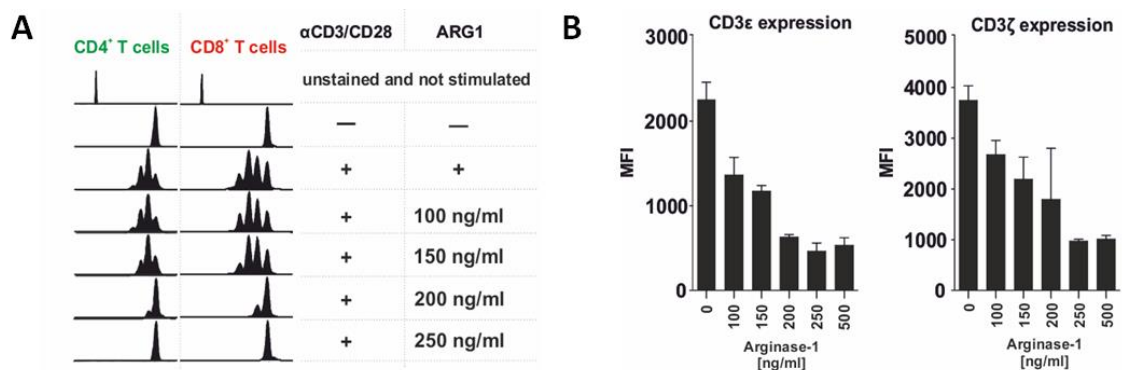
Figure 26. Analysis of the effect of recombinant human ARG1 on proliferation (left) and CD3 expression (right) in murine CD4$^+$ and CD8$^+$ T -cells. CD4$^+$ and CD8$^+$ T cells were negatively isolated from the spleens of C57BL/6 mice. Cells were stained with cell trace violet (CTV) and incubated with anti-CD3/CD28 beads to trigger activation. Recombinant human ARG1 was added to some groups at concentrations ranging from 100 to 500 ng/ml. Proliferation in presence of various concentrations of recombinant human ARG1 was analyzed by flow cytometry (A). Expression of CD3ε and CD3ζ chains presented as mean fluorescence intensity (MFI) measured in CD8$^+$ T cells by flow cytometry (B). Data show means ± SD.

Another important point of the study was to determine how rapid are the changes in expression of CD3 complex chains upon ARG1 increment. A high concentration of recombinant human ARG1 (1 µg/ml) was implemented to CD4$^+$ and CD8$^+$ T-cells cultures and the expression profile was measured in time ranging from 2 to 72 hours. At a 6 hour time-point, there was a slight up-regulation in expression of CD3ε implying that activation signaling was triggered by the anti-CD3/CD28-coupled beads (Figure 27). Nevertheless, a high concentration of ARG1 caused escalating down-regulation of both CD3ε and CD3ζ expression. The alterations of the CD3 chains expression in time are very similar in both CD4$^+$ and CD8$^+$ T-cells reaching the lowest values of at maximum 72 hour time-point (CD3ε: 29% ± 2% and 33% ± 1%; CD3ζ: 33% ± 5% and 33% ± 0% for CD4$^+$ and CD8$^+$ T-cells, respectively). Examples of representative overlay histograms showing CD3ε and CD3ζ expression on CD4$^+$ T-cells at selected time points are presented in Figure 28. Collectively, these results indicate that ARG1 acts on T-cells by attenuating the expression of crucial signaling molecules that play an essential role in the initiation of T-cell activation.
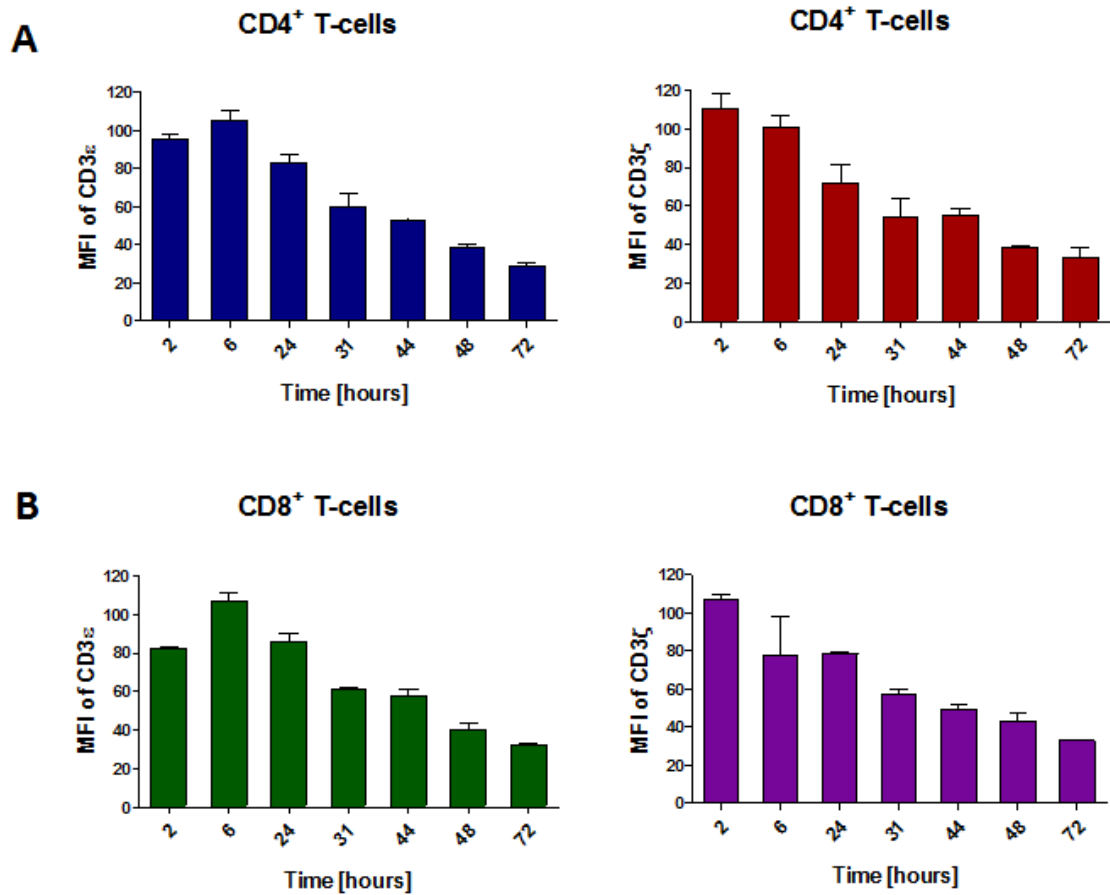
Figure 27. *Time-course analysis of CD3ε and CD3ζ expression on CD4$^+$ (A) and CD8$^+$ (B) T-cells in presence of high recombinant human ARG1 concentration (1 µg/ml). The expression is presented as **a** percentage of positive control with no ARG1 added that was set as 100%. Data show means ± SD.*
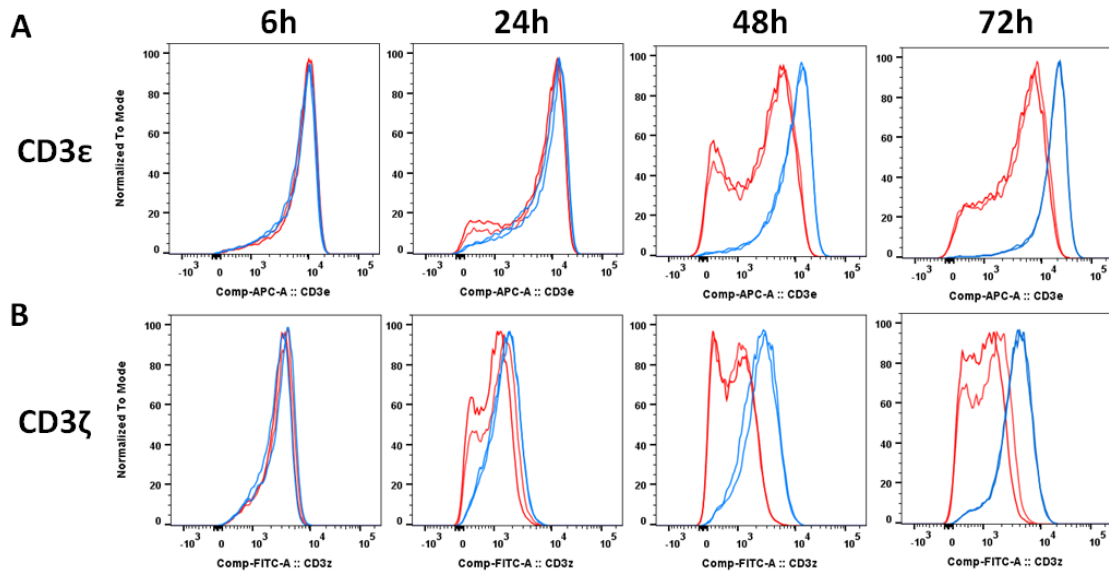
Figure 28. *Representative examples of overlay histograms representing CD3ε (A) and CD3ζ (B) expression on CD4⁺ T-cells in presence of high recombinant human ARG1 concentration (1 µg/ml; red) and untreated cells (positive control; blue) at selected time points. Each sample is shown in a technical duplicate.*

4.7 Evaluation of lack of ι-arginine on the *in vitro* T-cells proliferation and CD3 expression

In the next step, it was verified whether T-cells ability to proliferate is dependent on ι-arginine concentration in the microenvironment. Thus, to provide the evidence, CD4⁺ T-cells were cultured in a medium with various ι-arginine concentrations (none 0 µM, low 15 µM, physiologic 150 µM and high 1500 µM) and results fully supported the dependence assumption. Worsening of proliferation was observed in lack of ι-arginine in medium (0 µM) and low concentration 15 µM however physiologic concentration such as 150 µM was sufficient to recover the complete proliferation profile (Figure 29). Regarding the CD3ε and CD3ζ expression, in both cases, significant improvement of expression was noticed in 150 µM ι-arginine concentration as compared to 0 µM ι-arginine (Figure 30).
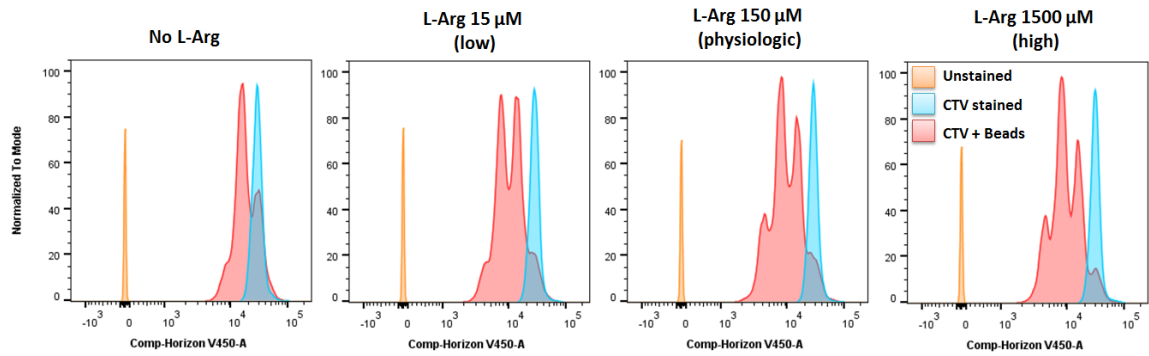
Figure 29. *Comparison of CD4+ T-cells proliferation cultured in medium with no (0 μM), low (15 μM), physiologic (150 μM) and high (1500 μM) ι-arginine concentrations. CD4+ were negatively isolated from the spleens of healthy C57BL/6 mice. Cells were stained with cell trace violet (CTV) and incubated with anti-CD3/CD28 beads to trigger activation and analyzed by flow cytometry.*
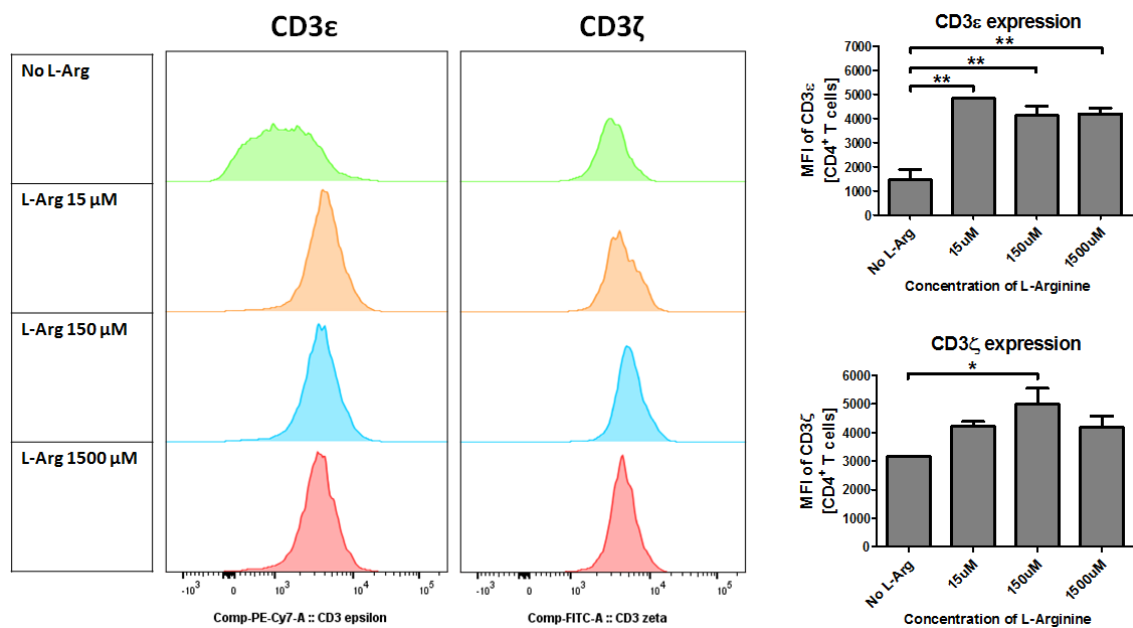
Figure 30. *Comparison of CD3ε and CD3ζ expression on CD4+ T-cells cultured in medium with no (0 μM), low (15 μM), physiologic (150 μM) and high (1500 μM) ι-arginine concentrations. CD4+ T-cells were negatively isolated from the spleens of healthy C57BL/6 mice. Cells were stained with cell trace violet (CTV), incubated with anti-CD3/CD28 beads to trigger activation and analyzed by flow cytometry. Data show means ± SD. One-way ANOVA with Tukey post-hoc test was used to compare groups. *p<0.05 **p≤0.01.*

Importantly, supplementation of extracellular ι-citrulline fully rescued the proliferative potential of T-cells cultured in a medium with no ι-arginine showing that T-cells have active ASS-1 and ASL enzymes and are able to rebuild required for proliferation ι-arginine from extracellular ι-citrulline (Figure 31).
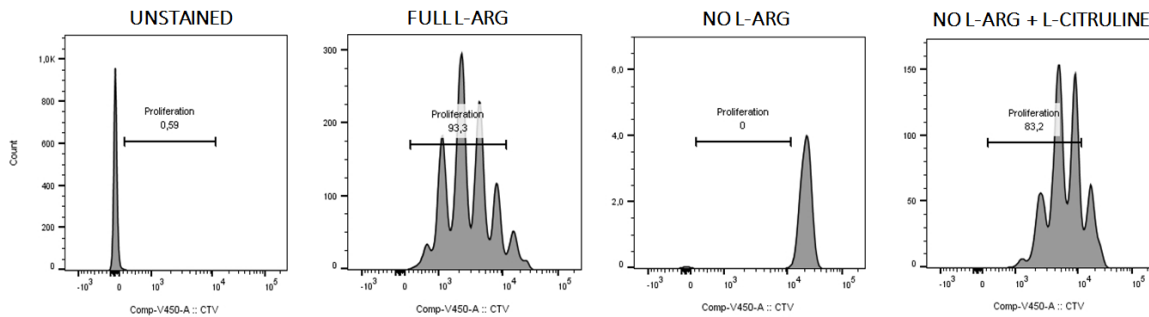
Figure 31. *Analysis of CD4$^+$ T-cells proliferation in medium lacking ι-arginine supplemented with ι-citrulline. Murine CD4$^+$ T-cells were negatively isolated from the spleens of healthy C57BL/6 mice. Cells were stained with cell trace violet (CTV), incubated with anti-CD3/CD28 beads to trigger activation and analyzed by flow cytometry.*

Since the exaggerated activity of ARG1 enzyme might cause both: fast depletion of the reaction substrate supplies along with an excessive accumulation of reaction products, it was questioned which of those events has a more profound impact on the T-cells proliferation. To accomplish that task CD4$^+$ T-cells were incubated with diversified concentrations of urea or ι-ornithine or both reaction products at once. None of the supplemented ARG1 reaction products at any concentration influenced the proliferation indicating that their accumulation has no impact (Figure 32).
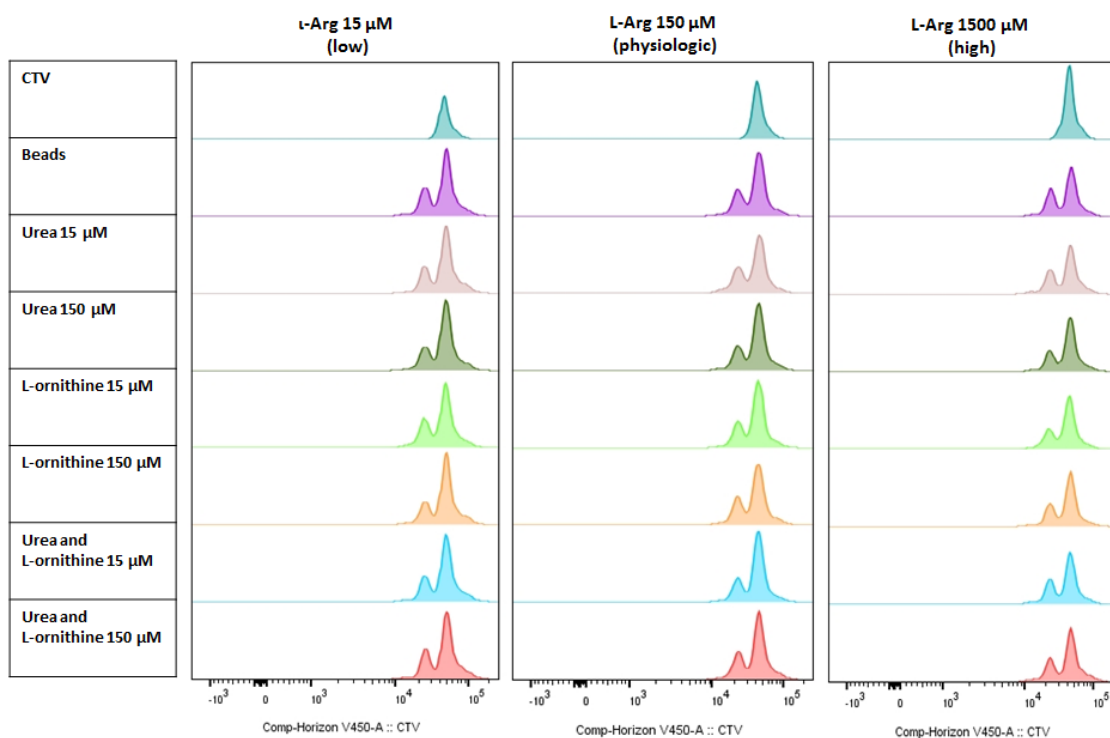
Figure 32. *Evaluation of the effect of ARG1 metabolites in various ι-arginine concentrations on the proliferation of murine CD4^{+} T-cells. CD4^{+} T-cells were negatively isolated from the spleens of healthy C57BL/6 mice. Cells were stained with cell trace violet (CTV) and activated with anti-CD3/CD28 beads. T-cells were cultured in medium with low (15 µM), physiologic (150 µM) and high (1500 µM) ι-arginine concentrations. ARG1 enzyme products such as urea and ι-ornithine or both were added to selected wells at the concentrations 15 µM or 150 µM and samples were analyzed by flow cytometry.*

4.8 Assessment of the treatment with ARG inhibitors on the *in vitro* T-cells proliferation and CD3 expression

Several compounds exhibiting inhibition activity against ARGs have been developed so far. This study aimed at a comparison of three small-molecule ARG inhibitors: reference compound ABH (2(S)-amino-6-boronohexanoic acid), newer and improved compound OAT-1617 and the most recently developed compound OAT-1746. Based on previous optimization experiments concentration of 250 µg/ml of ARG1 was selected as a fully inhibiting concentration for *in vitro* experiments evaluating the potential of ARGs inhibitor. Experiments were focused on blocking the activity of ARG1 and finding

the lowest concentration of inhibitor needed to recover the full proliferation profile and CD3 expression inhibited by a recombinant enzyme.

4.8.1 Studies evaluating ABH

ABH demonstrated very poor activity, as the required effective concentration to restore full proliferation was 10 µM in the case of human $CD4^+$ T-cells. On the other hand, a concentration of 5 µM allowed to achieve proliferation with one less division peak in comparison with the positive control ($CD4^+$ T-cells activated with beads but no ARG1 added). Apart from proliferation, the essential readout of inhibitor potential was the recovery of CD3 expression. In both cases, CD3ε and CD3ζ concentration of 10 µM ABH was the lowest to retrieve a statistically significant level (Figure 33).
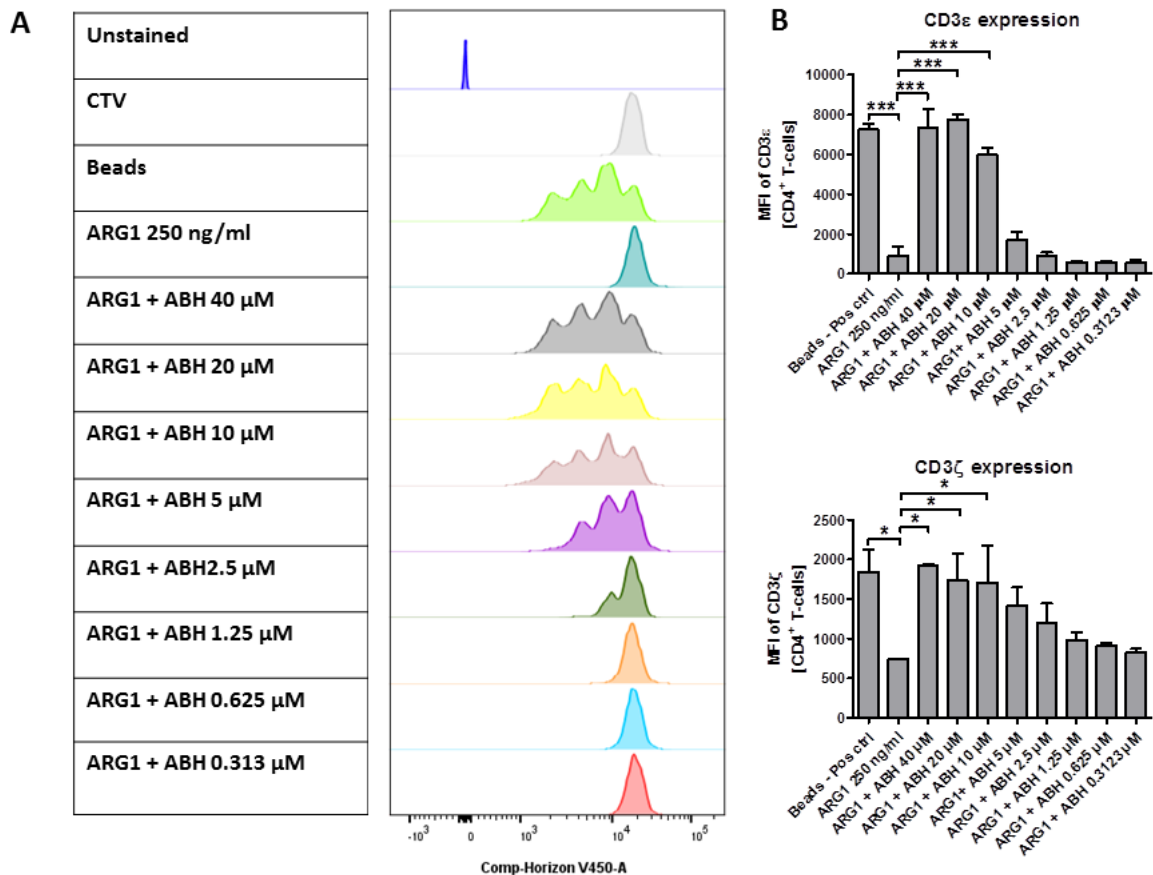
Figure 33. Evaluation of the effect of various concentrations of ABH on the proliferation (A) as well as on CD3ε and CD3ζ expression (B) of human $CD4^+$ T-cells in presence of ARG1. $CD4^+$ T-cells were negatively isolated from the blood of healthy donors. Cells were stained with cell trace violet (CTV) and incubated with anti-CD3/CD28 beads to trigger activation. Recombinant

*human ARG1 was added to some groups at a concentration of 250 ng/ml while ABH was added at a wide concentrations range and samples were analyzed by flow cytometry after 5 days of incubation. Data show means ± SD. One-way ANOVA with Tukey post-hoc test was used to compare groups. *p<0.05, ***p≤0.001.*

4.8.2 Studies evaluating OAT-1617

As opposed to ABH, novel inhibitor OAT-1617 demonstrated much higher activity with an effective concentration of 100 nM in the case of human CD4$^+$ T-cells. Even a lower concentration such as 50 nM was enough to regain high levels of CD3ε and CD3ζ expression down-regulated by ARG1 (Figure 34).
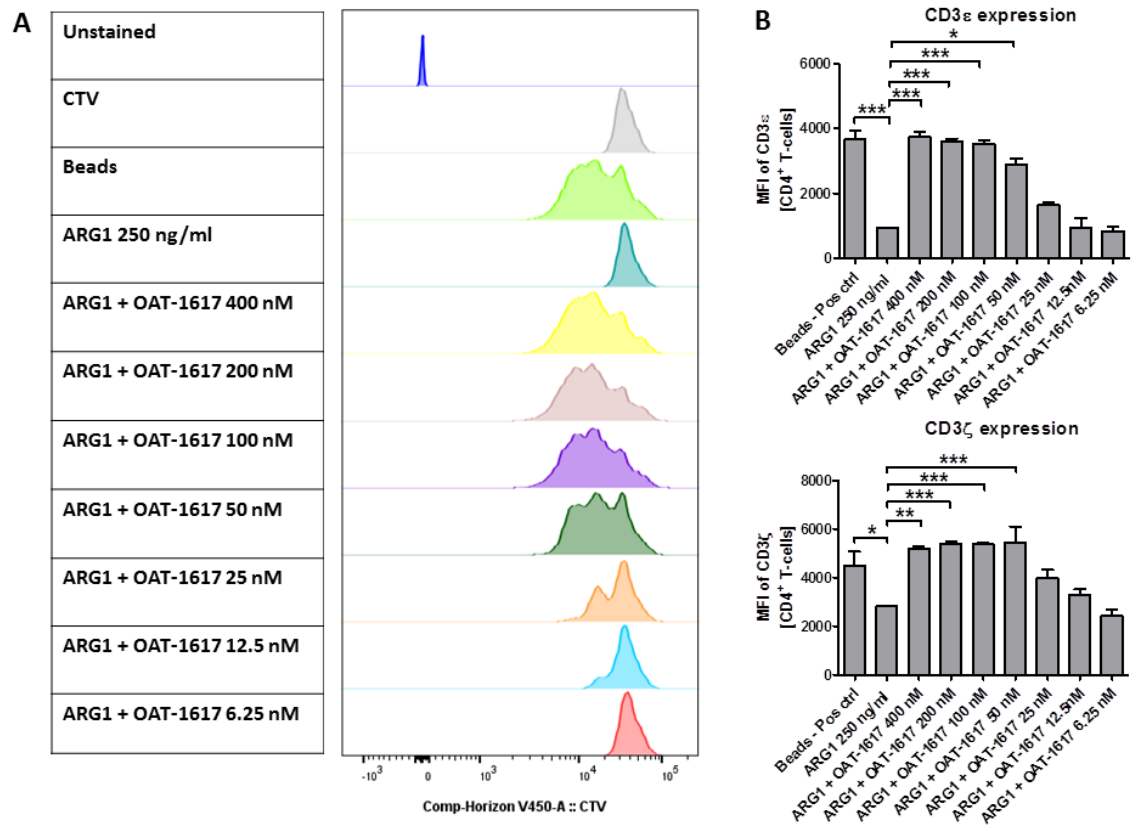
Figure 34. Evaluation of the effect of various concentrations of OAT-1617 on the proliferation (A) as well as on CD3ε and CD3ζ expression (B) of human CD4$^+$ T-cells in presence of ARG1. T-cells were negatively isolated from the blood of healthy donors. Cells were stained with cell trace violet (CTV) and incubated with anti-CD3/CD28 beads to trigger activation. Recombinant human ARG1 was added to some groups at a concentration of 250 ng/ml while OAT-1617 was added at a wide concentrations range and samples were analyzed by flow cytometry after 5

*days of incubation. Data show means ± SD. One-way ANOVA with Tukey post-hoc test was used to compare groups. *p<0.05, **p≤0.01, ***p≤0.001.*

4.8.3 Studies evaluating OAT-1746

A wide range of concentrations of OAT-1746 varying from 300 nM to 25 nM was tested to evaluate its inhibitory effects using both types of T-cells: CD4^{+} and CD8^{+}. In the case of CD4^{+} T-cells concentration of 100 nM was sufficient to recover full proliferation profile, whereas CD8^{+} T-cells required a higher concentration of 200 nM. It was probably linked to the faster proliferative rate of CD8^{+} T-cells, which are able to undergo more divisions than CD4^{+} T-cells at the same time. Importantly, even in presence of the lowest concentration of 25 nM of OAT-1746 some divisions were observed (Figure 35).
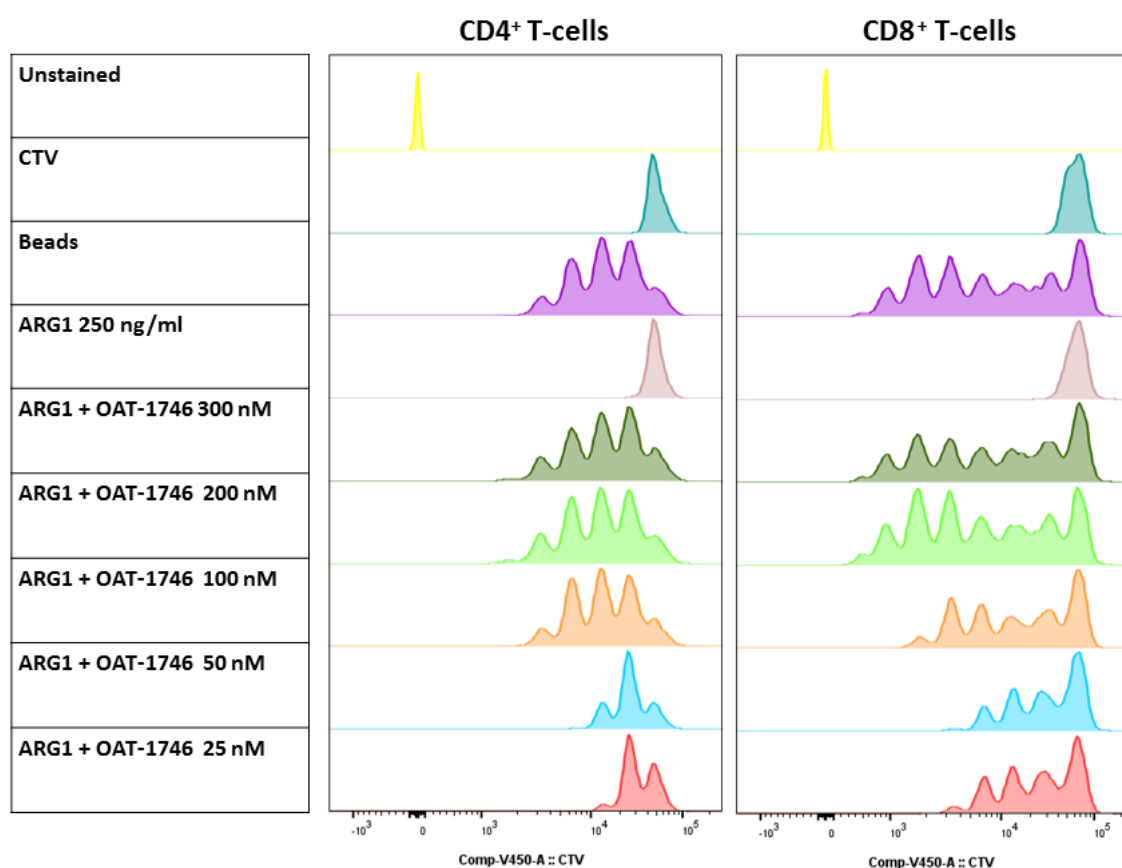
Figure 35. *Evaluation of the effect of various concentrations of OAT-1746 on the proliferation of human CD4^{+} and CD8^{+} T-cells in presence of ARG1. T-cells were negatively isolated from the blood of healthy donors. Cells were stained with cell trace violet (CTV) and incubated with anti-CD3/CD28 beads to trigger activation. Recombinant human ARG1 was added to some groups*

at a concentration of 250 ng/ml while OAT-1746 was added at a wide concentrations range and samples were analyzed by flow cytometry after 5 days of incubation.

Both effective doses of OAT-1746 (100 nM for CD4$^+$ and 200 nM for CD8$^+$ T-cells, respectively) were successfully employed to restore CD3ε expression profoundly down-regulated by ARG1 (Figure 36). What was repeatedly seen selected concentration of 250 µg/ml of recombinant human ARG1 imposed a more robust down-regulation effect on the CD3ε expression in comparison with CD3ζ expression.

***Figure 36.** Evaluation of the effect of a wide range of OAT-1746 concentrations on the CD3ε expression of human CD4$^+$ and CD8$^+$ T-cells in presence of ARG1. T-cells were negatively isolated from the blood of healthy donors. Cells were stained with cell trace violet (CTV) and incubated with anti-CD3/CD28 beads to trigger activation. Recombinant human ARG1 was added to some groups at a concentration of 250 ng/ml while OAT-1746 was added at a wide concentrations range and samples were analyzed by flow cytometry after 5 days of incubation. Representative histograms are shown and graphs represent Mean Fluorescence Intensity (MFI). Data show means ± SD. One-way ANOVA with Tukey post-hoc test was used to compare groups. ***p≤0.001.*

In this experiment concentration of 250 µg/ml caused a statistically significant drop in CD3ζ expression in CD8^{+} T-cells. However, it was visible but not statistically significant in the case of CD4^{+} T-cells (p = 0.0554, one-way ANOVA with Tukey post-hoc test). On the other hand, a wide range of OAT-1746 concentrations including even low concentration such as 50 nM was enough to preserve the high CD3ζ expression in CD4^{+} T-cells comparable with the positive control (T-cells stimulated with beads and no ARG1 and no OAT-1746 added). Interestingly, OAT-1746 concentration of 25 nM was substantial to retain the relatively high expression level of the CD3ζ chain in CD4^{+} T-cells, however this change was not statistically significant (Figure 37).

Figure 37. *Evaluation of the effect of a wide range of OAT-1746 concentrations on the CD3ζ expression of human CD4^{+} and CD8^{+} T-cells in presence of ARG1. T-cells were negatively isolated from the blood of healthy donors. Cells were stained with cell trace violet (CTV) and incubated with anti-CD3/CD28 beads to trigger activation. Recombinant human ARG1 was added to some groups at a concentration of 250 ng/ml while OAT-1746 was added at a wide concentrations range and samples were analyzed by flow cytometry after 5 days of incubation. Representative histograms are shown and graphs represent Mean Fluorescence Intensity (MFI). Data show means ± SD. One-way ANOVA with Tukey post-hoc test was used to compare groups. *p<0.05.*

Furthermore, OAT-1746 essentially supported the proper production level of TNF-α and INF-γ cytokines by human CD4^{+} T-cells, that was comparable with positive control. Considering TNF-α positive cells only OAT-1746 concentration of 300 nM retained the statistically significant result. What is more, remaining lower concentrations generated visible but not statistically significant up-regulation in the percentage of TNF-α positive cells. Despite not statistically significant difference between positive control and cells treated with ARG1 all tested concentrations of OAT-1746 resulted in an evidently increased percentage of IFN-γ in human CD4^{+} T-cells (Figure 38).
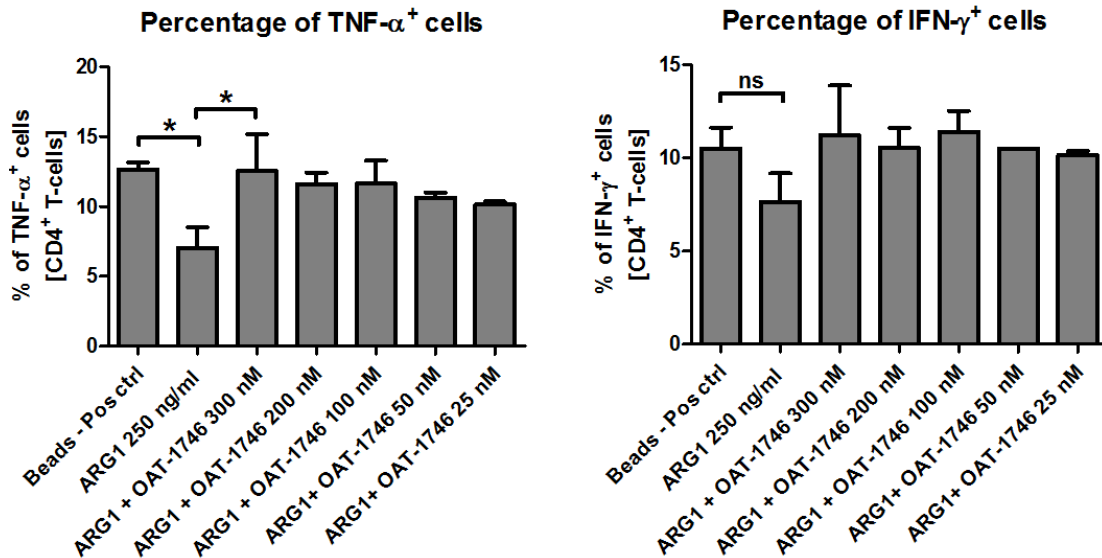
Figure 38. *Evaluation of the effect of a wide range of OAT-1746 concentrations on the percentage of TNF-α^{+} and IFN-γ^{+} human CD4^{+} T-cells in presence of ARG1. T-cells were negatively isolated from the blood of healthy donors. Cells were stained with cell trace violet (CTV) and incubated with anti-CD3/CD28 beads to trigger activation. Recombinant human ARG1 was added to some groups at a concentration of 250 ng/ml while OAT-1746 was added at concentrations ranging from 25 to 300 nM and samples were analyzed by flow cytometry after 6 days of incubation. Cytokines were measured after addition for the last 4h of incubation Brefeldin A and Golgi Stop. Data show means ± SD. One-way ANOVA with Tukey post-hoc test was used to compare groups. *p<0.05.*

4.9 Evaluation of the ARG inhibitors effectiveness in blocking the activity of tumor cells associated and secreted ARG1 and ARG2

Above results show the ability of the mentioned ARG inhibitors to inhibit the free, easily accessible form of recombinant human ARG1 diluted in medium. Next, it becomes important to verify the potential of these compounds in inhibiting the enzymes that are produced within the cell. To achieve this goal tumor cell lines overexpressing ARG1 enzyme generated by lentiviral transduction system were used. Cell lines overexpressing ARG2 were generated before and provided by the laboratory of Vincenzo Cerundolo at the University of Oxford. As the controls, matching WT cell lines or transduced with empty vector pLVX were used. As the results, B16F10-pLVX-ARG1 cell line had 45 times higher urea production than control one (4.14 ± 0,04% vs -0.01 ± 0,04%), whereas B16F10-ARG2 cell line had 55 times higher ARG activity than WT control (9.82 ± 0.30% vs 0.18 ± 0.00%). Moreover, overexpression of ARG1 or ARG2 enzymes was confirmed in modified ID8-ARG1 and THP-1-ARG2 cell lines in comparison with WT control cell lines (ID8 WT and THP-1 WT). All cell lines were incubated either with ABH or OAT-1617 or OAT-1746 ARG inhibitor and then supernatants as well as cell lysates were collected and analyzed for ARG activity in an enzymatic assay. In all cases, ABH used at 20 µM had no effect on tumor cell-associated ARG1 or ARG2 which confirms its poor activity. Furthermore, OAT-1617 showed blocking effect that was equal to 15%, 61%, 45% and 61% for B16F10-ARG1, B16F10-ARG2, ID8-ARG1 and THP-1-ARG2, respectively. Importantly, OAT-1746 inhibitor exerted more considerable effect resulting in 24%, 74%, 59% and 80% activity blocking in mentioned cell lines (Figure 39).
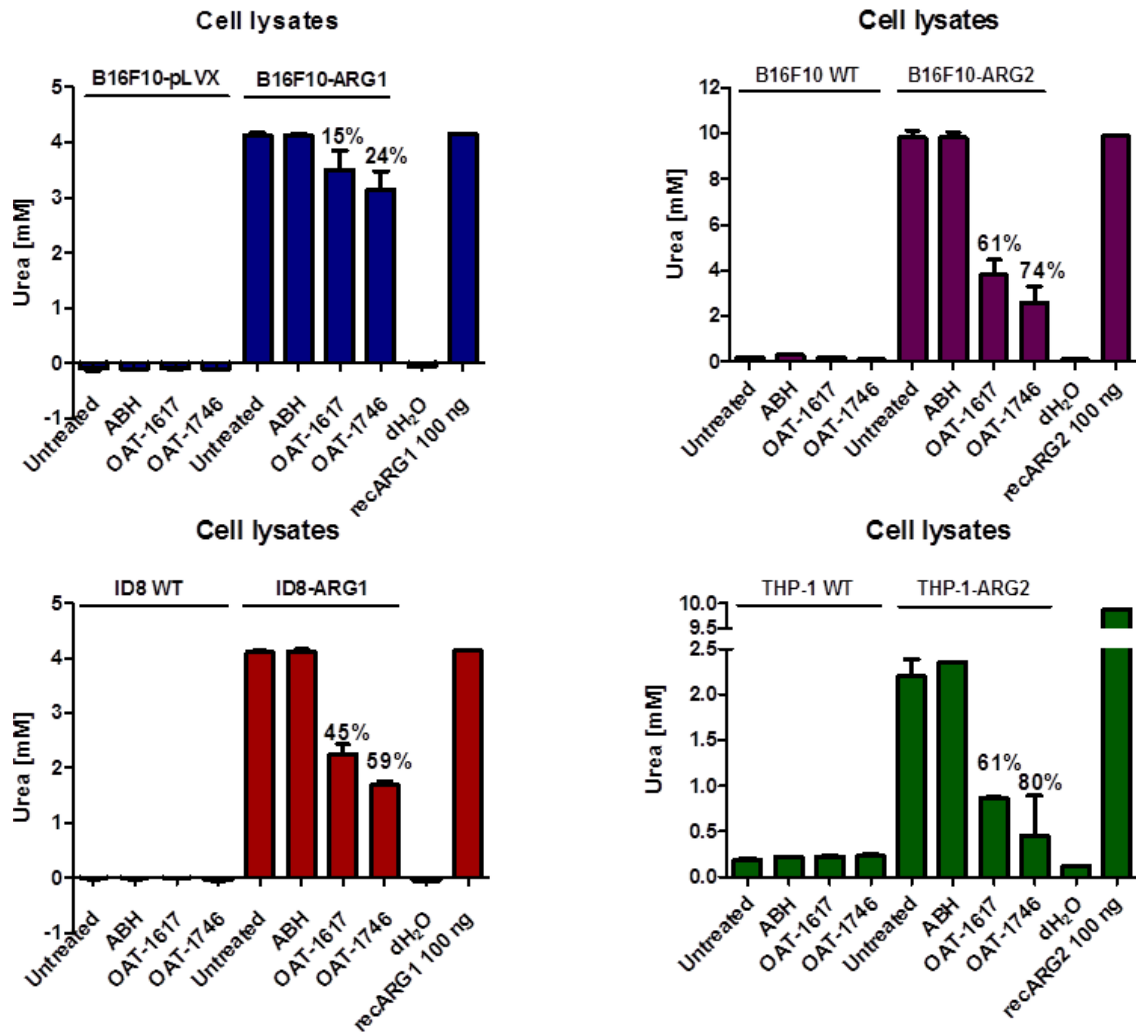
Figure 39. *Assessment of ABH, OAT-1617 and OAT-1746 inhibitors effectiveness in blocking the activity of tumor cells associated ARG1 and ARG2. ARG1-overexpressing tumor cells (B16F10-ARG1 and ID8-ARG1) or plasmid control cells line (B16F10-pLVX) were modified by lentiviral transduction. $1x10^6$ of tumor cells were seeded in 6-well plates. Cells were treated with 20 µM of ABH or OAT-1617 or OAT-1746 for 20 hours or were left untreated. Lysates of tumor cells were analyzed for ARGs activity measured as urea production using a 2-hour enzymatic assay with spectrophotometric readout. The percentage of ARG inhibition by the selected compound is shown in comparison with untreated samples with ARG1 overexpression. Data show means ± SD.*

Similarly, in tested tumor cell culture supernatants, ABH had none (as observed in B16F10-ARG2) or only a minor impact on inhibition of secreted ARG1 and ARG2 to the medium (10% and 12% inhibition in comparison with untreated B16F10-ARG1 and

107

THP-1-ARG2 cells, respectively). OAT-1617 showed improved efficacy but OAT-1746 used at the same concentration caused even better inhibition of ARG activity (presented as urea production) in the supernatant of B16F10-ARG1 and THP-1-ARG2 cell lines. Noteworthy, none of the inhibitor at 20 μM concentration induced the adverse condition of cells or dying after 20 hours of treatment (Figure 40).
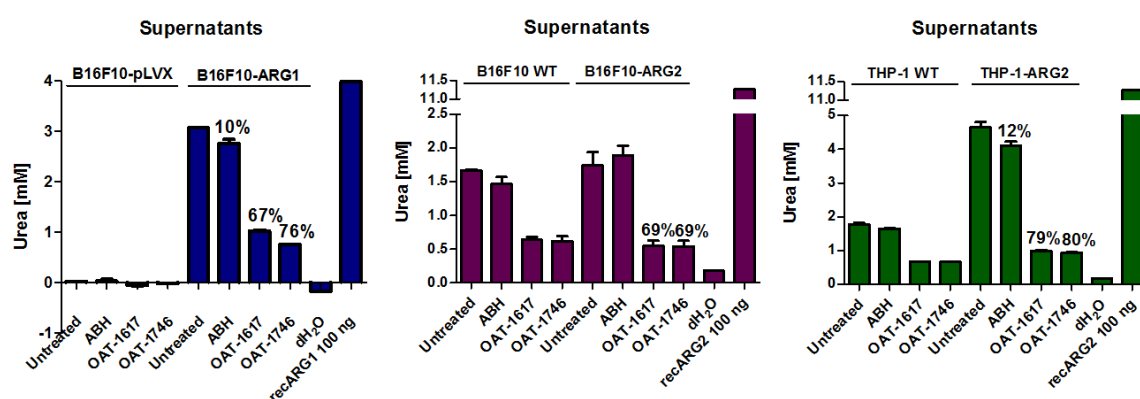
Figure 40. *Assessment of ABH, OAT-1746 and OAT-1617 inhibitors effectiveness in blocking the activity of tumor cells secreted ARG1 and ARG2. ARG1-overexpressing tumor cells (B16F10-ARG1) or plasmid control cells line (B16F10-pLVX) were modified by lentiviral transduction. 1×10^6 of tumor cells were seeded in 6-well plates. Cells were treated with 20 μM of ABH or OAT-1746 or OAT-1617 for 20 hours or were left untreated. Supernatants of tumor cells were first depleted from urea accrued during cell culture. Samples were analyzed for ARGs activity measured as urea production using a 2-hour enzymatic assay with spectrophotometric readout. The percentage of ARG inhibition by the selected compound is shown in comparison with untreated samples with ARG1 overexpression. Data show means ± SD.*

4.10 Evaluation of antitumor efficacy of ARG inhibitors in lung cancer model

4.10.1 Monotherapy with OAT-1746 or ABH

As the LLC tumor microenvironment is highly infiltrated with myeloid cells expressing ARG1 and OAT-1746 is able to inhibit the cell-associated enzyme, the therapeutic potential of this inhibitor was evaluated *in vivo* in LLC mouse model. Two weeks of treatment with 20 mg/kg of OAT-1746 did not result in tumor remission but significantly inhibited the tumor growth (p <0.0001, unpaired two-tailed t-test) as well as prolonged survival for 6 days in this very aggressive model (Figure 41). On the other

hand, treatment with 100 mg/kg of reference ARG inhibitor ABH did not affect the tumor growth at all (Figure 42).
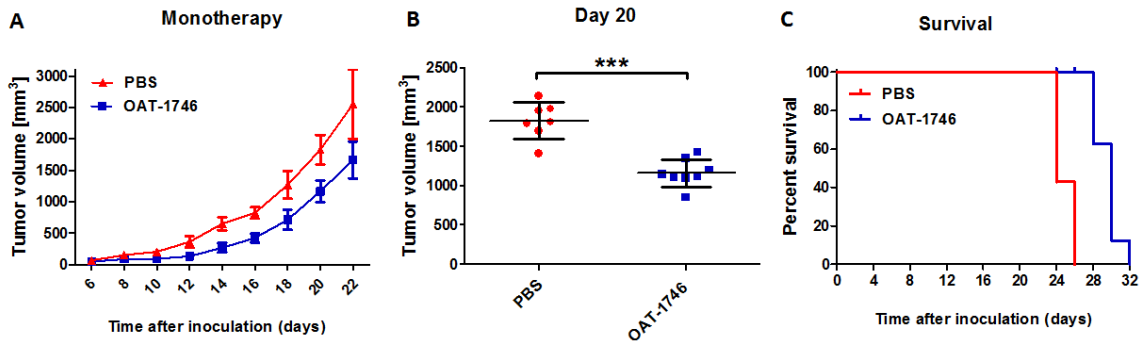
Figure 41. *Evaluation of antitumor efficacy of therapy with OAT-1746 ARG inhibitor. C57BL/6 mice were inoculated subcutaneously with 0.1x10^6 of LLC tumor cells. OAT-1746 was administered twice daily by an intraperitoneal route at the dose of 20 mg/kg for the first 14 days, whereas the control group received PBS. The graphs show tumor growth dynamics over time (A), individual mice tumor volume display from measurements performed on day 18 (B) and survival (C). Each experimental group consisted of n = 7-8 mice. Data are presented as mean ± SD. An unpaired two-tailed t-test was used to compare groups. ***p≤0.001.*
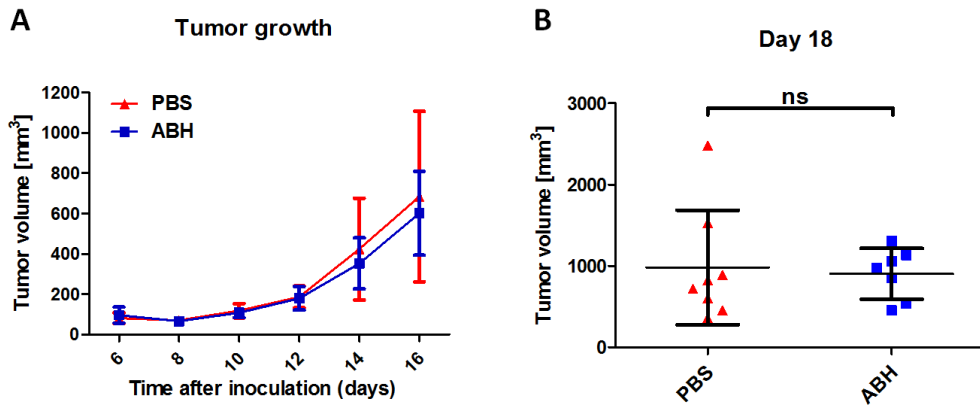
Figure 42. *Evaluation of antitumor efficacy of therapy with ABH ARG inhibitor. C57BL/6 mice were inoculated subcutaneously with 0.5x10^6 of LLC tumor cells. ABH was administered twice daily by oral route at the dose of 100 mg/kg for the first 14 days, whereas the control group received PBS. The graphs show tumor growth dynamics over time (A) and individual mice tumor volume display from measurements performed on day 18 (B). Each experimental group consisted of n = 7-8 mice. Data are presented as mean ± SD. An unpaired two-tailed t-test was used to compare groups. ns – not significant.*

Next, it was questioned whether OAT-1746 would impede the accelerated progression of LLC overexpressing ARG1. Therapy with ARG inhibitor strongly inhibited the growth of LLC-pLVX-ARG1 tumor (p <0.0001, one-way ANOVA with Tukey post-hoc test), and what is important, inhibition was to a similar extent as in the case of control LLC WT tumor (Figure 43). These results implicate that OAT-1746 not only can block the activity of ARG in the tumor microenvironment but also that overexpressed by tumor cells.
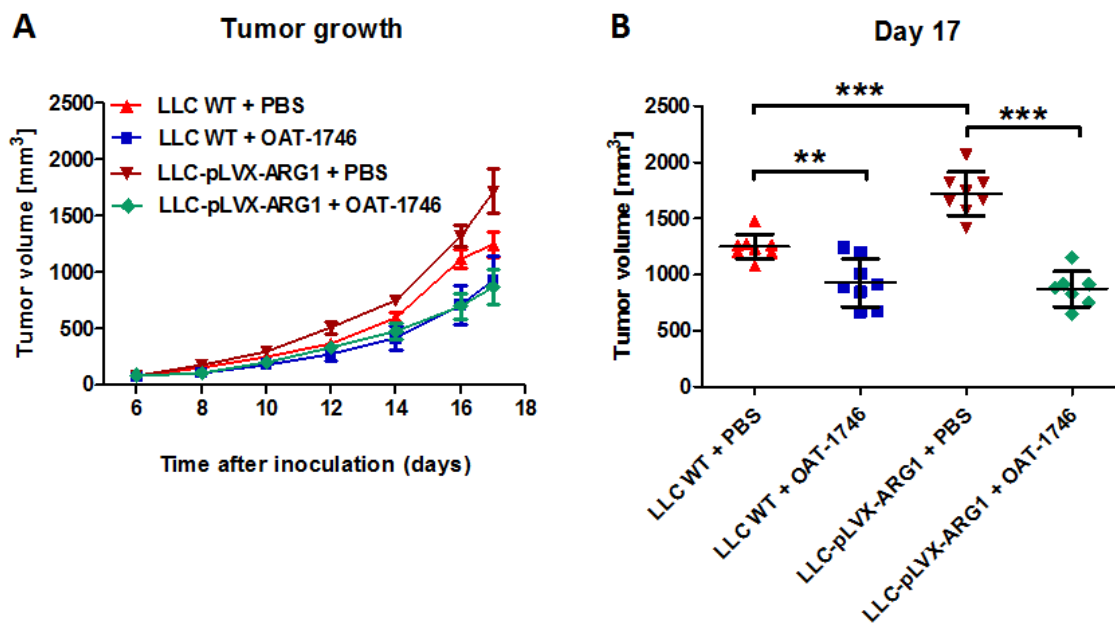
Figure 43. *Comparison of tumor growth in C57BL/6 mice inoculated with $0.1x10^6$ of LLC WT or LLC-pLVX-ARG1 cell line treated with OAT-1746 (20 mg/kg) or PBS for the whole experiment. The graphs show tumor growth dynamics over time (A), individual mice tumor volume display from measurements performed on day 17 (B). Each experimental group consisted of n = 7-8 mice. Data are presented as mean ± SD. One-way ANOVA with Tukey post-hoc test was used to compare groups. $**p \leq 0.01$, $***p \leq 0.001$.*

4.10.2 Mechanism of action studies using OAT-1746

To elucidate the mechanisms of therapeutic activity of OAT-1746 in above *in vivo* studies the proliferation of OT-I T-cells in a tumor-draining lymph node of mice with advanced LLC WT tumors was again verified. In OAT-1746 treated group proliferation

was improved as compared to mice with advanced tumors treated only with PBS (p = 0.0273, unpaired two-tailed t-test, Figure 44).
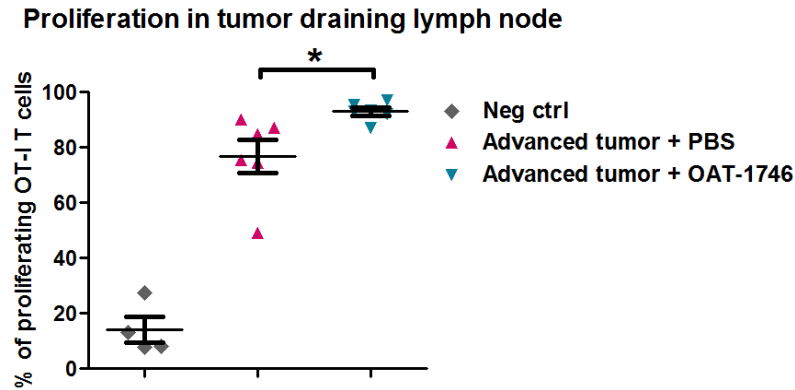
Proliferation in tumor draining lymph node

Figure 44. *Study of the antigen-specific proliferation in vivo in C57BL/6 mice with advanced tumors treated with OAT-1746. 0.5x10^6 of LLC tumor cells were inoculated subcutaneously on days 0 and 14 of the experiment in order to generat advanced and initial tumors, respectively. Isolated, CTV stained, OT-I CD8$^+$ lymphocytes were transferred intravenously on day 17. Antigen-specific proliferation was triggered by ovalbumin protein injected subcutaneously in the tumor area on day 18. In the selected group OAT-1746 was administered twice daily by an intraperitoneal route at the dose of 20 mg/kg on days 16-21, whereas the control group received PBS. The proliferation of OT-I T cells in tumor-draining lymph node (inguinal) was evaluated on day 21 by flow cytometry. Data are presented as means ± SD. An unpaired two-tailed t-test was used to compare groups. *p<0.05.*

To further resolve the clue of antitumor efficacy transgenic mice B6.Cg-Foxp3^{tm2Tch}/J were used. These mice co-express green fluorescence protein (GFP) and the T regulatory cell-specific transcription factor FoxP3. Mice were inoculated with LLC WT cells and were split into two groups treated either with OAT-1746 or PBS. The tumor growth rate was analogous to normal C57BL/6 with significant inhibition in OAT-1746 treated mice (p <0.0001, unpaired two-tailed t-test). Subpopulations of T-cells were analyzed by flow cytometry showing that ARG inhibitor receiving group had a significantly decreased percentage of regulatory T cells in the tumor (gated as CD25$^+$ FoxP3$^+$ cells among all CD3$^+$ CD4$^+$ cells, p = 0.0306, unpaired two-tailed t-test). Furthermore, OAT-1746 treated group had increased percentage in non-T regulatory lymphocytes (gated as CD3$^+$ FoxP3$^-$ cells among CD45$^+$ CD11b$^-$ F40/80$^-$ cells, p = 0.0278,

unpaired one-tailed t-test, Figure 45). These data suggest that OAT-1746 acts by changing the proportions of specific T-cell populations in the tumor microenvironment, especially by switching the balance towards less immunosuppressive T-cell phenotype.
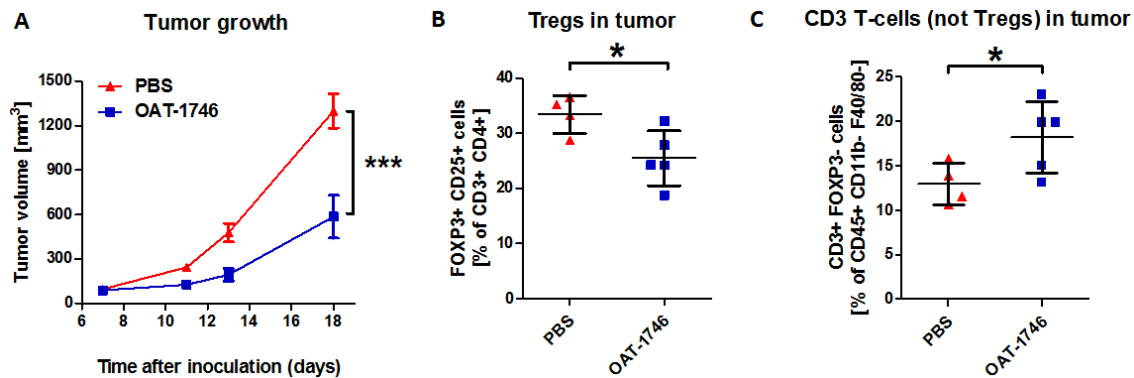
Figure 45. *Analysis of OAT-1746 immunomodulatory mechanisms on the immune cells in the tumor microenvironment of the lung cancer model. B6.Cg-Foxp3^{tm2Tch}/J mice were inoculated with 1x10^6 of LLC tumor cells and were treated twice daily with OAT-1746 by an intraperitoneal route at the dose of 20 mg/kg for the whole experiment, whereas control groups received PBS. Tumor growth was measured with a digital caliper. Mice were sacrificed on day 18 and tumors were harvested, processed, stained with antibodies and analyzed by flow cytometry. Tumor growth (A). Percentage of T regulatory cells identified as FoxP3$^+$ CD25$^+$ (B). Percentage of lymphocytes but not T regulatory cells identified as CD3$^+$ FoxP3$^-$ (C). Each experimental group consisted of n = 4-5 mice. Data are presented as mean ± SD. Unpaired one or two-tailed t-test was used to compare groups. *p<0.05, ***p≤0.001.*

4.10.3 Combination therapy with OAT-1746 and anti-PD-1

Considering that OAT-1746 given as monotherapy does not fully cure the mice in LLC model, it was important to verify whether combination therapy with a checkpoint blockade would amplify its antitumor effect. Mice received OAT-1746 alone or in combination with anti-PD-1, whereas the control group was injected with isotype control antibodies and PBS. The scheme of the *in vivo* experiment is presented in Figure 46.
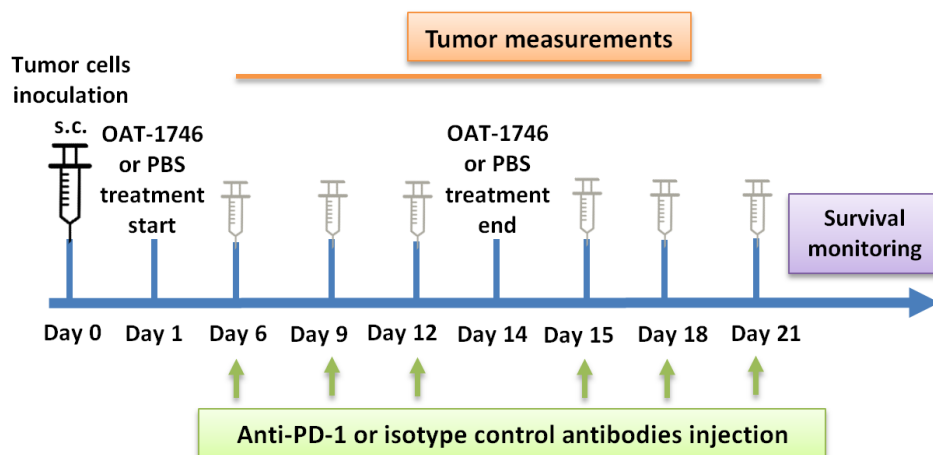
Figure 46. *Timeline of the in vivo experiment evaluating antitumor efficacy of the combination of OAT-1746 with anti-PD-1 therapy in the mouse lung cancer model LLC in C57BL/6 mice.*

In comparison with anti-PD-1 treatment, monotherapy with OAT-1746 more effectively inhibited tumor progression (mean tumor volumes measured on day 22: 2090 ± 260 mm^3 vs 1599 ± 340 mm^3). Importantly, the combination of anti-PD-1 with OAT-1746 significantly reduced tumor growth (1079 ± 153 mm^3) in comparison to single therapies confirming that combination therapies impose enhanced effects. Survival was equal 30 days for both OAT-1746 monotherapy and OAT-1746 combined with anti-PD-1 groups, being superior by 6 days in comparison with the control group that received PBS and isotype control antibody (Figure 47).
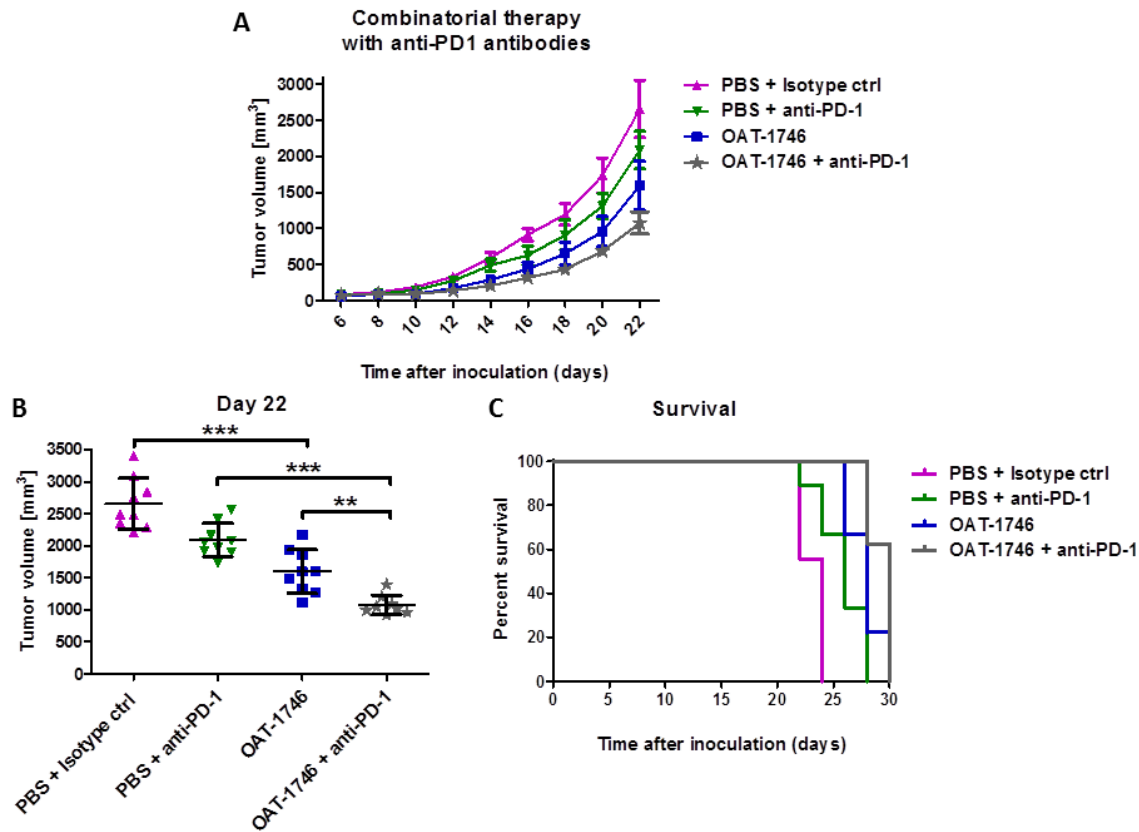
Figure 47. *Evaluation of antitumor efficacy of OAT-1746 combined with anti-PD-1 therapy. C57BL/6 mice were inoculated with 0.1×10^6 of LLC tumor cells. OAT-1746 was administered twice daily by an intraperitoneal route at the dose of 20 mg/kg for the first 14 days (control groups received PBS) while anti-PD-1 or isotype control antibodies by an intraperitoneal route at the dose of 10 mg/kg on selected days: 6, 9, 12, 15, 18, 21. Tumor growth over time (A). Individual mice tumor volume display from measurements performed on day 22 (B). Percent survival (C). Each experimental group consisted of n = 8-9 mice. Data are presented as mean ± SD. One-way ANOVA with Tukey post-hoc test was used to compare groups. **p≤0.01, ***p≤0.001.*

4.10.4 Combination therapy with OAT-1746, anti-PD-1 and DMXAA

As dual therapy did not result in total tumor remission in LLC tumor model the search for the other immunotherapies to combine with ARG inhibitor was continued. DMXAA, which is a stimulator of interferon genes (STING) agonist, has been chosen to add to the dual therapy. Accordingly, in this experiment triple combination group received: ARG inhibitor for the first 14 subsequent days, anti-PD-1 on selected days and DMXAA

given by intratumoral injection on day 8. As the result, the antitumor activity of OAT-1746 was even more potentiated in this combination (Figure 48, pink line). Noteworthy, dual therapies such as a combination of OAT-1746 with DMXAA or OAT-1746 with anti-PD-1 achieved better outcomes than monotherapies but were less effective than therapy with three immunomodulatory agents. Finally, the triple combination treatment prolonged the survival of mice until 36 days (Figure 48).
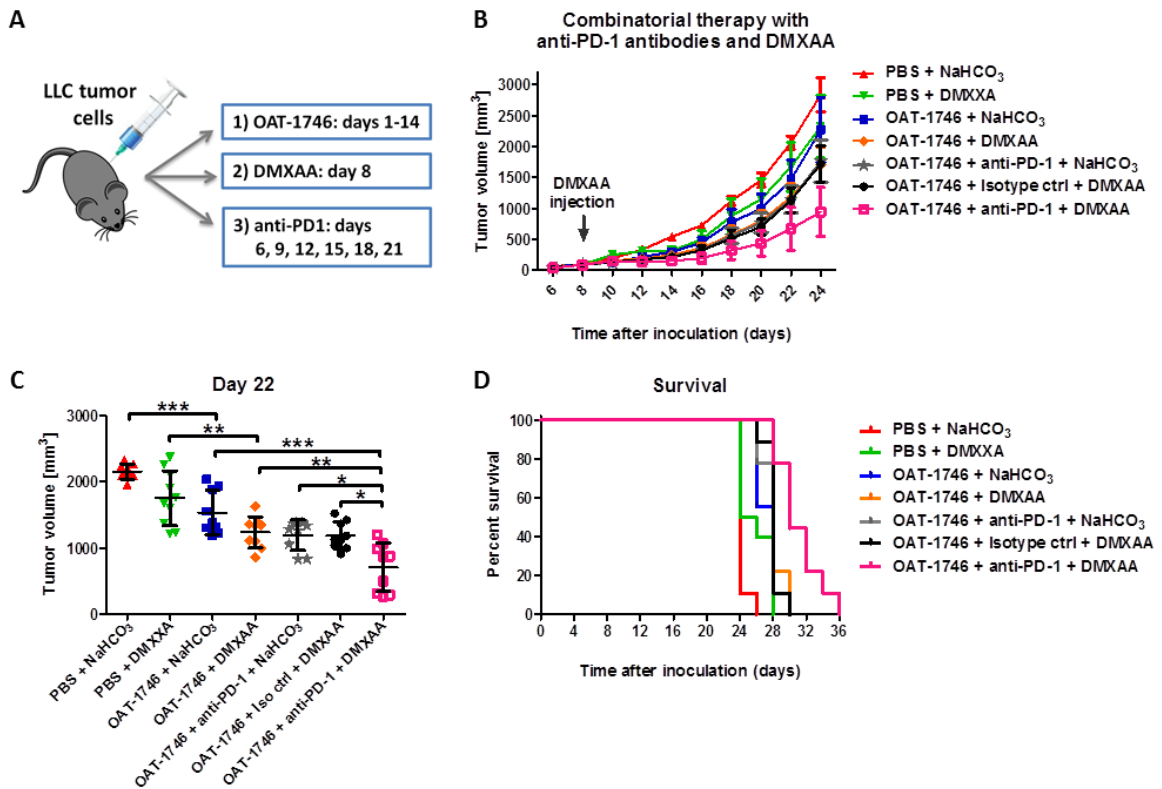
Figure 48. *Evaluation of antitumor efficacy of OAT-1746 combined with anti-PD-1 and DMXAA therapies. C57BL/6 mice were inoculated with 0.1×10^6 of LLC tumor cells. OAT-1746 was administered twice daily by intraperitoneal route at the dose of 20 mg/kg for the first 14 days (control groups received PBS), anti-PD-1 or isotype control antibodies by an intraperitoneal route at the dose of 10 mg/kg on days: 6, 9, 12, 15, 18, 21 and DMXAA by intratumoral injection at 0.5 µg/mouse on day 8 (control groups received $NaHCO_3$, which is DMXAA diluent). Scheme of the triple combination group showing received therapies (A). Tumor growth over time (B Individual mice tumor volume display from measurements performed on day 22 (C). Percent survival (D). Each experimental group consisted of n = 9-10 mice. Data are presented as mean ± SD. One-way ANOVA with Tukey post-hoc test was used to compare groups. *p<0.05, **p≤0.01, ***p≤0.001.*

5. DISCUSSION

5.1 ARG expression in the tumor microenvironment

Tumor development is linked with alterations in ʟ-arginine metabolic pathways in the malignant lesion [89, 135]. In the present study, the pattern of accumulation of myeloid cells expressing ARG1 is shown in reference to the tumor progression stage in murine lung tumor model with further differentiation of TAMs, M-MDSC and G-MDSC. Last decade it became increasingly relevant for researchers to elucidate the function of these cells in the tumor microenvironment leading to conclusions that tumor cells harbor them for creating the immune-suppressive microenvironment. Many mechanisms responsible for this strategy have been identified, including depletion of amino acids, production of NO and reactive oxygen species, expression of PD-L1 molecule, induction of T regulatory cells and impairment of NK cell-mediated cytotoxicity [247-249]. The comparison of peritoneal macrophages, TAMs and other cells in the advanced LLC subcutaneous model (day 19 after inoculation) revealed that only macrophages associated with tumor express high levels of ARG1, among others mentioned [250]. It was also shown that the induction of ARG1 in polarized M2 macrophages is mediated by hypoxia-inducible factor 1α induced by tumor-derived lactic acid [250]. In myeloid cells, especially in alternatively activated macrophages M2, IL-4 induced ARG1 expression might be adversarially modulated by TNF [251]. Importantly, both types of macrophages such as tissue-resident and tumor-recruited contribute to the overall development of tumor in the lung [252]. Flow cytometric analysis of samples from YARG mice with colon adenocarcinoma revealed ARG1 expression only in the tumor but not in other evaluated organs. ARG1^{+} cells predominantly expressed F4/80 marker being TAMs and minority expressed CD11c and MHC class II being activated dendritic cells. Moreover, tumor *in vivo* imaging allowed to clearly assess ARG1^{+} cells' distribution across the tumor microenvironment [253]. Accumulation of MDSCs is a characteristic feature of a variety of tumors originating from distinct tissues [254]. Extracted on day 30 MOC1 tumors, that represent a tumor model of head and neck squamous cell carcinoma, were highly infiltrated with myeloid cells mostly expressing markers characteristic for G-MDSC (Ly6G^{high}, Ly6C[inter]) and

displaying an up-regulated expression of ARG and iNOS, but not tryptophan-degrading indoleamine 2,3-dioxygenase (IDO) enzyme [255]. In cancer patients, the highest percentage of MDSCs (identified as CD14$^+$ HLA-DR$^{-/low}$) was reached in the tumor compared to tumor-draining lymph nodes and blood [256]. In this project mechanism of switching on the ARG1 expression in myeloid cells present in the tumor microenvironment was not studied. However, it is known that ARG1 expression in MDSCs is controlled by cyclic GMP, which is in turn regulated by phosphodiesterase 5 activity. Thus, compounds modulating intracellular cGMP levels, including phosphodiesterase 5 inhibitors, might be useful for reducing MDSCs-mediated immunosuppression [257]. Also, STAT-3 dependent mechanisms are involved in switching on ARG1 expression in MDSCs, as a positive correlation of STAT-3 phosphorylation and ARG1 activity was found. Further studies confirmed that inhibition of pSTAT3 diminished the expression of ARG1 and revealed that STAT3 binds to the promoter region of ARG1 in MDSCs [256]. A research group led by Augusto Ochoa studied the same murine tumor model LLC, and by using immunohistochemistry, they observed an accumulation of mature myeloid cells expressing ARG1, which is consistent with results presented in this study [87]. Comparison of murine tumor models revealed that cells expressing ARG1 are more abundantly present in poorly immunogenic murine tumor models, including LLC and B16F10, than in highly immunogenic models like CT-26 and 4T1 [258]. Importantly, myeloid cells with increased ARG expression were seen not only in the tumor but also in local lymph nodes where development of effective immune response should take place [124].

5.2 Plasma ʟ-arginine concentration in cancer

In addition to progressive infiltration of LLC tumors with ARG$^+$ myeloid cells, the results presented here show that mice with advanced tumors have significantly decreased plasma ʟ-arginine concentration indicating high ARG activity. It suggests that in late-stage tumors, ARG expression by myeloid cells affects not only the local tumor microenvironment but also alters the systemic balance of ʟ-arginine metabolism. On

the other hand, ι-arginine is considered to be one of the amino acids the most prominently decreased in patients with cancer-related cachexia [259]. However, the condition of mice with advanced tumors was favorable and rather did not represent the cachectic stage. Plasma ι-arginine concentration in these mice reached 26.2 ± 9.3 μM, whereas, in healthy mice, it oscillated around 147.8 ± 24.3 μM. In another study, ι-arginine concentration in plasma collected from mice with intermediate pancreatic ductal adenocarcinoma varied between 50-234 μM with a mean of 130 μM, whereas in tumor interstitial fluid (TIF) it was only 2 μM. Consequently, ι-ornithine concentration in TIF was higher than that in plasma of the same tumor-bearing mice suggesting enormously robust ARG activity exactly in the tumor microenvironment [260]. Measurement of human plasma ι-arginine concentration indicated a significant drop in cancer patients versus sex- and age-matched control subjects that was irrespective of weight loss that usually occurs in pancreatic cancer [261]. In the group of cancer patients representing 13 different histologies, plasma ARG1 expression was highly upregulated whereas ι-arginine concentration was significantly downregulated again, indicating not only the local phenomenon limited to the tumor site but systemic effect [235]. Similar observations were seen in plasma of one hundred patients with esophageal cancer, however there was no difference between patients with and without distant organ metastasis [262]. To provide the evidence that tumor mass and its surrounding environment indeed contains the ARG producing cells, the ARG plasma levels in ovarian cancer patients' cohort were compared at the diagnosis and after three chemotherapy cycles, and the significant drop in ARG activity has been reported after the treatment [263]. Studies of breast tumor samples obtained from patients during mastectomy found elevated ARG activity in 74% of tumors in comparison to adjacent normal tissues with corresponding histology. Moreover, contrary to normal tissues, the cationic isoform of ARG was found to be dominant in breast tumor samples [264]. Mice with breast carcinoma showed significantly reduced ι-arginine as well as NO plasma levels indicating that in comparison to NOS, ARG enzyme is responsible for greater depletion of substrate amino acid that is ι-arginine [265].

5.3 Correlation of plasma ɪ-arginine concentration with cancer stage

The inverse correlation between advanced LLC tumor stage and reduced ɪ-arginine concentration in plasma was observed in the present study. Weekly tracking of changes in ɪ-arginine metabolism revealed significant alterations only at the advanced stages of metastatic murine breast cancer development [266]. Another study showed a positive correlation between breast cancer stage and elevated arginase activity in patients' serum, which is in accordance with this study [267]. It was also suggested that increasing ARG activity in patients with benign mastopathy might serve as the biomarker for transformation towards breast cancer [268]. After breast tumor removal surgery, a significant drop of ARG activity and expression was seen in patients' blood [124, 268]. However, according to contrary reports, ɪ-arginine concentration was further decreased 24 hours after surgery, implying still the high activity of ARG [269]. These discrepancies might results from the distant time points of measurements after surgery - too short 24h versus several weeks [124, 268, 269]. Concerning pulmonary malignancies, profiling of plasma free amino acid including ɪ-arginine was proposed for detection of early lung cancer [270, 271].

5.4 Effect of ARG activity and ARG inhibitors on T-cells proliferation and CD3 chains expression

ARG has been identified as of cells proliferation inhibiting factor many decades ago. At that moment, researchers isolated the enzyme from the liver, where is abundantly expressed as a part of the urea cycle [272]. The specificity of an unknown then 'inhibitor' has been verified by the addition of substrate ɪ-arginine and observed accumulation of ɪ-ornithine [272, 273]. Many years later, the inhibitory mechanisms of ARG have been well established. In terms of cancer immunotherapy, the most important issue raises the inhibition of T-cells as it impairs mounting the proper response against cancerous cells [81]. Experiments performed in this study show that human and murine recombinant ARG1 inhibits *in vitro* proliferation of both types of T-cells: cytotoxic and helper in a dose-dependent manner. Similar results were obtained using mouse recombinant enzyme ARG2 cultured with antigen-specific CD8^{+} T-cells.

Importantly, the addition of one among several ARG inhibitors (ABH, OAT-1617, OAT-1746) re-establish the normal T-cells proliferation. Other researchers discovered that ARG2 is the dominant isoform of this enzyme expressed in dendritic cells - the main population of APCs that play a crucial role in activating cytotoxic T-cells for the eradication of transformed cells. T-cells primed by dendritic cells with repressed expression of ARG2 displayed enhanced proliferative potential [274]. Furthermore, ARG1^{+} MDSCs isolated from human tumors inhibited autologous T-cell proliferation in a dose-dependent fashion, which indicates the same direction as the results presented in the present study [256]. Another study points at strong inhibition of CD4^{+} and CD8^{+} T-cells proliferation by increasing ratios of tumor isolated G-MDSC that was partially abolished in the presence of nor-NOHA ARG inhibitor [255]. The same inhibitor rescued the proliferation of T-cells exposed to ARG[+] neuroblastoma tumor cells [122]. Nor-NOHA also prolonged the survival of infiltrating T lymphocytes in prostate carcinoma organ cultures [275]. It was successfully applied to reverse the inhibitory influence of MDSCs isolated from 4T1 tumor-bearing mice on T-cells proliferation rate [276]. Furthermore, IPI-145, a selective PI3Kδ/γ inhibitor, was shown to reduce the expression of ARG1 in tumor and splenic MDSCs, thereby reversing their suppressive capacity on T-cell proliferation [255]. During studies presented in this thesis, the negative correlation between increasing ARG1 concentration and the downregulation of CD3ζ and CD3ε chains expression on *in vitro* cultured T-cells was found. It has decisive functional implications as the expression of CD3 complex together with TCR, plays a pivotal role in antigen recognition that leads to T-cell activation as a consequence of cascade signaling. Moreover, in the presented project, the dynamics of the changes mentioned above of CD3 chains were studied in detail in isolated T-cells in the presence of a high concentration of ARG1. Tracking it in time from 2 to 72h revealed not very rapid but gradual downregulation pattern. Similarly, using Jurkat CD4+ T-cell line, Rodriguez et al. showed progressive CD3ζ expression decline in ʟ-arginine free medium with the lowest point at 72h. The explanation was the induction of CD3ζ mRNA instability by post-transcriptional mechanisms [100]. Their further studies also confirmed the negative influence of a lack of ʟ-arginine on CD3ε chain [87].

Also, ARG-expressing neutrophils isolated from sepsis patients were found to negatively modulate CD3ζ [277]. Down-regulation of CD3ζ has been linked with the accumulation of MDSCs not only related to cancer in both murine and human settings [94, 278]. Importantly, in the present study, it was shown that the unfavorable effects of ARG1 on the expression of CD3ε and CD3ζ chains in T-cells could be propitiously abolished by treatment with OAT-1746. Another ARG inhibitor - nor-NOHA was utilized to explain the inhibitory mechanism of mouse embryonic stem cells that caused the downregulation of TCR-associated CD3ζ chain expression through the activity of ARG1 [227]. Very similar conclusions were drawn in the case of hematopoietic progenitor cells or polymorphonuclear leukocytes co-cultured with T-cells in the presence of nor-NOHA [138, 279]. It was shown that nor-NOHA is able to upregulate the expression of both CD3ζ and CD3ε on T-cells co-cultured with tumor-associated myeloid cells [87]. The results obtained during this study indicate that *in vivo* proliferation of antigen-specific OT-I T-cells and CD3ζ expression is diminished in late-stage tumors when the number of myeloid cells expressing ARG1 increases. Another group studied the *in vivo* proliferation of antigen-specific OT-II T-cells in the presence of dendritic cells overexpressing ARG2. In accordance with the results of this study, they observed down-regulated CD3ζ expression [274]. Furthermore, this study shows that impaired *in vivo* antigen-specific proliferation of OT-I T-cells in mice with advanced LLC tumors can be improved by OAT-1746. Nor-NOHA has been exploited to confirm that activation of antigen-specific T-cells (both OT-I and OT-II) depends on ARG activity in co-cultured *in vitro* myeloid cells derived from the tumor [87]. Already published results by our group from the Department of Immunology indicate the impairment of *in vivo* OT-I T-cells proliferation in the tumor-draining lymph node after local inoculation of ovarian tumor-derived extracellular vesicles containing ARG1. Furthermore, this negative effect was abrogated while mice were treated with OAT-1746 ARG inhibitor [121].

There is a possibility that the proliferative potential of isolated T-cells from the blood of healthy donors might vary very slightly between donors available at the blood station. This might results in fewer or more peaks of T-cells after the same period of incubation time. Therefore, ideally it would have been to compare all ARG inhibitors

using T-cells from one donor. However, this was not technically possible due to the limited availability of blood samples given by one donor. In each experiment, the proper controls were set to compare as reference for a selected donor to eliminate these discrepancies.

In the present study, the negative impact of ARG1 on the production of cytokines by T-cells such as IFN-γ and TNF-α was demonstrated. These cytokines secreted in the tumor microenvironment and secondary lymphoid organs are necessary to maintain the immune surveillance and mount the appropriate antitumor response [280, 281]. MDSCs depletion mediated by anti-Ly6G or anti-Gr1 antibodies in a murine model of lung cancer resulted in elevated intracellular expression of IFN-γ, perforin and granzyme by cytotoxic T-cells. In addition, total intratumoral cytokine expression such as IFN-γ, TNF-α and IL-12 was higher than in the group treated with isotype control antibodies [282]. In the present study, treatment of T-cells with OAT-1746 ARG inhibitor resulted in a reversal of T-cells percentage producing IFN-γ and TNF-α to the control level. In another study, an ARG inhibitor named compound 9 fully reversed the *ex vivo* activation and effector function of T-cells suppressed by recombinant ARG, causing the restoration of appropriately high concentrations of secreted IFN-γ, production of granzyme B and IL-2. Also, in the presence of compound 9, production of IFN-γ was re-established once murine splenocytes were co-cultured with peritoneal macrophages or MDSCs expressing ARG [283]. CB-1158 was shown to upregulate the secretion of IFN-γ and granzyme B by T-cells cultured in a medium conditioned by cancer patient ARG[+] granulocytes [235]. Another study showed that in hepatitis C virus infection, MDSCs-associated ARG1 expression suppressed the production of IFN-γ by NK cells, and this effect was reversible by supplementation of ι-arginine. More profound studies revealed that diminished IFN-γ production resulted from insufficient activation of the mammalian target of rapamycin, which is central for cellular metabolism regulation [284]. Moreover, antigen-specific stimulation of T-cells from tumor-draining lymph node resulted in elevated secretion of IFN-γ after treatment with IPI-145, which acts by reducing ARG1 expression in tumor MDSCs [255].

Based on several optimization experiments, 250 µg/ml concentration of recombinant human ARG1 was selected to use for all further *in vitro* proliferation studies. The initial readout to choose the concentration was total inhibition of proliferation of both CD4$^+$ and CD8$^+$ T-cells. ARG1 was very carefully titrated so that the highest concentration of the enzyme was selected to use in the search for the lowest concentration of the ARG inhibitor that unblocks inhibited divisions. With the progress of the project more readouts, than only proliferation of T-cells, were applied, including expression of CD3ε and CD3ζ chains as well as studies of cytokines production such as INF-γ and TNF-α. Unfortunately, in some experiments, an initially selected ARG1 concentration of 250 µg/ml was not enough to obtain the statistically significant drop in expression of CD3ζ or production of INF-γ. Nonetheless, in each case, a decline was observed. Considering the concentration selection strategy from the point of finished experiments, it should be selected based on more readouts.

5.6 The effect of supplementation of ι-citrulline on T-cells in ARG-depleted microenvironment

The first rescue of ARG-mediated inhibition of proliferation by the addition of ι-citrulline was described in 1960 [285]. Recycling of ι-arginine is possible from ι-citrulline in a two-step enzymatic process via the intermediate named argininosuccinate that requires the subsequent activity of ASS and ASL enzymes [91]. In T-cells, ALS is expressed constitutively, whereas ASS expression varies based on the ι-arginine level being highly induced in the low ι-arginine concentration [286]. We and others [286] show that externally added ι-citrulline is sufficient to reconstitute the proliferation of CD4$^+$ T-cells under ι-arginine restriction. Werner *et al.* studied further the mechanism beyond revealing that ι-citrulline transport in T-cells is mediated by L-type amino acid transporter 1 [286].

5.7 Effect of ARG deficiency on tumor growth

The present study provided evidence that mice with induced ARG1 KO in all types of cells develop smaller LLC tumors and that this event is mediated by enhanced response of TILs. Similarly, our results show that the genetic ablation of ARG1 only in myeloid

cells, which represent the main source of immunosuppressive enzyme in the tumor microenvironment, results in the development of smaller LLC tumors. Other very compelling findings were described by another research group also in LLC model: antibody-mediated depletion of MDSCs (by anti-Gr1 or anti-Ly6G antibodies) augmented the antitumor immune activity and lead to inhibition of tumor growth [282]. The increased frequency, as well as the activity of the CD8^{+} T and NK cell effectors in the tumor, were proved in comparison to controls [282]. Providing that ARG expression in depleted MDSCs was responsible for unfavorable effects on the immune system, these results fully support the findings of the present study. The expression of ARG1 in TAMs was confirmed to be crucial for faster tumor development as the weight of LLC tumors containing ARG1-deficient macrophages was considerably lower than those with WT macrophages [250]. Results of the present study showing that mice with KO of ARG1 in myeloid lineage develop smaller tumors that are very consistent with the results obtained by Steggerda *et al*. in the same LLC murine tumor model [235]. Another study shows that induction of ARG1 loss-of-function by shRNA interference repressed more invasive *in vitro* cellular behaviors of hepatocellular cancer cells [126]. Interestingly, mice with genetic deletion of ARG2 represented better response against growing B16F10 and MC38 tumors leading to considerably reduced tumors or even tumor-free mice [287]. Furthermore, ARG2$^{-/-}$ in mice with tumor yielded a higher percentage of TILs and further analysis revealed elevated CD8^{+} T-cells subpopulation [287]. These findings are consistent with the present study results showing an increased percentage of TILs in ARG total KO mice.

5.8 Effect of ARG overexpression on tumor growth

In the present study, the search for the murine tumor model in which tumor cells would display high ARG expression was undertaken. ARG expression was verified in seven tumor cells lines of various origin at the protein level using two independent methods. To our best knowledge, there is no mouse solid tumor model with such elevated expression. However, in humans, there are primary tumor cells in which ARG presence has been confirmed. This include lung cancer [283, 288], hepatocellular carcinoma [126], acute myeloid leukemia [119], neuroblastoma [122], prostate cancer

[289], breast cancer [290], thyroid carcinoma [133] and colorectal cancer [130]. One research group has investigated the ARG1 and ARG2 expression levels in lysates of murine LLC tumors and found that both enzymes were abundantly expressed in the tumor micromilieu as well as high enzymatic activity was confirmed [87]. Likewise, the present study results are consistent with their observations about ARG expression in LLC tumor microenvironment. Nonetheless, this tumor cell line itself contains very little amount of ARG (as verified by Western Blotting and FACS analysis) and exhibits no enzymatic activity. Therefore, to enhance the effect, it was decided to introduce the additional ARG1 enzyme into tumor cells. As a result, faster *in vivo* tumor growth in LLC and B16F10 models with ARG1 overexpression was observed. Similarly, in a previous study of ovarian carcinoma ID8, more intensified tumor development was observed once ARG1 was overexpressed [121]. ARG overexpression was shown to be the most prominent in the late stages of colorectal cancer, and it was associated with metastases to lymph nodes [130]. Genetic modification and elevation of ARG1 or ARG2 activity promoted *in vitro* proliferation, invasion and migration of hepatocellular cancer cells and glioblastoma, respectively [126, 291]. In cancer patients, higher expression of ARG1 was linked with bigger size and more aggressive tumor progression [126]. In the co-culture system, overexpression of ARG by macrophages enhanced tumor cells divisions [292]. Similar results were obtained in colon adenocarcinoma MC-38 that overexpressed ARG2 [287]. Importantly, results presented here show that more aggressive ARG1-overexpressing tumor growth was dependent on the presence of an intact host immune system as in immunodeficient RAG2 KO mice the effect of accelerated tumor growth was abrogated. In the literature, there is a report in which researchers used immunodeficient C57BL/6-Prkdc[scid] mice that lack functional B and T cells to evaluate the mechanism of action of ARG inhibitor nor-NOHA in LLC model. In accordance with the present study, it was suggested that the antitumor effect of ARG inhibitor is at least partially dependent on lymphocyte function [87].

5.9 Effect of ARGs inhibitor on tumor cells *in vitro*

In the present study, the inhibition activity of three ARG inhibitors (ABH, OAT-1617 and OAT-1746) was compared using several tumor cell lines overexpressing ARG1 or ARG2. Based on these experiments, the most potent inhibition properties were attributed to OAT-1746. On the other hand, the effect of ARG inhibitors on the growth of tumor cells *in vitro* was not studied in this project. However, there are reports that focus on revealing the effect of ARG inhibitors on *in vitro* tumor growth in the literature. For instance, *in vitro* growth of murine renal cancer cell line CL-19 was inhibited by incubation with nor-NOHA. Effective ARG inhibition was substantiated by measurement of amino acids showing that ʟ-arginine concentration remained very high, whereas ʟ-ornithine emerged as low [293]. Nor-NOHA reduced *in vitro* tube formation and migration of glioblastoma cells U-251 MG ARG2-overexpressing cells [291]. Similarly, nor-NOHA antitumor activity was tested *in vitro* on HepG2 hepatocellular carcinoma cells showing antiproliferative effects linked with inhibited migration and invasion, increased NO production and apoptosis induction [294]. NOHA usage significantly inhibited *in vitro* cell proliferation in high ARG expressing human breast cancer cell lines such as MDA-MB-468 [290], HCC1806 and HCC 70 [295]. Further mechanistic analysis revealed that cells died due to apoptosis induction, in detail by activation of caspase-3 and caspase-8 [295, 296]. Furthermore, the implementation of nor-NOHA to *in vitro* cultured chronic myeloid leukemia cells K562 that express high levels of ARG2 proved to have an anti-leukemic effect under the hypoxic but not normoxic conditions [297]. An analogous study evaluated the *in vitro* growth of osteosarcoma cell lines SaOS-2 and OS-17, which express relatively high levels of ARG2 under hypoxic conditions. As a result, all tested compounds NOHA, BEC and putative, but nonspecific ARG inhibitor α-difluoromethylornithine (DFMO) prevented the hypoxia-induced proliferation of tumor cells [298]. Additionally, the role of ARG2 was determined in the hypoxia-induced proliferation of cervical cancer HeLa cells by modulation of ARG activity again with DFMO. The authors indicated that fluorinated ornithine analog - DFMO abolished the increase in the number of viable cancer cells and pointed that induction of ARG2 expression under hypoxic conditions is

linked with epidermal growth factor receptor signaling pathway [299]. ARG overexpressing macrophages treated with ʟ-norvaline displayed significantly downregulated ARG activity that halted the production of ʟ-ornithine and putrescine being the substrate for polyamines synthesis essential for cell growth. This, in turn, reduced the growth of co-cultured breast cancer cells ZR-75-1. Furthermore, inhibition of macrophage ARG activity by ʟ-norvaline augmented the macrophage nitrite production enhancing the NO-mediated antitumor cytotoxicity [292]. Activity and mechanism of action of ʟ-norvaline (that has been described as ARG inhibitor) containing compound MF13 were investigated in human 7 hepatocellular carcinoma (HCC) cell lines *in vitro,* showing antiproliferative effects that were caused by cell cycle arrest at S-phase and activated pathway of apoptosis [244].

5.10 *In vivo* antitumor efficacy of ARG inhibitors as monotherapy

This study shows that dysregulated metabolism of ʟ-arginine by upregulated ARG1 expression in TAMs and MDSCs present in the tumor microenvironment can be successfully modulated by the treatment with OAT-1746 ARGs inhibitor aiming at reducing the immunotherapy brakes and potentiating T-cell mediated antitumor immune response. Moreover, in secondary lymphoid organs, the activity of immunosuppressive ARG2 was proved to be at a considerable level. Therefore, the dual inhibition of both ARGs seems to be an important therapeutic issue [287]. So far, due to the lack of ARG inhibitors with satisfying properties, many researchers have used supplementation of ʟ-arginine as the imitation of ARG blockade. In contrast, others tried to add enormous amounts of poor inhibitors such as nor-NOHA, BEC or ABH to achieve the desired effect [82, 300]. In LLC model, treatment with nor-NOHA resulted in the generation of antitumor immunity, thus inhibiting tumor growth. The result was escalated once nor-NOHA was combined with supplementation of ʟ-arginine, suggesting the fundamental role of this amino acid [87]. It was recently emphasized that supplementation of ʟ-arginine would be a promising strategy for boosting T-cell mediated antitumor immune response [301]. Importantly, treatment with nor-NOHA resulted in a reduction of the number and the size of lung metastases in the murine 4T1 breast cancer model [276]. In another study, ʟ-norvaline containing

compound, MF13 was administered intraperitoneally as monotherapy at 10 mg/kg *in vivo* in nude mice with hepatocellular carcinoma HepG2 or Bel-7402, and this treatment resulted in strong tumor growth inhibition [244]. MF13 used at 15 mg/kg dose also inhibited the growth of human melanoma and colon cancer in nude mice [302]. The recently developed compound by American company Calithera Biosciences, CB-1158, is a potent and orally-bioavailable small-molecule inhibitor of ARGs [303]. However, the tremendous difference between CB-1158 and OAT-1746 is the permeability through cell membranes. CB-1158 does not penetrate, so it can act only on the extracellular ARGs, while OAT-1746 also reaches the intracellular compartments of the cells. CB-1158 at the dose of 100 mg/kg (oral administration, twice daily) partially inhibited the tumor growth in several syngeneic tumor models, including LLC, B16F10, CT-26 and 4T1 [235]. In comparison, OAT-1746 given precisely the same way at 50 mg/kg reduced the tumor growth in the first 3 above mentioned tumors [233]. In turn, in this study the dose of 20 mg/kg of OAT-1746 given intraperitoneally was effective in inhibiting LLC tumor growth. Transgenic mice with tagged FoxP3 allowed to resolve the mechanisms of antitumor activity of OAT-1746 - together with increase of CD3$^+$ T-cells, the decrease of FoxP3$^+$CD25$^+$CD4$^+$ T-cells was observed after treatment. Considering pharmacological inhibition of ARGs as similar to ARG deletion models, it has been recently shown that ARG2 KO mice have reduced frequencies of regulatory T-cells in tumors [287]. Also increased frequency of TILs in ARG2$^{-/-}$ mice is consistent with results of mice treated with OAT-1746 presented in this study [287]. Previously studied mechanisms of antitumor activity of CB-1158 indicate that its action is dependent on the presence of immune cells such as CD8$^+$ and NK cells, which was confirmed by experiments with depletion of this cells subpopulation [235]. Notably, the treatment of mice lacking ARG1 expression in the myeloid lineage with CB-1158 did not further diminish tumor growth, indicating specific on-target activity of CB-1158 [235]. Another ARG inhibitor named 'compound 9' prevented the lung tumors growth in Kras mutant mice by creating an immune favorable tumor microenvironment that is by upregulating the percentage of CD3$^+$ and CD4$^+$ T cells as well as the ratio of CD8$^+$ to FoxP3$^+$ cells [283]. Moreover, a very meaningful finding was identified in mice lacking

ARG2 expression – it improved the effector function of antigen-specific CD8^{+} T-cells measured as *in vivo* killing [287]. The antigen-specific killing ability of effector CD8^{+} T cells is critical for protective immunity against developing cancer. In another study, *in vitro* cytotoxic activity of OT-I T-cells against target tumor cells was diminished in the presence of ARG1-positive G-MDSCs. Furthermore, effector functions of antigen-specific T-cells were partially restored by the addition of nor-NOHA [255]. This might further explain the mechanism of antitumor efficacy of OAT-1746 beyond only increasing the frequencies of TILs.

5.11 *In vivo* antitumor efficacy of ARG inhibitors in combinatorial therapies

The experiments performed in this project demonstrated that *in vivo* ARG inhibition by OAT-1746 abrogated local immunosuppression mediated by ARG1 in myeloid cells and, in combination, enhanced response to therapy with an anti-PD-1 monoclonal antibody. However, a recent study suggested that anti-PD-1 therapy should not be synergized with pharmacological inhibition of ARG1 as PD-1 blockade decreases the number of ARG1-positive TAMs favoring the ARG1-negative phenotype [253]. Nonetheless, ARG inhibitor CB-1158, while combined with anti-PD-L1 therapy in highly immunogenic model CT-26, resulted in 60% of complete responses and limited the number of lung metastases [235]. The same inhibitor used in poorly immunogenic tumor model B16F10 strongly potentiated the effect of adoptive T-cell therapy. On the other hand, in 4T1 model combination of CB-1158 with even two different checkpoint inhibitors anti-PD-1 and CTLA-4, only partially inhibited the tumor growth [235]. Moreover, it was shown that splenic CD11b^{+} GR1^{+} MDSCs isolated from mice with LLC tumors express PD-L1 that might be involved in creating an inhibitory microenvironment by suppressing T-cell activation through interaction with PD-1 immune checkpoint found on T-cells. Therefore, the combination of ARG inhibitor with anti-PD-1 or anti-PD-L1 antibodies seems to be a reasonable direction [27]. Obviously, immunotherapy approaches and outcomes depend on the immune profiles of murine tumor models [304]. *In vivo* application of low-dose selective PI3Kδ/γ inhibitor that indirectly down-regulates ARG1 expression in G-MDSC augmented the response to PD-L1 treatment in

head and neck squamous cell carcinomas [255]. The proposed mechanism beyond PI3Kδ/γ inhibitor effect included elevated number of CD8^{+} TILs, higher percentage of degranulated CD107a-positive CD8^{+} T-cells and upregulated expression of PD-1 and 4-1BB co-stimulatory molecule on TILs [255]. The idea of pharmacological ARG inhibition is supported by recent results in which 80% of ARG2^{-/-} mice rejected the MC-38 colon tumors in combination therapy with anti-PD-1 [287]. Milestone steps were undertaken to identify the biomarkers useful in selection of patients that would be likely to respond to checkpoint blockade therapy. Based on the results of the present study addition of ARG expression to the list would be additional clue that would be suggestive how widespread is the immunosuppression of the patient [305]. Murine studies using MC-38 tumors showed inhibited tumor growth upon four intraperitoneal injections of 100 μg ABH ARG inhibitor, however combination therapy with anti-PD-1 antibodies did not enhanced the effect. On the other hand, survival was prolonged by 10 days in the dual combination group as compared to monotherapy only with ABH inhibitor [253]. Another group studied the antitumor efficacy of combinatorial therapy of ARG inhibitor nor-NOHA in addition to DFMO, which targets ornithine decarboxylase - a key enzyme for polyamine synthesis. The results in lung cancer model LLC indicate that inhibition of tumor growth is at a similar level in both monotherapies and dual therapy. However, the combination therapy resulted in a reduction of the average volume of metastases [306]. In the murine model of urethane-induced lung carcinogenesis 6-gingerol, that was described to possess inhibitory activity towards ARG, reprogrammed macrophage polarization from tumor-promoting ARG positive M2 to immune-stimulatory iNOS positive M1 phenotype and prevented the tumor development. 6-gingerol mildly suppressed the growth of LLC tumor in the allograft model, but the combination with nor-NOHA inhibitor escalated the antitumor effect [246]. In the present study, vascular disrupting agent DMXAA (STING agonist) was chosen to enhance *in vivo* effect of OAT-1746 in combination with anti-PD-1. In non-small cell lung cancer (NSCLC) it was found that DMXAA activity not only has anti-vascular activity but also impacts the TAMs by re-educating anti-inflammatory M2 type towards a pro-inflammatory M1 phenotype [307]. Based on literature search it

appears that no one has ever studied the antitumor effect of combination of DMXAA with ARG inhibition, so the results of this study are the first to show that, similarly to checkpoint blockade, DMXAA potentiates antitumor efficacy of ARG inhibitor.

5.12 Concluding remarks

The generation of the immunosuppressive environment by tumor is a very complex process that involves not only one but numerous mechanisms. Undoubtedly, based on the results presented in this doctoral thesis, local ARG expression represents one of them, which is powerful in suppressing T-cells mediated responses. So far, CB-1158 is the only ARG inhibitor that has entered the clinical studies. It is currently designated for testing under the identifier INCB001158 in several clinical trials concerning Immuno-oncology (NCT02903914, NCT03910530, NCT03314935) [72]. However, OncoArendi Therapeutics company that developed OAT-1746, claims to enter the first phase of clinical trials in cancer patients in 2020/2021 [308]. In summary, the results of this study demonstrate that quenching ARG-mediated ι-arginine depletion by the use of ARG inhibitors in cancer settings makes a pivotal contribution to boosting the antitumor potential of T-cells. However, being aware of the existing opposite strategy based on amino acid deprivation, the use of ARG inhibitors must be carefully matched with the type of tumors to be treated, with special attention to ι-arginine auxotrophic malignancies [143].

Very recently, an entirely new therapeutic approach that is definitely worth attention is a phase I first-in-humans clinical trial with identifier NCT03689192 concerning the vaccine with ARG1 peptides that are currently tested in 10 patients with a variety of solid metastatic tumors. The scientific background for its supposed efficacy is the activation of ARG1-specific T-cells, which have been identified in cancer patients, that are expected to eliminate the immunosuppressive ARG1-positive cells in the tumor microenvironment [72, 309]. A research group lead by Mads Hald Andersen has previously described the existence of T-cells specific for ARG1 being able to recognize and react with ARG1-expressing cells such as dendritic cells [310]. In another study, they identified peptides derived from ARG1 that generated disease stage-dependent

response by CD4^{+} T-cells isolated from patients with chronic myeloproliferative neoplasms [311]. A very recently published study points at ARG2 as a novel target for designing vaccines with immune-modulatory potential. The authors identified the effector T-cells specific for ARG2 that can recognize the target tumor cells and myeloid cells expressing ARG2. Furthermore, twice vaccination using ARG2 peptide vaccine (on day of inoculation and day 7) of mice with LLC tumors resulted in a significant reduction of tumor growth, identifying the next candidate for development in the cancer immunotherapy field [312].

6. CONCLUSIONS

- The impaired antigen-specific local immune response is dependent on ARG activity as ARG expression in the tumor microenvironment increases, while ʟ-arginine plasma concentration decreases with tumor progression

- ARG1 deficiency delays, whereas ARG1 overexpression accelerates LLC tumor progression in a lymphocyte-dependent manner

- Both recombinant ARG1 and ARG2 suppress T-cells cultured *in vitro*. However, ARG inhibitors restore the T-cells proliferation, CD3 expression and cytokines production

- OAT-1746 better than OAT-1617 and ABH inhibits the activity of tumor-associated and secreted ARG1 and ARG2, exhibiting the highest potential

- ARG inhibition by OAT-1746 delays the LLC tumors progression by modulating T-cells response in the tumor microenvironment

- ARG is a relevant target in cancer immunotherapy and inhibition of ARG represents a promising approach among other antitumor therapies

7. REFERENCES

1.   Basu, A.K., *DNA Damage, Mutagenesis and Cancer.* Int J Mol Sci, 2018. **19**(4).
2.   Hanahan, D. and R.A. Weinberg, *The hallmarks of cancer.* Cell, 2000. **100**(1): p. 57-70.
3.   Loeb, L.A., K.R. Loeb, and J.P. Anderson, *Multiple mutations and cancer.* Proc Natl Acad Sci U S A, 2003. **100**(3): p. 776-81.
4.   Balkwill, F.R., M. Capasso, and T. Hagemann, *The tumor microenvironment at a glance.* J Cell Sci, 2012. **125**(Pt 23): p. 5591-6.
5.   Theocharis, A.D., et al., *Extracellular matrix structure.* Adv Drug Deliv Rev, 2016. **97**: p. 4-27.
6.   Guo, S. and C.X. Deng, *Effect of Stromal Cells in Tumor Microenvironment on Metastasis Initiation.* Int J Biol Sci, 2018. **14**(14): p. 2083-2093.
7.   Valkenburg, K.C., A.E. de Groot, and K.J. Pienta, *Targeting the tumour stroma to improve cancer therapy.* Nat Rev Clin Oncol, 2018. **15**(6): p. 366-381.
8.   Hanahan, D. and R.A. Weinberg, *Hallmarks of cancer: the next generation.* Cell, 2011. **144**(5): p. 646-74.
9.   Italiani, P. and D. Boraschi, *From Monocytes to M1/M2 Macrophages: Phenotypical vs. Functional Differentiation.* Front Immunol, 2014. **5**: p. 514.
10.   Murray, P.J., et al., *Macrophage activation and polarization: nomenclature and experimental guidelines.* Immunity, 2014. **41**(1): p. 14-20.
11.   Hao, N.B., et al., *Macrophages in tumor microenvironments and the progression of tumors.* Clin Dev Immunol, 2012. **2012**: p. 948098.
12.   Sica, A., et al., *Macrophage polarization in tumour progression.* Semin Cancer Biol, 2008. **18**(5): p. 349-55.
13.   Atanasov, G., et al., *TIE2-expressing monocytes and M2-polarized macrophages impact survival and correlate with angiogenesis in adenocarcinoma of the pancreas.* Oncotarget, 2018. **9**(51): p. 29715-29726.
14.   Pathria, P., T.L. Louis, and J.A. Varner, *Targeting Tumor-Associated Macrophages in Cancer.* Trends Immunol, 2019. **40**(4): p. 310-327.
15.   Sorensen, M.D., et al., *Tumour-associated microglia/macrophages predict poor prognosis in high-grade gliomas and correlate with an aggressive tumour subtype.* Neuropathol Appl Neurobiol, 2018. **44**(2): p. 185-206.
16.   Tiainen, S., et al., *High numbers of macrophages, especially M2-like (CD163-positive), correlate with hyaluronan accumulation and poor outcome in breast cancer.* Histopathology, 2015. **66**(6): p. 873-83.
17.   Wang, H., et al., *High numbers of CD68+ tumor-associated macrophages correlate with poor prognosis in extranodal NK/T-cell lymphoma, nasal type.* Ann Hematol, 2015. **94**(9): p. 1535-44.
18.   He, H., et al., *Endothelial cells provide an instructive niche for the differentiation and functional polarization of M2-like macrophages.* Blood, 2012. **120**(15): p. 3152-62.
19.   Chanmee, T., et al., *Tumor-associated macrophages as major players in the tumor microenvironment.* Cancers (Basel), 2014. **6**(3): p. 1670-90.
20.   Gil-Bernabe, A.M., et al., *Recruitment of monocytes/macrophages by tissue factor-mediated coagulation is essential for metastatic cell survival and premetastatic niche establishment in mice.* Blood, 2012. **119**(13): p. 3164-75.

21. Noy, R. and J.W. Pollard, *Tumor-associated macrophages: from mechanisms to therapy.* Immunity, 2014. **41**(1): p. 49-61.

22. Ruffell, B., et al., *Macrophage IL-10 blocks CD8+ T cell-dependent responses to chemotherapy by suppressing IL-12 expression in intratumoral dendritic cells.* Cancer Cell, 2014. **26**(5): p. 623-37.

23. Liu, J., et al., *Tumor-associated macrophages recruit CCR6+ regulatory T cells and promote the development of colorectal cancer via enhancing CCL20 production in mice.* PLoS One, 2011. **6**(4): p. e19495.

24. Millrud, C.R., C. Bergenfelz, and K. Leandersson, *On the origin of myeloid-derived suppressor cells.* Oncotarget, 2017. **8**(2): p. 3649-3665.

25. Veglia, F., M. Perego, and D. Gabrilovich, *Myeloid-derived suppressor cells coming of age.* Nat Immunol, 2018. **19**(2): p. 108-119.

26. Pawelec, G., C.P. Verschoor, and S. Ostrand-Rosenberg, *Myeloid-Derived Suppressor Cells: Not Only in Tumor Immunity.* Front Immunol, 2019. **10**: p. 1099.

27. Youn, J.I., et al., *Subsets of myeloid-derived suppressor cells in tumor-bearing mice.* J Immunol, 2008. **181**(8): p. 5791-802.

28. Diaz-Montero, C.M., et al., *Increased circulating myeloid-derived suppressor cells correlate with clinical cancer stage, metastatic tumor burden, and doxorubicin-cyclophosphamide chemotherapy.* Cancer Immunol Immunother, 2009. **58**(1): p. 49-59.

29. Condamine, T., et al., *Regulation of tumor metastasis by myeloid-derived suppressor cells.* Annu Rev Med, 2015. **66**: p. 97-110.

30. Kumar, V., et al., *The Nature of Myeloid-Derived Suppressor Cells in the Tumor Microenvironment.* Trends Immunol, 2016. **37**(3): p. 208-220.

31. Raber, P., A.C. Ochoa, and P.C. Rodriguez, *Metabolism of L-arginine by myeloid-derived suppressor cells in cancer: mechanisms of T cell suppression and therapeutic perspectives.* Immunol Invest, 2012. **41**(6-7): p. 614-34.

32. Rodriguez, P.C., et al., *Arginase I-producing myeloid-derived suppressor cells in renal cell carcinoma are a subpopulation of activated granulocytes.* Cancer Res, 2009. **69**(4): p. 1553-60.

33. Nagaraj, S., et al., *Mechanism of T cell tolerance induced by myeloid-derived suppressor cells.* J Immunol, 2010. **184**(6): p. 3106-16.

34. Hanson, E.M., et al., *Myeloid-derived suppressor cells down-regulate L-selectin expression on CD4+ and CD8+ T cells.* J Immunol, 2009. **183**(2): p. 937-44.

35. Srivastava, M.K., et al., *Myeloid-derived suppressor cells inhibit T-cell activation by depleting cystine and cysteine.* Cancer Res, 2010. **70**(1): p. 68-77.

36. Liu, C., et al., *Expansion of spleen myeloid suppressor cells represses NK cell cytotoxicity in tumor-bearing host.* Blood, 2007. **109**(10): p. 4336-42.

37. Huang, B., et al., *Gr-1+CD115+ immature myeloid suppressor cells mediate the development of tumor-induced T regulatory cells and T-cell anergy in tumor-bearing host.* Cancer Res, 2006. **66**(2): p. 1123-31.

38. Draghiciu, O., et al., *Myeloid derived suppressor cells-An overview of combat strategies to increase immunotherapy efficacy.* Oncoimmunology, 2015. **4**(1): p. e954829.

39. Ai, L., et al., *Prognostic role of myeloid-derived suppressor cells in cancers: a systematic review and meta-analysis.* BMC Cancer, 2018. **18**(1): p. 1220.

40. Weber, R., et al., *Myeloid-Derived Suppressor Cells Hinder the Anti-Cancer Activity of Immune Checkpoint Inhibitors.* Front Immunol, 2018. **9**: p. 1310.

41. Ohue, Y. and H. Nishikawa, *Regulatory T (Treg) cells in cancer: Can Treg cells be a new therapeutic target?* Cancer Sci, 2019. **110**(7): p. 2080-2089.

42. Togashi, Y., K. Shitara, and H. Nishikawa, *Regulatory T cells in cancer immunosuppression - implications for anticancer therapy.* Nat Rev Clin Oncol, 2019. **16**(6): p. 356-371.

43. Wing, K., et al., *CTLA-4 control over Foxp3+ regulatory T cell function.* Science, 2008. **322**(5899): p. 271-5.

44. Shi, L., et al., *Adenosine Generated by Regulatory T Cells Induces CD8(+) T Cell Exhaustion in Gastric Cancer through A2aR Pathway.* Biomed Res Int, 2019. **2019**: p. 4093214.

45. Plitas, G. and A.Y. Rudensky, *Regulatory T Cells in Cancer.* Annual Review of Cancer Biology, 2020. **4**(1): p. 459-477.

46. Saito, T., et al., *Two FOXP3(+)CD4(+) T cell subpopulations distinctly control the prognosis of colorectal cancers.* Nat Med, 2016. **22**(6): p. 679-84.

47. Dao, T., et al., *Depleting T regulatory cells by targeting intracellular Foxp3 with a TCR mimic antibody.* Oncoimmunology, 2019. **8**(7): p. 1570778.

48. Onda, M., K. Kobayashi, and I. Pastan, *Depletion of regulatory T cells in tumors with an anti-CD25 immunotoxin induces CD8 T cell-mediated systemic antitumor immunity.* Proc Natl Acad Sci U S A, 2019. **116**(10): p. 4575-4582.

49. deLeeuw, R.J., et al., *The prognostic value of FoxP3+ tumor-infiltrating lymphocytes in cancer: a critical review of the literature.* Clin Cancer Res, 2012. **18**(11): p. 3022-9.

50. Idos, G.E., et al., *The Prognostic Implications of Tumor Infiltrating Lymphocytes in Colorectal Cancer: A Systematic Review and Meta-Analysis.* Sci Rep, 2020. **10**(1): p. 3360.

51. Teng, M.W., et al., *From mice to humans: developments in cancer immunoediting.* J Clin Invest, 2015. **125**(9): p. 3338-46.

52. Prado-Garcia, H., et al., *Tumor-induced CD8+ T-cell dysfunction in lung cancer patients.* Clin Dev Immunol, 2012. **2012**: p. 741741.

53. Zamarron, B.F. and W. Chen, *Dual roles of immune cells and their factors in cancer development and progression.* Int J Biol Sci, 2011. **7**(5): p. 651-8.

54. Pages, F., et al., *International validation of the consensus Immunoscore for the classification of colon cancer: a prognostic and accuracy study.* Lancet, 2018. **391**(10135): p. 2128-2139.

55. Sun, G., et al., *The prognostic value of immunoscore in patients with colorectal cancer: A systematic review and meta-analysis.* Cancer Med, 2019. **8**(1): p. 182-189.

56. Miller, J.S. and L.L. Lanier, *Natural Killer Cells in Cancer Immunotherapy.* Annual Review of Cancer Biology, 2019. **3**(1): p. 77-103.

57. Souza-Fonseca-Guimaraes, F., J. Cursons, and N.D. Huntington, *The Emergence of Natural Killer Cells as a Major Target in Cancer Immunotherapy.* Trends Immunol, 2019. **40**(2): p. 142-158.

58. Algarra, I., et al., *The selection of tumor variants with altered expression of classical and nonclassical MHC class I molecules: implications for tumor immune escape.* Cancer Immunol Immunother, 2004. **53**(10): p. 904-10.

59. Talmadge, J.E., et al., *Role of natural killer cells in tumor growth and metastasis: C57BL/6 normal and beige mice.* J Natl Cancer Inst, 1980. **65**(5): p. 929-35.

60. Gorelik, E., et al., *Role of NK cells in the control of metastatic spread and growth of tumor cells in mice.* Int J Cancer, 1982. **30**(1): p. 107-12.

61. Aktas, O.N., et al., *Role of natural killer cells in lung cancer.* J Cancer Res Clin Oncol, 2018. **144**(6): p. 997-1003.

62. Strayer, D.R., W.A. Carter, and I. Brodsky, *Familial occurrence of breast cancer is associated with reduced natural killer cytotoxicity.* Breast Cancer Res Treat, 1986. **7**(3): p. 187-92.

63. Garcia-Iglesias, T., et al., *Low NKp30, NKp46 and NKG2D expression and reduced cytotoxic activity on NK cells in cervical cancer and precursor lesions.* BMC Cancer, 2009. **9**: p. 186.

64. Bassani, B., et al., *Natural Killer Cells as Key Players of Tumor Progression and Angiogenesis: Old and Novel Tools to Divert Their Pro-Tumor Activities into Potent Anti-Tumor Effects.* Cancers (Basel), 2019. **11**(4).

65. Hu, W., et al., *Cancer Immunotherapy Based on Natural Killer Cells: Current Progress and New Opportunities.* Front Immunol, 2019. **10**: p. 1205.

66. Guillerey, C., N.D. Huntington, and M.J. Smyth, *Targeting natural killer cells in cancer immunotherapy.* Nat Immunol, 2016. **17**(9): p. 1025-36.

67. Wculek, S.K., et al., *Dendritic cells in cancer immunology and immunotherapy.* Nat Rev Immunol, 2020. **20**(1): p. 7-24.

68. McDonnell, A.M., B.W. Robinson, and A.J. Currie, *Tumor antigen cross-presentation and the dendritic cell: where it all begins?* Clin Dev Immunol, 2010. **2010**: p. 539519.

69. Perez, C.R. and M. De Palma, *Engineering dendritic cell vaccines to improve cancer immunotherapy.* Nat Commun, 2019. **10**(1): p. 5408.

70. Palucka, K. and J. Banchereau, *Dendritic-cell-based therapeutic cancer vaccines.* Immunity, 2013. **39**(1): p. 38-48.

71. Lee, J.H., et al., *The Effect of the Tumor Microenvironment and Tumor-Derived Metabolites on Dendritic Cell Function.* J Cancer, 2020. **11**(4): p. 769-775.

72. *https://clinicaltrials.gov/.*

73. Kantoff, P.W., et al., *Sipuleucel-T immunotherapy for castration-resistant prostate cancer.* N Engl J Med, 2010. **363**(5): p. 411-22.

74. Mastelic-Gavillet, B., et al., *Personalized Dendritic Cell Vaccines-Recent Breakthroughs and Encouraging Clinical Results.* Front Immunol, 2019. **10**: p. 766.

75. Narita, Y., et al., *The key role of IL-6-arginase cascade for inducing dendritic cell-dependent CD4(+) T cell dysfunction in tumor-bearing mice.* J Immunol, 2013. **190**(2): p. 812-20.

76. Ma, Y., et al., *Tumor associated regulatory dendritic cells.* Semin Cancer Biol, 2012. **22**(4): p. 298-306.

77. Veglia, F. and D.I. Gabrilovich, *Dendritic cells in cancer: the role revisited.* Curr Opin Immunol, 2017. **45**: p. 43-51.

78. Wu, G., et al., *Arginine deficiency in preterm infants: biochemical mechanisms and nutritional implications.* J Nutr Biochem, 2004. **15**(8): p. 442-51.

79. Caldwell, R.W., et al., *Arginase: A Multifaceted Enzyme Important in Health and Disease.* Physiol Rev, 2018. **98**(2): p. 641-665.

80. Morris, S.M., Jr., *Recent advances in arginine metabolism: roles and regulation of the arginases.* Br J Pharmacol, 2009. **157**(6): p. 922-30.

81. Grzywa, T.M., et al., *Myeloid Cell-Derived Arginase in Cancer Immune Response.* Front Immunol, 2020. **11**: p. 938.

82. Boger, R.H., *The pharmacodynamics of L-arginine.* J Nutr, 2007. **137**(6 Suppl 2): p. 1650S-1655S.

83. Szefel, J., A. Danielak, and W.J. Kruszewski, *Metabolic pathways of L-arginine and therapeutic consequences in tumors.* Adv Med Sci, 2019. **64**(1): p. 104-110.

84. Closs, E.I., et al., *Plasma membrane transporters for arginine.* J Nutr, 2004. **134**(10 Suppl): p. 2752S-2759S; discussion 2765S-2767S.

85. Cimen Bozkus, C., et al., *Expression of Cationic Amino Acid Transporter 2 Is Required for Myeloid-Derived Suppressor Cell-Mediated Control of T Cell Immunity.* J Immunol, 2015. **195**(11): p. 5237-50.

86. Werner, A., et al., *Induced arginine transport via cationic amino acid transporter-1 is necessary for human T-cell proliferation.* Eur J Immunol, 2016. **46**(1): p. 92-103.

87. Rodriguez, P.C., et al., *Arginase I production in the tumor microenvironment by mature myeloid cells inhibits T-cell receptor expression and antigen-specific T-cell responses.* Cancer Res, 2004. **64**(16): p. 5839-49.

88. Rodriguez, P.C. and A.C. Ochoa, *T cell dysfunction in cancer: role of myeloid cells and tumor cells regulating amino acid availability and oxidative stress.* Semin Cancer Biol, 2006. **16**(1): p. 66-72.

89. Albaugh, V.L., C. Pinzon-Guzman, and A. Barbul, *Arginine-Dual roles as an onconutrient and immunonutrient.* J Surg Oncol, 2017. **115**(3): p. 273-280.

90. Schairer, D.O., et al., *The potential of nitric oxide releasing therapies as antimicrobial agents.* Virulence, 2012. **3**(3): p. 271-9.

91. Husson, A., et al., *Argininosuccinate synthetase from the urea cycle to the citrulline-NO cycle.* Eur J Biochem, 2003. **270**(9): p. 1887-99.

92. Bogdan, C., *Nitric oxide and the immune response.* Nat Immunol, 2001. **2**(10): p. 907-16.

93. Morris, S.M., Jr., *Enzymes of arginine metabolism.* J Nutr, 2004. **134**(10 Suppl): p. 2743S-2747S; discussion 2765S-2767S.

94. Rodriguez, P.C. and A.C. Ochoa, *Arginine regulation by myeloid derived suppressor cells and tolerance in cancer: mechanisms and therapeutic perspectives.* Immunol Rev, 2008. **222**: p. 180-91.

95. Park, I.S., et al., *Arginine deiminase: a potential inhibitor of angiogenesis and tumour growth.* Br J Cancer, 2003. **89**(5): p. 907-14.

96. Durante, W., F.K. Johnson, and R.A. Johnson, *Arginase: a critical regulator of nitric oxide synthesis and vascular function.* Clin Exp Pharmacol Physiol, 2007. **34**(9): p. 906-11.

97. Hesse, M., et al., *Differential regulation of nitric oxide synthase-2 and arginase-1 by type 1/type 2 cytokines in vivo: granulomatous pathology is shaped by the pattern of L-arginine metabolism.* J Immunol, 2001. **167**(11): p. 6533-44.

98. Munder, M., et al., *Th1/Th2-regulated expression of arginase isoforms in murine macrophages and dendritic cells.* J Immunol, 1999. **163**(7): p. 3771-7.

99. Lemos, H., et al., *Immune control by amino acid catabolism during tumorigenesis and therapy.* Nat Rev Cancer, 2019. **19**(3): p. 162-175.

100. Rodriguez, P.C., et al., *Regulation of T cell receptor CD3zeta chain expression by L-arginine.* J Biol Chem, 2002. **277**(24): p. 21123-9.

101. Rodriguez, P.C., et al., *L-arginine consumption by macrophages modulates the expression of CD3 zeta chain in T lymphocytes.* J Immunol, 2003. **171**(3): p. 1232-9.

102. Taheri, F., et al., *L-Arginine regulates the expression of the T-cell receptor zeta chain (CD3zeta) in Jurkat cells.* Clin Cancer Res, 2001. **7**(3 Suppl): p. 958s-965s.

103. Whiteside, T.L., *Down-regulation of zeta-chain expression in T cells: a biomarker of prognosis in cancer?* Cancer Immunol Immunother, 2004. **53**(10): p. 865-78.

104. Dworacki, G., et al., *Decreased zeta chain expression and apoptosis in CD3+ peripheral blood T lymphocytes of patients with melanoma.* Clin Cancer Res, 2001. **7**(3 Suppl): p. 947s-957s.

105. Zea, A.H., et al., *L-Arginine modulates CD3zeta expression and T cell function in activated human T lymphocytes.* Cell Immunol, 2004. **232**(1-2): p. 21-31.

106. Rodriguez, P.C., D.G. Quiceno, and A.C. Ochoa, *L-arginine availability regulates T-lymphocyte cell-cycle progression.* Blood, 2007. **109**(4): p. 1568-73.

107. Grohmann, U. and V. Bronte, *Control of immune response by amino acid metabolism.* Immunol Rev, 2010. **236**: p. 243-64.

108. Tate, D.J., Jr., et al., *Interferon-gamma-induced nitric oxide inhibits the proliferation of murine renal cell carcinoma cells.* Int J Biol Sci, 2012. **8**(8): p. 1109-20.

109. Geiger, R., et al., *L-Arginine Modulates T Cell Metabolism and Enhances Survival and Anti-tumor Activity.* Cell, 2016. **167**(3): p. 829-842 e13.

110. Bronte, V. and P. Zanovello, *Regulation of immune responses by L-arginine metabolism.* Nat Rev Immunol, 2005. **5**(8): p. 641-54.

111. Caldwell, R.B., et al., *Arginase: an old enzyme with new tricks.* Trends Pharmacol Sci, 2015. **36**(6): p. 395-405.

112. Dizikes, G.J., et al., *Isolation of human liver arginase cDNA and demonstration of nonhomology between the two human arginase genes.* Biochem Biophys Res Commun, 1986. **141**(1): p. 53-9.

113. Gotoh, T., et al., *Molecular cloning of cDNA for nonhepatic mitochondrial arginase (arginase II) and comparison of its induction with nitric oxide synthase in a murine macrophage-like cell line.* FEBS Lett, 1996. **395**(2-3): p. 119-22.

114. Gotoh, T., M. Araki, and M. Mori, *Chromosomal localization of the human arginase II gene and tissue distribution of its mRNA.* Biochem Biophys Res Commun, 1997. **233**(2): p. 487-91.

115. Sparkes, R.S., et al., *The gene for human liver arginase (ARG1) is assigned to chromosome band 6q23.* Am J Hum Genet, 1986. **39**(2): p. 186-93.

116. Munder, M., *Arginase: an emerging key player in the mammalian immune system.* Br J Pharmacol, 2009. **158**(3): p. 638-51.

117. Ash, D.E., *Structure and function of arginases.* J Nutr, 2004. **134**(10 Suppl): p. 2760S-2764S; discussion 2765S-2767S.

118. Bronte, V., et al., *L-arginine metabolism in myeloid cells controls T-lymphocyte functions.* Trends Immunol, 2003. **24**(6): p. 302-6.

119. Mussai, F., et al., *Acute myeloid leukemia creates an arginase-dependent immunosuppressive microenvironment.* Blood, 2013. **122**(5): p. 749-58.

120. Suer Gokmen, S., et al., *Arginase and ornithine, as markers in human non-small cell lung carcinoma.* Cancer Biochem Biophys, 1999. **17**(1-2): p. 125-31.

121. Czystowska-Kuzmicz, M., et al., *Small extracellular vesicles containing arginase-1 suppress T-cell responses and promote tumor growth in ovarian carcinoma.* Nat Commun, 2019. **10**(1): p. 3000.

122. Mussai, F., et al., *Neuroblastoma Arginase Activity Creates an Immunosuppressive Microenvironment That Impairs Autologous and Engineered Immunity.* Cancer Res, 2015. **75**(15): p. 3043-53.

123. Ino, Y., et al., *Arginase II expressed in cancer-associated fibroblasts indicates tissue hypoxia and predicts poor outcome in patients with pancreatic cancer.* PLoS One, 2013. **8**(2): p. e55146.

124. de Boniface, J., et al., *Expression patterns of the immunomodulatory enzyme arginase 1 in blood, lymph nodes and tumor tissue of early-stage breast cancer patients.* Oncoimmunology, 2012. **1**(8): p. 1305-1312.

125. Ochoa, A.C., et al., *Arginase, prostaglandins, and myeloid-derived suppressor cells in renal cell carcinoma.* Clin Cancer Res, 2007. **13**(2 Pt 2): p. 721s-726s.

126. You, J., et al., *The Oncogenic Role of ARG1 in Progression and Metastasis of Hepatocellular Carcinoma.* Biomed Res Int, 2018. **2018**: p. 2109865.

127. Obiorah, I.E., et al., *Prognostic Implications of Arginase and Cytokeratin 19 Expression in Hepatocellular Carcinoma After Curative Hepatectomy: Correlation With Recurrence-Free Survival.* Gastroenterology Res, 2019. **12**(2): p. 78-87.

128. Gokmen, S.S., et al., *Significance of arginase and ornithine in malignant tumors of the human skin.* J Lab Clin Med, 2001. **137**(5): p. 340-4.

129. Bedoya, A.M., et al., *Immunosuppression in cervical cancer with special reference to arginase activity.* Gynecol Oncol, 2014. **135**(1): p. 74-80.

130. Ma, Z., et al., *Overexpression of Arginase-1 is an indicator of poor prognosis in patients with colorectal cancer.* Pathol Res Pract, 2019. **215**(6): p. 152383.

131. Grabon, W., et al., *L-arginine as a factor increasing arginase significance in diagnosis of primary and metastatic colorectal cancer.* Clin Biochem, 2009. **42**(4-5): p. 353-7.

132. Gabitass, R.F., et al., *Elevated myeloid-derived suppressor cells in pancreatic, esophageal and gastric cancer are an independent prognostic factor and are associated with significant elevation of the Th2 cytokine interleukin-13.* Cancer Immunol Immunother, 2011. **60**(10): p. 1419-30.

133. Cerutti, J.M., et al., *A preoperative diagnostic test that distinguishes benign from malignant thyroid carcinoma based on gene expression.* J Clin Invest, 2004. **113**(8): p. 1234-42.

134. Bron, L., et al., *Prognostic value of arginase-II expression and regulatory T-cell infiltration in head and neck squamous cell carcinoma.* Int J Cancer, 2013. **132**(3): p. E85-93.

135. Kim, S.H., et al., *Impact of l-Arginine Metabolism on Immune Response and Anticancer Immunotherapy.* Front Oncol, 2018. **8**: p. 67.

136. Fletcher, M., et al., *l-Arginine depletion blunts antitumor T-cell responses by inducing myeloid-derived suppressor cells.* Cancer Res, 2015. **75**(2): p. 275-83.

137. Cao, Y., et al., *L-Arginine supplementation inhibits the growth of breast cancer by enhancing innate and adaptive immune responses mediated by suppression of MDSCs in vivo.* BMC Cancer, 2016. **16**: p. 343.

138. Munder, M., et al., *Suppression of T-cell functions by human granulocyte arginase.* Blood, 2006. **108**(5): p. 1627-34.
139. Singer, K., et al., *Suppression of T-cell responses by tumor metabolites.* Cancer Immunol Immunother, 2011. **60**(3): p. 425-31.
140. Munder, M., et al., *Cytotoxicity of tumor antigen specific human T cells is unimpaired by arginine depletion.* PLoS One, 2013. **8**(5): p. e63521.
141. Kropf, P., et al., *Arginase activity mediates reversible T cell hyporesponsiveness in human pregnancy.* Eur J Immunol, 2007. **37**(4): p. 935-45.
142. Wang, Y., et al., *Exosomes released by granulocytic myeloid-derived suppressor cells attenuate DSS-induced colitis in mice.* Oncotarget, 2016. **7**(13): p. 15356-68.
143. Patil, M.D., et al., *Arginine dependence of tumor cells: targeting a chink in cancer's armor.* Oncogene, 2016. **35**(38): p. 4957-72.
144. Sosnowska, A., M. Czystowska-Kuzmicz, and J. Golab, *Extracellular vesicles released by ovarian carcinoma contain arginase 1 that mitigates antitumor immune response.* Oncoimmunology, 2019. **8**(11): p. e1655370.
145. Zou, S., et al., *Arginine metabolism and deprivation in cancer therapy.* Biomed Pharmacother, 2019. **118**: p. 109210.
146. Fultang, L., et al., *Molecular basis and current strategies of therapeutic arginine depletion for cancer.* Int J Cancer, 2016. **139**(3): p. 501-9.
147. Takaku, H., et al., *Chemical modification by polyethylene glycol of the anti-tumor enzyme arginine deiminase from Mycoplasma arginini.* Jpn J Cancer Res, 1993. **84**(11): p. 1195-200.
148. Gupta, V., et al., *Protein PEGylation for cancer therapy: bench to bedside.* J Cell Commun Signal, 2019. **13**(3): p. 319-330.
149. Feun, L., et al., *Arginine deprivation as a targeted therapy for cancer.* Curr Pharm Des, 2008. **14**(11): p. 1049-57.
150. Phillips, M.M., M.T. Sheaff, and P.W. Szlosarek, *Targeting arginine-dependent cancers with arginine-degrading enzymes: opportunities and challenges.* Cancer Res Treat, 2013. **45**(4): p. 251-62.
151. Delage, B., et al., *Arginine deprivation and argininosuccinate synthetase expression in the treatment of cancer.* Int J Cancer, 2010. **126**(12): p. 2762-72.
152. Ni, Y., U. Schwaneberg, and Z.H. Sun, *Arginine deiminase, a potential anti-tumor drug.* Cancer Lett, 2008. **261**(1): p. 1-11.
153. Lam, T.L., et al., *Recombinant human arginase inhibits the in vitro and in vivo proliferation of human melanoma by inducing cell cycle arrest and apoptosis.* Pigment Cell Melanoma Res, 2011. **24**(2): p. 366-76.
154. Chow, A.K., et al., *Anti-tumor efficacy of a recombinant human arginase in human hepatocellular carcinoma.* Curr Cancer Drug Targets, 2012. **12**(9): p. 1233-43.
155. De Santo, C., et al., *The arginine metabolome in acute lymphoblastic leukemia can be targeted by the pegylated-recombinant arginase I BCT-100.* Int J Cancer, 2018. **142**(7): p. 1490-1502.
156. Mussai, F., et al., *Arginine dependence of acute myeloid leukemia blast proliferation: a novel therapeutic target.* Blood, 2015. **125**(15): p. 2386-96.
157. Xu, S., et al., *Recombinant human arginase induces apoptosis through oxidative stress and cell cycle arrest in small cell lung cancer.* Cancer Sci, 2018. **109**(11): p. 3471-3482.

158. Lam, S.K., et al., *Growth suppressive effect of pegylated arginase in malignant pleural mesothelioma xenografts.* Respir Res, 2017. **18**(1): p. 80.

159. Morrow, K., et al., *Anti-leukemic mechanisms of pegylated arginase I in acute lymphoblastic T-cell leukemia.* Leukemia, 2013. **27**(3): p. 569-77.

160. Hernandez, C.P., et al., *Pegylated arginase I: a potential therapeutic approach in T-ALL.* Blood, 2010. **115**(25): p. 5214-21.

161. Wheatley, D.N., *Controlling cancer by restricting arginine availability--arginine-catabolizing enzymes as anticancer agents.* Anticancer Drugs, 2004. **15**(9): p. 825-33.

162. Vander Heiden, M.G., *Targeting cancer metabolism: a therapeutic window opens.* Nat Rev Drug Discov, 2011. **10**(9): p. 671-84.

163. Agrawal, V., et al., *Targeting methionine auxotrophy in cancer: discovery & exploration.* Expert Opin Biol Ther, 2012. **12**(1): p. 53-61.

164. Qie, S., et al., *Glutamine depletion and glucose depletion trigger growth inhibition via distinctive gene expression reprogramming.* Cell Cycle, 2012. **11**(19): p. 3679-90.

165. Heo, Y.A., Y.Y. Syed, and S.J. Keam, *Correction to: Pegaspargase: A Review in Acute Lymphoblastic Leukaemia.* Drugs, 2019. **79**(8): p. 901.

166. Seidel, J.A., A. Otsuka, and K. Kabashima, *Anti-PD-1 and Anti-CTLA-4 Therapies in Cancer: Mechanisms of Action, Efficacy, and Limitations.* Front Oncol, 2018. **8**: p. 86.

167. *https://www.nobelprize.org/prizes/medicine/2018/press-release/.*

168. Chemnitz, J.M., et al., *SHP-1 and SHP-2 associate with immunoreceptor tyrosine-based switch motif of programmed death 1 upon primary human T cell stimulation, but only receptor ligation prevents T cell activation.* J Immunol, 2004. **173**(2): p. 945-54.

169. de la Fuente, H., D. Cibrian, and F. Sanchez-Madrid, *Immunoregulatory molecules are master regulators of inflammation during the immune response.* FEBS Lett, 2012. **586**(18): p. 2897-2905.

170. Loke, P. and J.P. Allison, *PD-L1 and PD-L2 are differentially regulated by Th1 and Th2 cells.* Proc Natl Acad Sci U S A, 2003. **100**(9): p. 5336-41.

171. Rozali, E.N., et al., *Programmed death ligand 2 in cancer-induced immune suppression.* Clin Dev Immunol, 2012. **2012**: p. 656340.

172. Ma, W., et al., *Current status and perspectives in translational biomarker research for PD-1/PD-L1 immune checkpoint blockade therapy.* J Hematol Oncol, 2016. **9**(1): p. 47.

173. Nishimura, H., et al., *Development of lupus-like autoimmune diseases by disruption of the PD-1 gene encoding an ITIM motif-carrying immunoreceptor.* Immunity, 1999. **11**(2): p. 141-51.

174. Wang, J., et al., *Establishment of NOD-Pdcd1-/- mice as an efficient animal model of type I diabetes.* Proc Natl Acad Sci U S A, 2005. **102**(33): p. 11823-8.

175. Myklebust, J.H., et al., *High PD-1 expression and suppressed cytokine signaling distinguish T cells infiltrating follicular lymphoma tumors from peripheral T cells.* Blood, 2013. **121**(8): p. 1367-76.

176. Kitano, A., et al., *Tumour-infiltrating lymphocytes are correlated with higher expression levels of PD-1 and PD-L1 in early breast cancer.* ESMO Open, 2017. **2**(2): p. e000150.

177. Tamura, T., et al., *Programmed Death-1 Ligand-1 (PDL1) Expression Is Associated with the Prognosis of Patients with Stage II/III Gastric Cancer.* Anticancer Res, 2015. **35**(10): p. 5369-76.

178. Zhang, Y., et al., *Prognostic significance of programmed cell death 1 (PD-1) or PD-1 ligand 1 (PD-L1) Expression in epithelial-originated cancer: a meta-analysis.* Medicine (Baltimore), 2015. **94**(6): p. e515.

179. Park, H., et al., *Prognostic implications of soluble programmed death-ligand 1 and its dynamics during chemotherapy in unresectable pancreatic cancer.* Sci Rep, 2019. **9**(1): p. 11131.

180. Okadome, K., et al., *Prognostic and clinical impact of PD-L2 and PD-L1 expression in a cohort of 437 oesophageal cancers.* Br J Cancer, 2020. **122**(10): p. 1535-1543.

181. Kim, H.R., et al., *Tumor microenvironment dictates regulatory T cell phenotype: Upregulated immune checkpoints reinforce suppressive function.* J Immunother Cancer, 2019. **7**(1): p. 339.

182. Park, J.J., et al., *B7-H1/CD80 interaction is required for the induction and maintenance of peripheral T-cell tolerance.* Blood, 2010. **116**(8): p. 1291-8.

183. Chan, D.V., et al., *Differential CTLA-4 expression in human CD4+ versus CD8+ T cells is associated with increased NFAT1 and inhibition of CD4+ proliferation.* Genes Immun, 2014. **15**(1): p. 25-32.

184. Contardi, E., et al., *CTLA-4 is constitutively expressed on tumor cells and can trigger apoptosis upon ligand interaction.* Int J Cancer, 2005. **117**(4): p. 538-50.

185. Harper, K., et al., *CTLA-4 and CD28 activated lymphocyte molecules are closely related in both mouse and human as to sequence, message expression, gene structure, and chromosomal location.* J Immunol, 1991. **147**(3): p. 1037-44.

186. van der Merwe, P.A., et al., *CD80 (B7-1) binds both CD28 and CTLA-4 with a low affinity and very fast kinetics.* J Exp Med, 1997. **185**(3): p. 393-403.

187. Qureshi, O.S., et al., *Trans-endocytosis of CD80 and CD86: a molecular basis for the cell-extrinsic function of CTLA-4.* Science, 2011. **332**(6029): p. 600-3.

188. Tu, L., et al., *Assessment of the expression of the immune checkpoint molecules PD-1, CTLA4, TIM-3 and LAG-3 across different cancers in relation to treatment response, tumor-infiltrating immune cells and survival.* Int J Cancer, 2020. **147**(2): p. 423-439.

189. Gough, S.C., L.S. Walker, and D.M. Sansom, *CTLA4 gene polymorphism and autoimmunity.* Immunol Rev, 2005. **204**: p. 102-15.

190. Waldman, A.D., J.M. Fritz, and M.J. Lenardo, *A guide to cancer immunotherapy: from T cell basic science to clinical practice.* Nat Rev Immunol, 2020.

191. Spranger, S. and T.F. Gajewski, *Mechanisms of Tumor Cell–Intrinsic Immune Evasion.* Annual Review of Cancer Biology, 2018. **2**(1): p. 213-228.

192. Schreiber, R.D., L.J. Old, and M.J. Smyth, *Cancer immunoediting: integrating immunity's roles in cancer suppression and promotion.* Science, 2011. **331**(6024): p. 1565-70.

193. Burnet, F.M., *The concept of immunological surveillance.* Prog Exp Tumor Res, 1970. **13**: p. 1-27.

194. Shankaran, V., et al., *IFNgamma and lymphocytes prevent primary tumour development and shape tumour immunogenicity.* Nature, 2001. **410**(6832): p. 1107-11.

195. Kaplan, D.H., et al., *Demonstration of an interferon gamma-dependent tumor surveillance system in immunocompetent mice.* Proc Natl Acad Sci U S A, 1998. **95**(13): p. 7556-61.

196. van den Broek, M.E., et al., *Decreased tumor surveillance in perforin-deficient mice.* J Exp Med, 1996. **184**(5): p. 1781-90.

197. Smyth, M.J., et al., *Differential tumor surveillance by natural killer (NK) and NKT cells.* J Exp Med, 2000. **191**(4): p. 661-8.

198. Hodi, F.S., et al., *Improved survival with ipilimumab in patients with metastatic melanoma.* N Engl J Med, 2010. **363**(8): p. 711-23.

199. Robert, C., et al., *Ipilimumab plus dacarbazine for previously untreated metastatic melanoma.* N Engl J Med, 2011. **364**(26): p. 2517-26.

200. Robert, C., et al., *Nivolumab in previously untreated melanoma without BRAF mutation.* N Engl J Med, 2015. **372**(4): p. 320-30.

201. Postow, M.A., et al., *Nivolumab and ipilimumab versus ipilimumab in untreated melanoma.* N Engl J Med, 2015. **372**(21): p. 2006-17.

202. Wolchok, J.D., et al., *Nivolumab plus ipilimumab in advanced melanoma.* N Engl J Med, 2013. **369**(2): p. 122-33.

203. Wei, S.C., C.R. Duffy, and J.P. Allison, *Fundamental Mechanisms of Immune Checkpoint Blockade Therapy.* Cancer Discov, 2018. **8**(9): p. 1069-1086.

204. Poole, R.M., *Pembrolizumab: first global approval.* Drugs, 2014. **74**(16): p. 1973-1981.

205. Gettinger, S. and R.S. Herbst, *B7-H1/PD-1 blockade therapy in non-small cell lung cancer: current status and future direction.* Cancer J, 2014. **20**(4): p. 281-9.

206. Buder-Bakhaya, K. and J.C. Hassel, *Biomarkers for Clinical Benefit of Immune Checkpoint Inhibitor Treatment-A Review From the Melanoma Perspective and Beyond.* Front Immunol, 2018. **9**: p. 1474.

207. Vaddepally, R.K., et al., *Review of Indications of FDA-Approved Immune Checkpoint Inhibitors per NCCN Guidelines with the Level of Evidence.* Cancers (Basel), 2020. **12**(3).

208. Cogdill, A.P., M.C. Andrews, and J.A. Wargo, *Hallmarks of response to immune checkpoint blockade.* Br J Cancer, 2017. **117**(1): p. 1-7.

209. Chen, D.S. and I. Mellman, *Elements of cancer immunity and the cancer-immune set point.* Nature, 2017. **541**(7637): p. 321-330.

210. Simeone, E., et al., *Immunological and biological changes during ipilimumab treatment and their potential correlation with clinical response and survival in patients with advanced melanoma.* Cancer Immunol Immunother, 2014. **63**(7): p. 675-83.

211. Martens, A., et al., *Baseline Peripheral Blood Biomarkers Associated with Clinical Outcome of Advanced Melanoma Patients Treated with Ipilimumab.* Clin Cancer Res, 2016. **22**(12): p. 2908-18.

212. Subrahmanyam, P.B., et al., *Distinct predictive biomarker candidates for response to anti-CTLA-4 and anti-PD-1 immunotherapy in melanoma patients.* J Immunother Cancer, 2018. **6**(1): p. 18.

213. Darvin, P., et al., *Immune checkpoint inhibitors: recent progress and potential biomarkers.* Exp Mol Med, 2018. **50**(12): p. 1-11.

214. Zhao, P., et al., *Mismatch repair deficiency/microsatellite instability-high as a predictor for anti-PD-1/PD-L1 immunotherapy efficacy.* J Hematol Oncol, 2019. **12**(1): p. 54.

215. Overman, M.J., et al., *Durable Clinical Benefit With Nivolumab Plus Ipilimumab in DNA Mismatch Repair-Deficient/Microsatellite Instability-High Metastatic Colorectal Cancer.* J Clin Oncol, 2018. **36**(8): p. 773-779.

216. Michot, J.M., et al., *Immune-related adverse events with immune checkpoint blockade: a comprehensive review.* Eur J Cancer, 2016. **54**: p. 139-148.

217. Friedman, C.F., T.A. Proverbs-Singh, and M.A. Postow, *Treatment of the Immune-Related Adverse Effects of Immune Checkpoint Inhibitors: A Review.* JAMA Oncol, 2016. **2**(10): p. 1346-1353.

218. Postow, M.A., R. Sidlow, and M.D. Hellmann, *Immune-Related Adverse Events Associated with Immune Checkpoint Blockade.* N Engl J Med, 2018. **378**(2): p. 158-168.

219. Custot, J., et al., *The new α-amino acid N ω-hydroxy-nor-L-arginine: a high-affinity inhibitor of arginase well adapted to bind to its manganese cluster.* Journal of the American Chemical Society, 1997. **119**(17): p. 4086-4087.

220. Di Costanzo, L., et al., *Inhibition of human arginase I by substrate and product analogues.* Arch Biochem Biophys, 2010. **496**(2): p. 101-8.

221. Baggio, R., et al., *Biochemical and functional profile of a newly developed potent and isozyme-selective arginase inhibitor.* J Pharmacol Exp Ther, 1999. **290**(3): p. 1409-16.

222. Kim, N.N., et al., *Probing erectile function: S-(2-boronoethyl)-L-cysteine binds to arginase as a transition state analogue and enhances smooth muscle relaxation in human penile corpus cavernosum.* Biochemistry, 2001. **40**(9): p. 2678-88.

223. Tenu, J.P., et al., *Effects of the new arginase inhibitor N(omega)-hydroxy-nor-L-arginine on NO synthase activity in murine macrophages.* Nitric Oxide, 1999. **3**(6): p. 427-38.

224. Mondanelli, G., et al., *The immune regulation in cancer by the amino acid metabolizing enzymes ARG and IDO.* Curr Opin Pharmacol, 2017. **35**: p. 30-39.

225. Havlinova, Z., et al., *Comparative pharmacokinetics of N(omega)-hydroxy-nor-L-arginine, an arginase inhibitor, after single-dose intravenous, intraperitoneal and intratracheal administration to brown Norway rats.* Xenobiotica, 2013. **43**(10): p. 886-94.

226. Ivanenkov, Y.A. and N.V. Chufarova, *Small-molecule arginase inhibitors.* Pharm Pat Anal, 2014. **3**(1): p. 65-85.

227. Yachimovich-Cohen, N., et al., *Human embryonic stem cells suppress T cell responses via arginase I-dependent mechanism.* J Immunol, 2010. **184**(3): p. 1300-8.

228. Golebiowski, A., et al., *2-Substituted-2-amino-6-boronohexanoic acids as arginase inhibitors.* Bioorg Med Chem Lett, 2013. **23**(7): p. 2027-30.

229. Van Zandt, M.C., et al., *Discovery of (R)-2-amino-6-borono-2-(2-(piperidin-1-yl)ethyl)hexanoic acid and congeners as highly potent inhibitors of human arginases I and II for treatment of myocardial reperfusion injury.* J Med Chem, 2013. **56**(6): p. 2568-80.

230. Ilies, M., et al., *Binding of alpha,alpha-disubstituted amino acids to arginase suggests new avenues for inhibitor design.* J Med Chem, 2011. **54**(15): p. 5432-43.

231. Van Zandt, M.C., et al., *Discovery of N-Substituted 3-Amino-4-(3-boronopropyl)pyrrolidine-3-carboxylic Acids as Highly Potent Third-*

Generation Inhibitors of Human Arginase I and II. J Med Chem, 2019. **62**(17): p. 8164-8177.

232. Guo, X., Y. Chen, and C.T. Seto, *Rational design of novel irreversible inhibitors for human arginase.* Bioorg Med Chem, 2018. **26**(14): p. 3939-3946.

233. Grzybowski, M.M., et al., *71PNovel dual arginase 1/2 inhibitor OATD-02 (OAT-1746) improves the efficacy of immune checkpoint inhibitors.* Annals of Oncology, 2017. **28**(suppl_11).

234. Stanczak, P., et al., *Development of OAT-1746, a novel arginase 1 and 2 inhibitor for cancer immunotherapy.* . 42nd ESMO Congress, 2017. **ESMO**.

235. Steggerda, S.M., et al., *Inhibition of arginase by CB-1158 blocks myeloid cell-mediated immune suppression in the tumor microenvironment.* J Immunother Cancer, 2017. **5**(1): p. 101.

236. Naing, A., et al., *Phase 1 study of the arginase inhibitor INCB001158 (1158) alone and in combination with pembrolizumab (PEM) in patients (PTS) with advanced/metastatic (ADV/MET) solid tumors.* . 44th ESMO Congress, 2019. **Barcelona**.

237. Pudlo, M., C. Demougeot, and C. Girard-Thernier, *Arginase Inhibitors: A Rational Approach Over One Century.* Med Res Rev, 2017. **37**(3): p. 475-513.

238. Abdelkawy, K.S., K. Lack, and F. Elbarbry, *Pharmacokinetics and Pharmacodynamics of Promising Arginase Inhibitors.* Eur J Drug Metab Pharmacokinet, 2017. **42**(3): p. 355-370.

239. Pham, T.N., et al., *Research of novel anticancer agents targeting arginase inhibition.* Drug Discov Today, 2018. **23**(4): p. 871-878.

240. Boucher, J.L., et al., *N omega-hydroxyl-L-arginine, an intermediate in the L-arginine to nitric oxide pathway, is a strong inhibitor of liver and macrophage arginase.* Biochem Biophys Res Commun, 1994. **203**(3): p. 1614-21.

241. Selamnia, M., et al., *Alpha-difluoromethylornithine (DFMO) as a potent arginase activity inhibitor in human colon carcinoma cells.* Biochem Pharmacol, 1998. **55**(8): p. 1241-5.

242. Samardzic, K. and K.J. Rodgers, *Cytotoxicity and mitochondrial dysfunction caused by the dietary supplement l-norvaline.* Toxicol In Vitro, 2019. **56**: p. 163-171.

243. Ming, X.F., et al., *Inhibition of S6K1 accounts partially for the anti-inflammatory effects of the arginase inhibitor L-norvaline.* BMC Cardiovasc Disord, 2009. **9**: p. 12.

244. Hu, Q.Y., et al., *Inhibition of human hepatocellular carcinoma by L-proline-m-bis (2-chloroethyl) amino-L-phenylalanyl-L-norvaline ethyl ester hydrochloride (MF13) in vitro and in vivo.* Int J Oncol, 2004. **25**(5): p. 1289-96.

245. Trujillo-Ferrara, J., et al., *Antitumor effect and toxicity of two new active-site-directed irreversible ornithine decarboxylase and extrahepatic arginase inhibitors.* Cancer Lett, 1992. **67**(2-3): p. 193-7.

246. Yao, J., et al., *6-Gingerol as an arginase inhibitor prevents urethane-induced lung carcinogenesis by reprogramming tumor supporting M2 macrophages to M1 phenotype.* Food Funct, 2018. **9**(9): p. 4611-4620.

247. Gabrilovich, D.I. and S. Nagaraj, *Myeloid-derived suppressor cells as regulators of the immune system.* Nat Rev Immunol, 2009. **9**(3): p. 162-74.

248. Parker, K.H., D.W. Beury, and S. Ostrand-Rosenberg, *Myeloid-Derived Suppressor Cells: Critical Cells Driving Immune Suppression in the Tumor Microenvironment.* Adv Cancer Res, 2015. **128**: p. 95-139.

249. Speiser, D.E., P.C. Ho, and G. Verdeil, *Regulatory circuits of T cell function in cancer.* Nat Rev Immunol, 2016. **16**(10): p. 599-611.

250. Colegio, O.R., et al., *Functional polarization of tumour-associated macrophages by tumour-derived lactic acid.* Nature, 2014. **513**(7519): p. 559-63.

251. Schleicher, U., et al., *TNF-Mediated Restriction of Arginase 1 Expression in Myeloid Cells Triggers Type 2 NO Synthase Activity at the Site of Infection.* Cell Rep, 2016. **15**(5): p. 1062-1075.

252. Loyher, P.L., et al., *Macrophages of distinct origins contribute to tumor development in the lung.* J Exp Med, 2018. **215**(10): p. 2536-2553.

253. Arlauckas, S.P., et al., *Arg1 expression defines immunosuppressive subsets of tumor-associated macrophages.* Theranostics, 2018. **8**(21): p. 5842-5854.

254. Youn, J.I. and D.I. Gabrilovich, *The biology of myeloid-derived suppressor cells: the blessing and the curse of morphological and functional heterogeneity.* Eur J Immunol, 2010. **40**(11): p. 2969-75.

255. Davis, R.J., et al., *Anti-PD-L1 Efficacy Can Be Enhanced by Inhibition of Myeloid-Derived Suppressor Cells with a Selective Inhibitor of PI3Kdelta/gamma.* Cancer Res, 2017. **77**(10): p. 2607-2619.

256. Vasquez-Dunddel, D., et al., *STAT3 regulates arginase-I in myeloid-derived suppressor cells from cancer patients.* J Clin Invest, 2013. **123**(4): p. 1580-9.

257. Adams, J.L., et al., *Big opportunities for small molecules in immuno-oncology.* Nat Rev Drug Discov, 2015. **14**(9): p. 603-22.

258. Lechner, M.G., et al., *Immunogenicity of murine solid tumor models as a defining feature of in vivo behavior and response to immunotherapy.* J Immunother, 2013. **36**(9): p. 477-89.

259. Cala, M.P., et al., *Multiplatform plasma fingerprinting in cancer cachexia: a pilot observational and translational study.* J Cachexia Sarcopenia Muscle, 2018. **9**(2): p. 348-357.

260. Sullivan, M.R., et al., *Quantification of microenvironmental metabolites in murine cancers reveals determinants of tumor nutrient availability.* Elife, 2019. **8**.

261. Vissers, Y.L., et al., *Plasma arginine concentrations are reduced in cancer patients: evidence for arginine deficiency?* Am J Clin Nutr, 2005. **81**(5): p. 1142-6.

262. Kaplan, I., et al., *The evaluation of plasma arginine, arginase, and nitric oxide levels in patients with esophageal cancer.* Turkish Journal of Medical Sciences, 2012. **42**(3): p. 403-409.

263. Coosemans, A., et al., *Immunosuppressive parameters in serum of ovarian cancer patients change during the disease course.* Oncoimmunology, 2016. **5**(4): p. e1111505.

264. Porembska, Z., et al., *Arginase in patients with breast cancer.* Clinica chimica acta; international journal of clinical chemistry, 2003. **328**(1-2): p. 105-111.

265. Erbas, H., et al., *Asymmetric dimethylarginine in experimental breast cancer; action of Vitamin C and E.* J Pak Med Assoc, 2015. **65**(8): p. 829-33.

266. Kus, K., et al., *Alterations in arginine and energy metabolism, structural and signalling lipids in metastatic breast cancer in mice detected in plasma by targeted metabolomics and lipidomics.* Breast Cancer Res, 2018. **20**(1): p. 148.

267. Polat, M.F., et al., *Elevated serum arginase activity levels in patients with breast cancer.* Surg Today, 2003. **33**(9): p. 655-61.

268. Straus, B., I. Cepelak, and G. Festa, *Arginase, a new marker of mammary carcinoma.* Clin Chim Acta, 1992. **210**(1-2): p. 5-12.

269. Engelen, M., et al., *Major surgery diminishes systemic arginine availability and suppresses nitric oxide response to feeding in patients with early stage breast cancer.* Clin Nutr, 2018. **37**(5): p. 1645-1653.

270. Maeda, J., et al., *Possibility of multivariate function composed of plasma amino acid profiles as a novel screening index for non-small cell lung cancer: a case control study.* BMC Cancer, 2010. **10**: p. 690.

271. Shingyoji, M., et al., *The significance and robustness of a plasma free amino acid (PFAA) profile-based multiplex function for detecting lung cancer.* BMC Cancer, 2013. **13**: p. 77.

272. Lieberman, I. and P. Ove, *Inhibition of growth of cultured mammalian cells by liver extracts.* Biochim Biophys Acta, 1960. **38**: p. 153.

273. Holley, R.W., *Evidence that a rat liver "inhibitor" of the synthesis of DNA in cultured mammalian cells is arginase.* Biochim Biophys Acta, 1967. **145**(2): p. 525-7.

274. Dunand-Sauthier, I., et al., *Repression of arginase-2 expression in dendritic cells by microRNA-155 is critical for promoting T cell proliferation.* J Immunol, 2014. **193**(4): p. 1690-700.

275. Bronte, V., et al., *Boosting antitumor responses of T lymphocytes infiltrating human prostate cancers.* J Exp Med, 2005. **201**(8): p. 1257-68.

276. Secondini, C., et al., *Arginase inhibition suppresses lung metastasis in the 4T1 breast cancer model independently of the immunomodulatory and anti-metastatic effects of VEGFR-2 blockade.* Oncoimmunology, 2017. **6**(6): p. e1316437.

277. Darcy, C.J., et al., *Neutrophils with myeloid derived suppressor function deplete arginine and constrain T cell function in septic shock patients.* Crit Care, 2014. **18**(4): p. R163.

278. Ezernitchi, A.V., et al., *TCR zeta down-regulation under chronic inflammation is mediated by myeloid suppressor cells differentially distributed between various lymphatic organs.* J Immunol, 2006. **177**(7): p. 4763-72.

279. Kim, E.M., et al., *Embryonic stem cell-derived haematopoietic progenitor cells down-regulate the CD3 xi chain on T cells, abrogating alloreactive T cells.* Immunology, 2014. **142**(3): p. 421-30.

280. Castro, F., et al., *Interferon-Gamma at the Crossroads of Tumor Immune Surveillance or Evasion.* Front Immunol, 2018. **9**: p. 847.

281. Josephs, S.F., et al., *Unleashing endogenous TNF-alpha as a cancer immunotherapeutic.* J Transl Med, 2018. **16**(1): p. 242.

282. Srivastava, M.K., et al., *Myeloid suppressor cell depletion augments antitumor activity in lung cancer.* PLoS One, 2012. **7**(7): p. e40677.

283. Miret, J.J., et al., *Suppression of Myeloid Cell Arginase Activity leads to Therapeutic Response in a NSCLC Mouse Model by Activating Anti-Tumor Immunity.* J Immunother Cancer, 2019. **7**(1): p. 32.

284. Goh, C.C., et al., *Hepatitis C Virus-Induced Myeloid-Derived Suppressor Cells Suppress NK Cell IFN-gamma Production by Altering Cellular Metabolism via Arginase-1.* J Immunol, 2016. **196**(5): p. 2283-92.

285. Tytell, A.A. and R.E. Neuman, *Growth response of stable and primary cell cultures to L-ornithine, L-citrulline, and L-arginine.* Exp Cell Res, 1960. **20**: p. 84-91.

286. Werner, A., et al., *Reconstitution of T Cell Proliferation under Arginine Limitation: Activated Human T Cells Take Up Citrulline via L-Type Amino Acid Transporter 1 and Use It to Regenerate Arginine after Induction of Argininosuccinate Synthase Expression.* Front Immunol, 2017. **8**: p. 864.

287. Marti i Lindez, A.A., et al., *Mitochondrial arginase-2 is a cellautonomous regulator of CD8+ T cell function and antitumor efficacy.* JCI Insight, 2019. **4**(24).

288. Rotondo, R., et al., *Arginase 2 is expressed by human lung cancer, but it neither induces immune suppression, nor affects disease progression.* Int J Cancer, 2008. **123**(5): p. 1108-16.

289. Gannon, P.O., et al., *Androgen-regulated expression of arginase 1, arginase 2 and interleukin-8 in human prostate cancer.* PLoS One, 2010. **5**(8): p. e12107.

290. Singh, R., et al., *Arginase activity in human breast cancer cell lines: N(omega)-hydroxy-L-arginine selectively inhibits cell proliferation and induces apoptosis in MDA-MB-468 cells.* Cancer Res, 2000. **60**(12): p. 3305-12.

291. Costa, H., et al., *Human cytomegalovirus may promote tumour progression by upregulating arginase-2.* Oncotarget, 2016. **7**(30): p. 47221-47231.

292. Chang, C.I., J.C. Liao, and L. Kuo, *Macrophage arginase promotes tumor cell growth and suppresses nitric oxide-mediated tumor cytotoxicity.* Cancer Res, 2001. **61**(3): p. 1100-6.

293. Tate, D.J., Jr., et al., *Effect of arginase II on L-arginine depletion and cell growth in murine cell lines of renal cell carcinoma.* J Hematol Oncol, 2008. **1**: p. 14.

294. Li, X., et al., *[Arginase inhibitor nor-NOHA induces apoptosis and inhibits invasion and migration of HepG2 cells].* Xi Bao Yu Fen Zi Mian Yi Xue Za Zhi, 2017. **33**(4): p. 477-482.

295. Singh, R., et al., *Activation of caspase-3 activity and apoptosis in MDA-MB-468 cells by N(omega)-hydroxy-L-arginine, an inhibitor of arginase, is not solely dependent on reduction in intracellular polyamines.* Carcinogenesis, 2001. **22**(11): p. 1863-9.

296. Singh, R., S. Pervin, and G. Chaudhuri, *Caspase-8-mediated BID cleavage and release of mitochondrial cytochrome c during Nomega-hydroxy-L-arginine-induced apoptosis in MDA-MB-468 cells. Antagonistic effects of L-ornithine.* J Biol Chem, 2002. **277**(40): p. 37630-6.

297. Ng, K.P., et al., *The arginase inhibitor Nomega-hydroxy-nor-arginine (nor-NOHA) induces apoptosis in leukemic cells specifically under hypoxic conditions but CRISPR/Cas9 excludes arginase 2 (ARG2) as the functional target.* PLoS One, 2018. **13**(10): p. e0205254.

298. Setty, B.A., et al., *Hypoxic Proliferation of Osteosarcoma Cells Depends on Arginase II.* Cell Physiol Biochem, 2016. **39**(2): p. 802-13.

299. Setty, B.A., et al., *Hypoxia-induced proliferation of HeLa cells depends on epidermal growth factor receptor-mediated arginase II induction.* Physiol Rep, 2017. **5**(6).

300. Dhanak, D., et al., *Small-Molecule Targets in Immuno-Oncology.* Cell Chem Biol, 2017. **24**(9): p. 1148-1160.

301. Kang, J.S., *Dietary restriction of amino acids for Cancer therapy.* Nutr Metab (Lond), 2020. **17**: p. 20.

302. Jiang, J.D., et al., *High anticancer efficacy of L-proline-m-bis (2-chloroethyl) amino-L-phenylalanyl-L-norvaline ethyl ester hydrochloride (MF13) in vivo.* Anticancer Res, 2001. **21**(3B): p. 1681-9.

303. Papadopoulos, K.P., et al., *CX-1158-101: A first-in-human phase 1 study of CB-1158, a small molecule inhibitor of arginase, as monotherapy and in combination with an anti-PD-1 checkpoint inhibitor in patients (pts) with solid tumors.* 2017, American Society of Clinical Oncology.

304. Sanmamed, M.F., et al., *Defining the optimal murine models to investigate immune checkpoint blockers and their combination with other immunotherapies.* Ann Oncol, 2016. **27**(7): p. 1190-8.

305. Arora, S., et al., *Existing and Emerging Biomarkers for Immune Checkpoint Immunotherapy in Solid Tumors.* Adv Ther, 2019. **36**(10): p. 2638-2678.

306. Samoilenko capital O, C.A.C., et al., *Effect of polyamine metabolism inhibitors on Lewis lung carcinoma growth and metastasis.* Exp Oncol, 2015. **37**(2): p. 151-3.

307. Downey, C.M., et al., *DMXAA causes tumor site-specific vascular disruption in murine non-small cell lung cancer, and like the endogenous non-canonical cyclic dinucleotide STING agonist, 2'3'-cGAMP, induces M2 macrophage repolarization.* PLoS One, 2014. **9**(6): p. e99988.

308. Blaszczyk, R., et al., *Discovery and Pharmacokinetics of Sulfamides and Guanidines as Potent Human Arginase 1 Inhibitors.* ACS Med Chem Lett, 2020. **11**(4): p. 433-438.

309. Andersen, M.H., *The targeting of tumor-associated macrophages by vaccination.* Cell Stress, 2019. **3**(5): p. 139-140.

310. Martinenaite, E., et al., *Frequent adaptive immune responses against arginase-1.* Oncoimmunology, 2018. **7**(3): p. e1404215.

311. Jorgensen, M.A., et al., *Spontaneous T-cell responses against Arginase-1 in the chronic myeloproliferative neoplasms relative to disease stage and type of driver mutation.* Oncoimmunology, 2018. **7**(9): p. e1468957.

312. Weis-Banke, S.E., et al., *The metabolic enzyme arginase-2 is a potential target for novel immune modulatory vaccines.* OncoImmunology, 2020. **9**(1): p. 1771142.

UCHWAŁA NR 68/2013
z dnia 26 listopada 2013r.

II Lokalnej Komisji Etycznej ds. Doświadczeń na Zwierzętach w Warszawie, ul. Żwirki i Wigury 61, 02-091 Warszawa.

§1

Na podstawie art.30 ust 1 pkt1 ustawy z dnia 21 stycznia 2005r. o doświadczeniach na zwierzętach (Dz.U.Nr 33, poz. 289) i §14 ust 3 rozporządzenia Ministra Nauki i Informatyzacji z dnia 29 lipca 2005r. w sprawie Krajowej Komisji Etycznej do Spraw Doświadczeń na Zwierzętach oraz lokalnych komisji etycznych do spraw doświadczeń na zwierzętach (Dz. U. Nr 153, poz. 1275), po rozpatrzeniu wniosku pt.
„Opracowanie nowych związków stymulujących przeciwnowotworowe działanie układu odpornościowego.".

z dnia 15. 11. 2013r. złożonego
przez: Prof. dr hab. Jakuba GOŁĄBA
z :   Zakładu Immunologii I WL WUM
                 ul. Banacha 1a Blok „ F" , 02-097 Warszawa

WYRAŻA ZGODĘ
~~ODMAWIA WYRAŻENIA ZGODY~~
na przeprowadzenie doświadczeń na zwierzętach w zakresie wniosku.

§2

W wyniku rozpatrzenia wniosku, o którym mowa w §1, II Lokalna Komisja Etyczna ds. Doświadczeń na Zwierzętach ustaliła, że:

1.Wniosek należy zaliczyć do kategorii:
                 Badania naukowe na zwierzętach
                 ~~**Doświadczenia na zwierzętach w dydaktyce**~~
                 Doświadczenia na tkankach, narządach odzwierzęcych

2.Najwyższy stopień inwazyjności proponowanych procedur i nie przekracza wartości ..../....

3.Doświadczenia będą przeprowadzone na zwierzętach :(gatunek, liczba zwierząt)
   Gatunek (liczba zwierząt) :

   Myszy   324..............

4.Doświadczenia będą przeprowadzone przez : (nazwisko i imię, nazwa jednostki doświadczalnej)
   Imię i nazwisko wnioskodawcy: **Prof. dr hab. Jakub GOŁĄB**
   Nazwa jednostki doświadczalnej: **Zakład Immunologii I WL WUM**
                                        ul. Banacha 1a Blok „ F" , 02-097 Warszawa

§3

Integralną częścią niniejszej uchwały stanowi uzasadnienie i kopia wniosku, o którym mowa w §1.

II LOKALNA KOMISJA ETYCZNA
Ds. Doświadczen na Zwierzętach
przy Warszawskim Uniwersytecie Medycznym
Pieczęć II LKE ul. Żwirki i Wigury 61, 02-091 Warszawa
tel. 022 5720-110, 5720-304, fax. 022 5720-169
pok. 304

Przewodniczący II Lokalnej Komisji Etycznej

Prof. dr hab. Bogdan Ciszek

Strona niezadowolona z niniejszej uchwały może wnieść odwołanie do Krajowej Komisji Etycznej do Spraw. Doświadczeń na Zwierzętach w terminie 14 dni od dnia otrzymania uchwały. Odwołanie składa się za pomocą lokalnych komisji etycznych do spraw doświadczeń na zwierzętach (Dz. U Nr 153 poz.1275).

UCHWAŁA NR 193/2016

z dnia 14 grudnia 2016

I Lokalnej Komisji Etycznej do spraw doświadczeń na zwierzętach w Warszawie

§ 1

Na podstawie art. 48 pkt. 1 ustawy z dnia 15 stycznia 2015r. o ochronie zwierząt wykorzystywanych do celów naukowych lub edukacyjnych (Dz. U. poz. 266) po rozpatrzeniu wniosku pt. **Badanie przeciwnowotworowego działania inhibitora arginazy w połączeniu z inhibitorami punktów kontrolnych w mysich modelach nowotworowych** z dnia **02.12.2016** złożonego przez **I Wydział Lekarski, Warszawski Uniwersytet Medyczny ul. Żwirki i Wigury 61, 02-081 Warszawa** zaplanowanego przez **prof. dr hab. Jakuba Gołąba** lokalna komisja etyczna

WYRAŻA ZGODĘ
Na przeprowadzenie doświadczeń na zwierzętach w zakresie wniosku.

§ 2

W wyniku rozpatrzenia wniosku o którym mowa w § , Lokalna Komisja Etyczna ustaliła, że:

1. Wniosek należy przypisać do kategorii: **DOŚWIADCZENIA NA ZWIERZĘTACH (A)**
2. Najwyższy stopień dotkliwości proponowanych procedur to: **DOTKLIWY**
3. Doświadczenia będą przeprowadzane na gatunkach lub grupach gatunków **Mysz C57BL/6, samica   8-12 tygodni   320 osobników**
4. Doświadczenia będą przeprowadzane przez: **Jakub Gołąb, Dominika Nowis, Anna Sosnowska, Kavita Ramji, Zofia Pilch, Justyna Chlebowska, Olga Sokołowska**
5. Doświadczenie będzie przeprowadzane w terminie[1] **01.01.2017 – 01.07.2018 r.**
6. Doświadczenie będzie przeprowadzone w ośrodku[2]:
7. Doświadczenie będzie przeprowadzone poza ośrodkiem w:
8. Użyte do procedur zwierzęta dzikie zostaną odłowione przez............. w sposób
9. Doświadczenie zostanie/~~nie zostanie~~ poddane ocenie retrospektywnej w terminie: 6 m-cy po zakończeniu doświadczenia.

---

[1] Nie dłużej niż 5 lat
[2] Podać jeśli jest to inny ośrodek niż użytkownik

§ 3

Uzasadnienie:

Głównym celem leczenia onkologicznego jest niszczenie komórek nowotworowych jednak obecnie stosowane metody leczenia nowotworów często nie eliminują przerzutów oraz powodują wiele skutków ubocznych.

Projekt przedstawiony we wniosku nr 193/206 ma na celu zbadanie czy inhibitory arginazy mogą potęgować przeciwnowotworowe działanie tak zwanych inhibitorów punktu kontrolnego. Badania zostaną wykonane na dwóch modelach nowotworów – czerniaku oraz raku płuc gdzie będzie porównywany efekt zahamowania wzrostu guzów w grupach leczonych tylko inhibitorem lub tylko przeciwciałami w porównaniu do grup kontrolnych oraz nasilone zahamowanie wzrostu guzów w terapii łączonej.

Wciąż trwają poszukiwania nowych metod, które odznaczałyby się większą skutecznością oraz selektywnością wobec komórek nowotworowych a uzyskane wyniki pozwolą na lepsze zrozumienie mechanizmów przeciwnowotworowego działania układu odpornościowego, oraz mogą być pomocne w opracowaniu skutecznych metod leczenia nowotworów u ludzi.

Kategoria dotkliwości procedury, uzasadnienie jej przeprowadzenia oraz liczebność grup doświadczalnych zostały określone prawidłowo. Większość Członków Komisji nie zgłosiła zastrzeżeń do procedury oraz czynności doświadczalnych opisanych w przedłożonym wniosku i uznała, że realizacja tego projektu badawczego jest dopuszczalna.

Ze względu na najwyższy stopień dotkliwości proponowanych procedur przeprowadzona zostanie ocena retrospektywna 6 m-cy po zakończeniu doświadczenia

Niniejsza uchwała wchodzi w życie z dniem wydania i jest ważna do 01.07.2018 r.

§ 4

Integralną część niniejszej uchwały stanowi kopia wniosku, o którym mowa w § 1

I LOKALNA KOMISJA ETYCZNA
ds. Doświadczeń na Zwierzętach
przy Wydziale Biologii UW
ul. Ilji Miecznikowa 1, 02-096 Warszawa
tel. 022 5541028, e-mail: Ike1waw@biol.uw.edu.pl

(Pieczęć lokalnej komisji etycznej)   Podpisy przewodniczącego komisji

Otrzymuje Użytkownik

Pouczenie:

Od decyzji komisji można wnieść odwołanie do Krajowej Komisji Etycznej w terminie 14 od dnia otrzymania uchwały.

Użytkownik kopie przekazuje:

- Osoba planująca doświadczenie
- Zespół ds. dobrostanu

UCHWAŁA NR 289/2017

z dnia 26 kwietnia 2017 r.

I Lokalnej Komisji Etycznej do spraw doświadczeń na zwierzętach w Warszawie

§ 1

Na podstawie art. 48 pkt. 1 ustawy z dnia 15 stycznia 2015r. o ochronie zwierząt wykorzystywanych do celów naukowych lub edukacyjnych (Dz. U. poz. 266) po rozpatrzeniu wniosku pt. **Badanie roli arginazy w regulacji odpowiedzi przeciwnowotworowej w mysich modelach nowotworowych – część 1** z dnia **13.04.2017 r.** złożonego przez **Centrum Nowych Technologii Uniwersytetu Warszawskiego ul. Banacha 2c, 02-097 Warszawa** zaplanowanego przez **prof. dr hab. med. Dominikę Nowis** lokalna komisja etyczna

WYRAŻA ZGODĘ
Na przeprowadzenie doświadczeń na zwierzętach w zakresie wniosku.

§ 2

W wyniku rozpatrzenia wniosku o którym mowa w § , Lokalna Komisja Etyczna ustaliła, że:

1. Wniosek należy przypisać do kategorii: **DOŚWIADCZENIA NA ZWIERZĘTACH (A)**
2. Najwyższy stopień dotkliwości proponowanych procedur to: **UMIARKOWANY**
3. Doświadczenia będą przeprowadzane na gatunkach lub grupach gatunków: **Mysz C57BL/6 8-12 tygodni- 54 os., Mysz B6.129S4-Arg1tm1Lky (YARG), 8-12 tygodni- 108 os.**
4. Doświadczenia będą przeprowadzane przez: **Jakub Gołąb, Dominika Nowis, Anna Sosnowska, Kavita Ramji, Zofia Pilch, Justyna Chlebowska -Tuz**
5. Doświadczenie będzie przeprowadzane w terminie[1] **01.05.2017 - 01.05.2019 r.**
6. Doświadczenie będzie przeprowadzone w ośrodku[2]: **Centralne Laboratorium Zwierząt Doświadczalnych WUM ul. Banacha 1B, 02-097 Warszawa**
7. Doświadczenie będzie przeprowadzone poza ośrodkiem w:
8. Użyte do procedur zwierzęta dzikie zostaną odłowione przez............. w sposób
9. Doświadczenie nie zostanie poddane ocenie retrospektywnej

---

[1] Nie dłużej niż 5 lat
[2] Podać jeśli jest to inny ośrodek niż użytkownik

§ 3

Uzasadnienie:

Nowotwory są drugą przyczyną zgonów w Polsce a liczba zachorowań na nowotwory złośliwe w ciągu ostatnich trzech dekad wrosła ponad dwukrotnie. Projekt przedstawiony we wniosku nr 289/2017 ma na celu zweryfikowanie hipotezy, że arginaza upośledza rozwój przeciwnowotworowej swoistej odpowiedzi immunologicznej a inhibitor tego enzymu przywraca prawidłową funkcję komórek układu odpornościowego Planowana jest ocena w którym z mysich modeli nowotworów dochodzi do najbardziej nasilonej indukcji wytwarzania arginazy a następnie wyłonienie tych rodzajów, które charakteryzują się najwyższą produkcją tego enzymu. Wykonana zostanie również ocena dynamiki pojawiania się w guzach arginazy w czasie oraz zidentyfikowane zostaną wytwarzające ją komórki. Dokładnie scharakteryzowany profil ekspresji arginazy pozwoli na lepsze poznanie mechanizmów przeciwnowotworowego działania układu odpornościowego a uzyskane wyniki w przyszłości mogą być pomocne w tworzeniu skutecznych metod leczenia nowotworów u ludzi.

Kategoria dotkliwości procedur, uzasadnienie ich przeprowadzenia oraz liczebność grup doświadczalnych zostały określone prawidłowo. Większość Członków Komisji nie zgłosiła zastrzeżeń do procedur oraz czynności doświadczalnych opisanych w przedłożonym wniosku i uznała, że realizacja tego projektu badawczego jest dopuszczalna.

Niniejsza uchwała wchodzi w życie z dniem wydania i jest ważna do 01.05.2019 r.

§ 4

Integralną część niniejszej uchwały stanowi kopia wniosku, o którym mowa w § 1

I LOKALNA KOMISJA ETYCZNA
ds. Doświadczeń na Zwierzętach
przy Wydziale Biologii UW
ul. Ilji Miecznikowa 1, 02-096 Warszawa
tel. 022 5541028, e-mail: lke1waw@biol.uw.edu.pl

(Pieczęć lokalnej komisji etycznej)

Podpisy przewodniczącego komisji
....

Otrzymuje Użytkownik

Pouczenie:

Od decyzji komisji można wnieść odwołanie do Krajowej Komisji Etycznej w terminie 14 od dnia otrzymania uchwały.

Użytkownik kopie przekazuje:

- Osoba planująca doświadczenie
- Zespół ds. dobrostanu

UCHWAŁA NR 317/2017

z dnia 24 maja 2017 r.

I Lokalnej Komisji Etycznej do spraw doświadczeń na zwierzętach w Warszawie

§ 1

Na podstawie art. 48 pkt. 1 ustawy z dnia 15 stycznia 2015r. o ochronie zwierząt wykorzystywanych do celów naukowych lub edukacyjnych (Dz. U. poz. 266) po rozpatrzeniu wniosku pt. **Badanie roli arginazy w regulacji odpowiedzi przeciwnowotworowej w mysich modelach nowotworowych – część 2** z dnia **12.05.2017 r.** złożonego przez **Centrum Nowych Technologii Uniwersytetu Warszawskiego ul. Banacha 2c, 02-097 Warszawa** zaplanowanego przez **prof. dr hab. med. Dominikę Nowis** lokalna komisja etyczna

WYRAŻA ZGODĘ
Na przeprowadzenie doświadczeń na zwierzętach w zakresie wniosku.

§ 2

W wyniku rozpatrzenia wniosku o którym mowa w §, Lokalna Komisja Etyczna ustaliła, że:

1. Wniosek należy przypisać do kategorii: **DOŚWIADCZENIA NA ZWIERZĘTACH (A)**
2. Najwyższy stopień dotkliwości proponowanych procedur to: **UMIARKOWANY**
3. Doświadczenia będą przeprowadzane na gatunkach lub grupach gatunków:
   Mysz C57BL/6, 8-12 tygodni, 237 os.;
   Mysz C57BL/6-Tg(TcraTcrb)1100Mjb/J (OT-I) , 8-12 tygodni, 50 os.;
   Myszy B6(Cg)-Rag2tm1.1Cgn/J (RAG2 KO), 8-12 tygodni 60 os.
4. Doświadczenia będą przeprowadzane przez: **Jakub Gołąb, Dominika Nowis, Anna Sosnowska, Kavita Ramji, Zofia Pilch, Justyna Chlebowska –Tuz, Olga Sokołowska**
5. Doświadczenie będzie przeprowadzane w terminie[1] **01.06.2017 – 30.12.2019 r.**
6. Doświadczenie będzie przeprowadzone w ośrodku[2]: **Centralne Laboratorium Zwierząt Doświadczalnych WUM ul. Banacha 1B, 02-097 Warszawa**
7. Doświadczenie będzie przeprowadzone poza ośrodkiem w:
8. Użyte do procedur zwierzęta dzikie zostaną odłowione przez............. w sposób
9. Doświadczenie <u>nie zostanie</u> poddane ocenie retrospektywnej

---

[1] Nie dłużej niż 5 lat
[2] Podać jeśli jest to inny ośrodek niż użytkownik

§ 3

Uzasadnienie:

Projekt przedstawiony we wniosku nr 317/2017 ma na celu poznanie roli arginazy w regulacji antygenowo-swoistej odpowiedzi przeciwnowotworowej w mysim modelu czerniaka. Do tej pory taka terapia nie była badana. Badania funkcjonalności układu odpornościowego mogą być przeprowadzone jedynie w organizmie zwierzęcym z rozwiniętym układem immunologicznym, odwzorowującym układ immunologiczny człowieka. Arginaza jest enzymem, który degraduje aminokwas niezbędny do proliferacji limfocytów upośledzając ich prawidłowe funkcjonowanie. Wysoka aktywność tego enzymu występuje u chorych na różne rodzaje nowotworów. Wyniki doświadczenia mogą być pomocne w zrozumieniu mechanizmów przeciwnowotworowego działania układu odpornościowego oraz mogą przyczynić się do rozwoju bardziej skutecznych metod leczenia nowotworu u ludzi.

Kategoria dotkliwości procedur, uzasadnienie ich przeprowadzenia oraz liczebność grup doświadczalnych zostały określone prawidłowo. Większość Członków Komisji nie zgłosiła zastrzeżeń do procedur oraz czynności doświadczalnych opisanych w przedłożonym wniosku i uznała, że realizacja tego projektu badawczego jest dopuszczalna.

Niniejsza uchwała wchodzi w życie z dniem wydania i jest ważna do 30.12.2019 r.
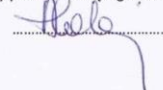
§ 4

Integralną część niniejszej uchwały stanowi kopia wniosku, o którym mowa w § 1

LOKALNA KOMISJA ETYCZNA
ds. Doświadczeń na Zwierzętach
przy Wydziale Biologii UW
ul. Ilji Miecznikowa 1, 02-096 Warszawa
tel. 022 5541028, e-mail: lke1waw@biol.uw.edu.pl

(Pieczęć lokalnej komisji etycznej)

Podpisy przewodniczącego komisji
....

Otrzymuje Użytkownik

Pouczenie:

Od decyzji komisji można wnieść odwołanie do Krajowej Komisji Etycznej w terminie 14 od dnia otrzymania uchwały.

Użytkownik kopie przekazuje:

- Osoba planująca doświadczenie
- Zespół ds. dobrostanu